SESSION IV

NOBLE GASES (1)

Tuesday, August 13, 1974
CHAIRMAN: Victor Benaroya

ADSORPTION OF KRYPTON FROM HELIUM BY LOW TEMPERATURE CHARCOAL
M.H. Cooper, C.R. Simmons, G.R. Taylor

ENGINEERING SCALE TESTS OF AN FFTF FISSION GAS DELAY BED
T.J. Kabele, A.P. Bohringer

SELECTIVE ADSORPTION-DESORPTION METHOD FOR THE ENRICHMENT OF Kr
Y. Yuasa, M. Ohta, A. Watanabe, A. Tani, N. Takashima

PRESSURE-SWING SORPTION CONCENTRATION OF KRYPTON-85 FOR PERMANENT STORAGE
A.S. Goldin, J.W. Ayers, D.W. Underhill

GENERAL ATOMIC'S RADIOACTIVE GAS RECOVERY SYSTEM
J.A. Mahn, C.A. Perry

DEVELOPMENT OF THE KRYPTON ABSORPTION IN LIQUID CARBON DIOXIDE (KALC) PROCESS FOR HTGR OFF-GAS REPROCESSING
R.W. Glass, H.W.R. Beaujean, H.D. Cochran, Jr., P.A. Haas, D.M. Levins, W.M. Woods

AKUT - A PROCESS FOR THE SEPARATION OF AERCSOLS, KRYPTON AND TRITIUM FROM BURNER OFF-GAS IN HTR-FUEL REPROCESSING
M. Laser, H. Barnert-Wiemer, H. Beaujean, E. Merz, H. Vygen

ABSORPTION PROCESS FOR REMOVING KRYPTON FROM THE OFF-GAS OF AN LMFBR FUEL REPROCESSING PLANT
M.J. Stephenson, W.D. Reed, D.I. Dunthorn, J.H. Pashley

ADSORPTION OF KRYPTON FROM HELIUM BY LOW TEMPERATURE CHARCOAL

M. H. Cooper, C. R. Simmons, and G. R. Taylor
Advanced Reactors Division
Westinghouse Electric Corporation
Madison, Pennsylvania

Abstract

Adsorption of krypton from helium by charcoal at temperatures from -100°C to -140°C was experimentally investigated to verify adsorption system design methods and to determine effects of regeneration for the Gas Purification System of the Liquid-Metal Fast Breeder Reactor. Helium with two krypton concentrations, traced by krypton-85 at 0.0044 $\mu Ci/cm^3$, was passed through a 1/2-inch diameter, three-inch long trap packed with Pittsburgh Activated Carbon, Type PCB 12x30, coconut charcoal. Breakthrough curves were measured by continuously recording the activity of the effluent gas using a Westinghouse Model 1440 Radio Gas Sampler with a krypton-85 detection limit of about $5x10^{-7}$ $\mu Ci/cm^3$.

Experimental breakthrough curves with continuous feed for both concentrations and for superficial gas velocities of 5 to 28 cm/sec were closely fitted when the pore diffusion term was omitted from the Anzelius linear equilibrium adsorption model indicating that the adsorption process for this system was controlled by gas phase mass transport kinetics. Adsorption capacities determined in these experiments at -140°C agreed closely with published data. A discontinuity, however, was observed in the krypton adsorption coefficient between -100 and -120°C. This discontinuity may be caused by capillary condensation of krypton in the charcoal pores.

Breakthrough times for pulse experiments at 400 ppm (vol.) krypton concentration were several times greater than breakthrough for continuous feed experiments at equivalent conditions. The differences in breakthrough times indicate that the adsorption isotherms are non-linear in this concentration range.

Regeneration experiments showed that purging with helium at room temperature for 16 hours was inadequate, since lower breakthrough times were obtained after this treatment. Regeneration under vacuum at 100°C or 200°C for 16 hours resulted in satisfactory regeneration (i.e., no reduction in breakthrough times occurred in subsequent runs).

I. Introduction

Both argon and helium are being considered for the covergas of the Liquid-Metal Fast Breeder Reactor (LMFBR) to protect the sodium coolant from reaction with atmospheric oxygen, moisture, carbon dioxide, and other trace contaminants. A small stream of covergas is continuously withdrawn and purified to remove radioactive fission gases released to the covergas from defect or failed fuel. The design basis for the gas purification system is continuous operation with 1% failed fuel. The reference design for the helium covergas purification is a low temperature charcoal adsorption system consisting of a pair of charcoal adsorption traps and a gas pressurization and storage system. One trap can be regenerated, while the other trap is used to purify the recirculating helium.

The purpose of this paper is a discussion of an experimental program supported by the Westinghouse Electric Corporation to investigate the removal of fission gases from helium by adsorption on low temperature charcoal. Specific objectives of this program were the verification of design methods used to predict breakthrough and determination of the effects of repeated regeneration on charcoal performance at high decontamination factors (DF's).

II. Apparatus

The experimental apparatus, shown schematically in Figure 1, is installed in a forced-draft fume hood to ensure removal and dilution of any radioactive gas leakage. The system is designed to perform both once-through and recirculating adsorption experiments at temperatures from ambient to liquid nitrogen temperature and to investigate regeneration at ambient and elevated temperatures. The equipment is designed for a maximum helium flow of 3.3 liters/min. at 2.4 atmospheres. System lines are fabricated of 3/8-inch and 1/2-inch copper tubing with silver soldered joints to reduce potential gas leakage.

Gas tagged with ^{85}Kr is supplied from either of two gas cylinders connected to the three cylinder manifold; the third cylinder is pure inert gas for purging prior to starting an experiment and during regeneration. The gas passes through an electronic flowmeter to a precooler and the primary test trap, both of which are installed in a Dewar filled with liquid nitrogen. The test trap consists of a 3-inch long bed of Pittsburgh Activated Charcoal, Type PCB 12x30, coconut charcoal packed in a copper tube, 0.45-inch ID. The precooler is a 2-inch diameter coil, consisting of 30 turns of 1/4-inch OD copper tubing. Both the trap tube and cooler coil are wound with heater cable in series connection and are installed in copper jackets with Fiberfrax insulation. The details of trap tube fabrication and cooler coil trap installation in the Dewar vessels are shown in Figures 2 and 3, respectively. The heaters are used to adjust trap temperatures during regeneration studies and to raise trap temperatures above liquid nitrogen temperatures during the experiments. Downstream of the primary test trap, the gas enters a Westinghouse Model 1440 Radio Gas Sampler with a ^{85}Kr detection limit of about 5×10^{-7} $\mu Ci/cm^3$ and then enters a second precooler and charcoal trap. The purpose of the second trap is to act as an integrator by adsorbing any ^{85}Kr passing through the first trap and to prevent release of ^{85}Kr to the atmosphere during breakthrough of the primary test trap. A mechanical vacuum pump is connected to the system downstream of the integrator trap for regeneration of the test trap. A bellows-sealed diaphragm pump has been installed in a bypass loop, so that closed loop, pulse-type experiments may also be performed with the system.

Temperatures of both traps are measured by stainless steel sheathed chromel-alumel thermocouples inserted to monitor gas temperatures at the inlet and outlet positions. Continuous strip chart records are made of temperatures, gas flow, and beta activity at the outlet of the primary test trap.

III. Breakthrough Analysis

The analytical model used to predict the breakthrough curve is based on the Anzelius linear equilibrium solution to the differential mass balance across an element of the charcoal:[1]

$$V_S \frac{\partial C}{\partial Z} + \varepsilon \frac{\partial C}{\partial t} + \rho_b \frac{\partial g}{\partial t} = D \frac{\partial^2 C}{\partial Z^2} \qquad (1)$$

$$\rho_b \frac{\partial g}{\partial t} = (ka)_{eff} (C - g/K) \qquad (2)$$

In the first equation, the first term is the mass of solute flowing into the differential element; the second term is the solute accumulation in the column voids; the third term is the solute accumulation on the adsorbent; and the fourth is the axial dispersion of the solute along the length of the column. The second equation is the mass transfer to the adsorbent assuming a linearized adsorption isotherm. In order to solve these equations, the axial dispersion term is neglected and the axial dispersion is imbedded into the overall mass transfer coefficient:

$$\frac{1}{(ka)_{eff}} = \frac{1}{(ka)_{gas}} + \frac{1}{(ka)_{pore}} + \frac{1}{(ka)_{ax}} \tag{3}$$

The individual terms comprising the overall mass transfer coefficient are:

$$(ka)_{gas} = \frac{10.9\ V_S\ (1-\varepsilon)}{d_p} \left(\frac{D}{V_S\ d_p}\right)^{0.51} (Sc)^{0.16} \tag{4}$$

$$(ka)_{ax} = \frac{V_S}{\frac{d_p}{1.8} + \frac{D}{\sqrt{2}\ V_S}} \tag{5}$$

$$(ka)_{pore} = \frac{60(1-\varepsilon)\ \delta}{d_p^2} \tag{6}$$

Equations (1) and (2) are solved using the following dimensionless terms:

$$Y = g/g_m$$

$$X = C/C_o$$

$$N = \frac{(ka)_{eff} Z}{V_S}$$

$$ZN = \frac{(ka)_{eff} C_o}{\rho_b\ gm} \left(t - \frac{\varepsilon Z}{V_S}\right)$$

The solution is:

$$X = J\ (N, ZN) \tag{7}$$

$$Y = 1\text{-}J\ (ZN, N) \tag{8}$$

where J may be represented by the Onsager error function approximation:

$$J(S,t) = 1/2\ [1\text{-erf}\ (\sqrt{S} - \sqrt{t} + \frac{\exp - \sqrt{S} - \sqrt{t})^2}{\pi\ (\sqrt{t} + \sqrt[4]{St})}] \tag{9}$$

Equations (7), (8) and (9) were programmed for digital computer solution to yield X as a function of time and Y as a function of time and distance.

IV. Results and Discussion

Eleven continuous feed experiments and two pulse experiments have been performed using helium carrier gas at one atmosphere pressure and ^{85}Kr adsorbate. Five continuous feed experiments were performed at krypton concentrations of 400 ppm (vol.) while the remainder were at krypton concentrations of 0.03 ppm (vol.); the specific ^{85}Kr activity at both concentrations was 0.0044 $\mu Ci/cm^3$. The higher concentrations were used to facilitate the experiments by reducing the time to breakthrough. The lower concentration was similar to that expected for the total krypton concentration in the cover gas of an LMFBR if operated continuously with 1% failed fuel. Table 1 summarizes these experiments.

The breakthrough curves for all continuous feed experiments were closely predicted by the computer analysis described in Section III, when the pore diffusion term in Equation (2) was neglected. Hence, the controlling mass transport mechanism for this system is gas phase transport. The charcoal adsorption capacity data of Romberg and Shorrock[2] were used for the -140°C experiments; capacity data extrapolated from the data of Burnette, Graham, and Morse[3] were used for the higher temperature experiments. Figure 2 is a comparison of the experimental breakthrough curve with the calculated curve for Run I-5 at 400 ppm and -140°C. This excellent agreement confirms both the analytic model and the published capacity data.

Figure 3 is the breakthrough curve for Run I-7, in which the krypton concentration was 0.03 ppm (vol.) and the charcoal temperature was -120°C. The experimental breakthrough curve is closely fitted by the analytic model with gas phase transport control, even though the velocity was 28 cm/sec. Gas phase control results in breakthrough curves with steeper slopes, compared to those with pore diffusion.

Adsorption capacities obtained by trial-and-error fitting of the analytic breakthrough curves with the experimental data were a factor of three higher at -120°C and a factor of two lower at -100°C than adsorption capacities extrapolated from the data of Burdette, et.al.[3] These results imply a discontinuity in krypton adsorption on charcoal between -100°C and -120°C. A discontinuity in this range is shown in Figure 6, which correlates adsorption coefficients for krypton in argon reported by Underhill[4] with reciprocal absolute temperature as well as the present data. A possible mechanism to explain this discontinuity is the condensation of krypton in the charcoal pores because of capillary forces. Although the normal boiling point of krypton is -152°C, the capillary forces in the charcoal could result in the formation of a condensed phase at higher temperature, i.e., between -100 and -120°C. The calculated pore size, neglecting charcoal surface effects, required to raise the boiling point of krypton to -115°C is 2.5°A, while the predominate pore sizes of the charcoal used ranges from 18 to 21°A. The difference in magnitude between the adsorption coefficients reported by Underhill and those measured in this work or those extrapolated from Burnette et al may be the result of significantly lower krypton concentration in the former work compared to the 0.03 ppm (vol.) concentration in the present work.

The second objective of these experiments was to determine a suitable regeneration method to be specified for the plant covergas purification system. Comparison of Runs I-1, I-3, and I-4 shows that the breakthrough time for constant trap temperature (-140°C) and gas flow was increased by regeneration at 100°C while under vacuum compared to regeneration by purging with pure helium at room temperature.

Increasing the regeneration temperature to 200°C while under vacuum did not significantly affect the breakthrough time. Hence, an overnight evacuation at 100°C was selected as the standard regeneration method for these experiments.

Prior to regeneration of the charcoal, the helium carrier was removed by evacuation while the trap was at low temperature to demonstrate a potential method of minimizing the carrier gas to be compressed with the ^{85}Kr for long-term storage. For a 400 ppm (vol.) Kr experiment, the regeneration gas composition was 98% Kr and 2% He. At low concentration, however, nitrogen, presumably present as an impruity in the helium carrier, comprised about 73% of the regeneration gas, while Kr was about 0.2%. However, the enrichment factor for Kr in the regeneration gas was greater than 6×10^4. This method of fractionation prior to regeneration appears to be a feasible method for minimizing the gas volume required for long-term storage.

Breakthrough times for the pulse injections were considerably longer than the breakthrough times for corresponding conditions with constant flow. The breakthrough times for the two types of experiments should be the same, if the adsorption isotherms are linear. Hence, the adsorption isotherm for Kr is probably non-linear at the 400 ppm (vol.) range and pulse data cannot be simply analyzed at this concentration. Pulse experiments were not performed at the lower concentration because of the expected long breakthrough times.

V. Conclusions

Tentative conclusions reached from this investigation are:

(1) The adsorption model accurately predicts the breakthrough curve when gas transport control is assumed and pore diffusion is neglected.

(2) Charcoal is satisfactorily regenerated at 100°C in vacuo for 15 hours (shorter time cycles may be adequate; the effect of regeneration time was not investigated).

(3) Purging for 15 hours with pure helium at room temperature resulted in incomplete regeneration.

(4) The volume of gas to be stored to allow krypton decay may be minimized by evacuation of the adsorption bed while at low temperature prior to regeneration by heating.

(5) Adsorption data of Romberg and Shorrock are confirmed at -140°C and 400 ppm (vol.) krypton.

(6) An apparent discontinuity in Kr adsorption on charcoal between -100 and -120°C may be caused by capillary condensation. This effect required further investigation.

References

[1] J. H. Perry, editor, Chemical Engineer's Handbook, Fourth Ed., McGraw-Hill Book Co., N.Y., 1963, pp. 16-32.

[2] E. Romberg and M. A. Shorrock, "The determination of adsorption equilibria for the helium-methane-krypton system on active charcoal using a dynamic method," Trans. Instn. Chem. Engrs., (London), 47, pp. T3-T10 (1969).

[3] R.D. Burnette, W.W. Graham, III, and D.C. Morse, "The removal of radioactive krypton and xenon from a flowing helium stream by fixed-bed adsorption," GA-2395, General Atomics (Oct. 1961).

[4] M. W. First and D. W. Underhill, et. al., "Semi-Annual Report - Harvard Air Cleaning Laboratory," NYO-841-25, pp. 29 (Nov. 1971).

Notation

C = concentration in gas phase, mol fraction

D = diffusion coefficient, cm^2/sec

g = concentration on adsorbent, cm^3/gm

t = time, seconds

V_S = linear gas velocity, cm/sec

Z = distance, cm

ka = mass transfer coefficient, gm mol/sec, mol fraction

ε = void fraction of bed (dimensionless)

ρ_b = bed density, gm/cm^3

K = equilibrium adsorption coefficient, i.e., g = KC

d_p = particle diameter, cm

δ = pore diameter, cm

Sc = Schmidt number = $\frac{\text{viscosity}}{(\text{density})(\text{diffusion coefficient})}$

Subscripts

o = initial

m = maximum

gas = gas phase

pore = pore diffusion

ax = axial diffusion

eff = effective

Table I Summary of experimental results

Run	Kr Conc. ppm (vol.)	Trap Temperature °C	Superficial Velocity cm/sec	Regeneration Method*	Breakthrough Time**, Hr.	Exp. Capacity, cm^3/gm	Lit. Capacity cm^3/gm
Continuous Flow:							
I-1	400	-139	12.5	He purge at 20°C	3.5	37	37[2]
I-2	400	-140	15.0	Vacuum at 100°C	4.0	37	37[2]
I-3	400	-140	12.5	Vacuum at 100°C	6.0	37	37[2]
I-4	400	-140	12.5	Vacuum at 200°C	5.8	37	37[2]
I-5	400	-140	20.0	Vacuum at 100°C	3.5	37	37[2]
I-6	0.03	-100	28.0	Vacuum at 100°C	0.25	0.00045	0.00091[3]
I-7	0.03	-120	20-29	Vacuum at 100°C	8.4	0.0045	0.0015[3]
I-8	0.03	-100	28.0	Vacuum at 100°C	0.38	0.00045	0.00091[3]
I-9	0.03	-100	10.0	Vacuum at 100°C	1.4	0.00045	0.00091[3]
I-10	0.03	-100	10.0	Vacuum at 200°C	1.0	0.00045	0.00091[3]
I-11	0.03	-100	5.0	Vacuum at 200°C	3.0	0.00045	0.00091[3]
Pulse Injections:							
II-1	400	-140	10.0	Vacuum at 100°C	14.0		
II-2	400	-140	63.0	Vacuum at 100°C	12.6		

* All regenerations were carried out over a period of 15-16 hours.

** Breakthrough defined as $C/C_0 = 1 \times 10^{-3}$ for continuous flow tests and C/C_0 (max.) for pulse tests.

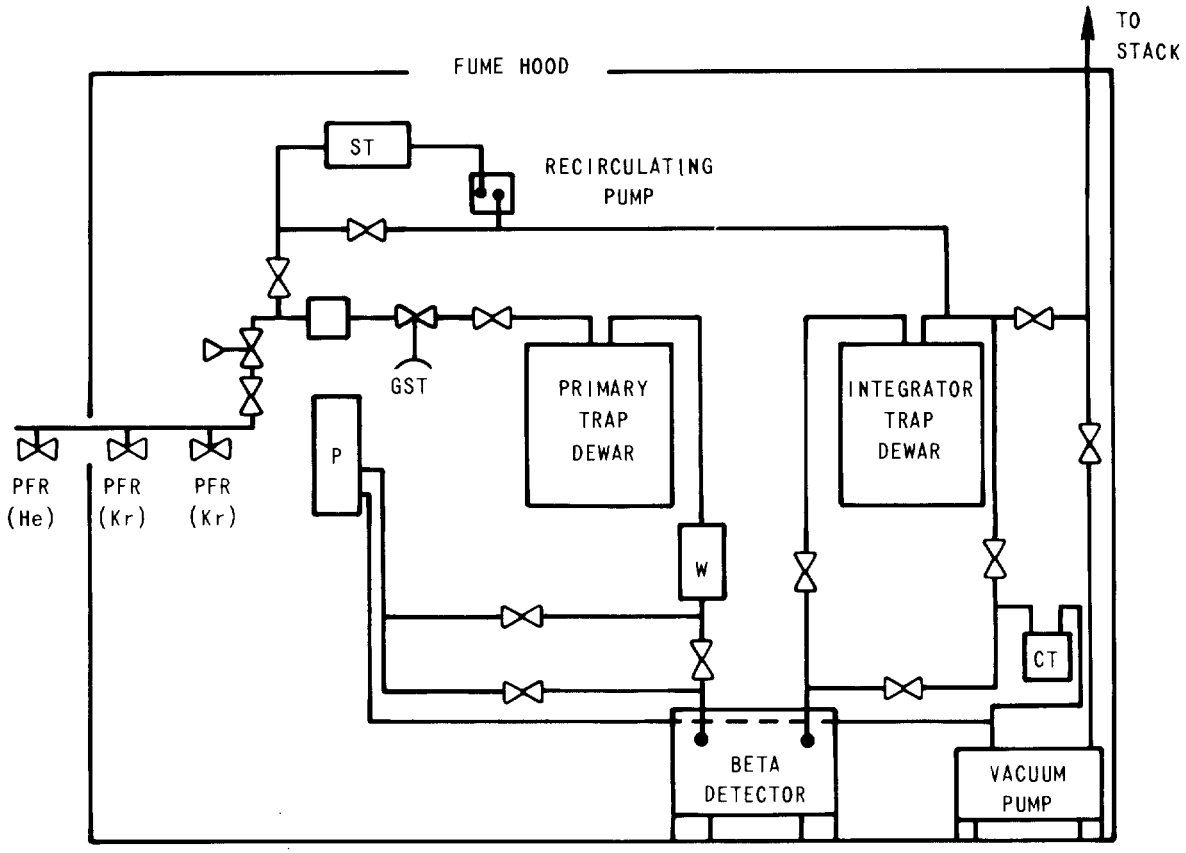

PFR: PRESSURE/FLOW REGULATOR
ST: SURGE TANK
F: FLOW METER
GST: GAS SAMPLING TRAP

P: McLEOD GAUGE
W: WARMER COIL
CT: VACUUM COLD TRAP

Figure 1. Experimental System Schematic Layout

6502-1

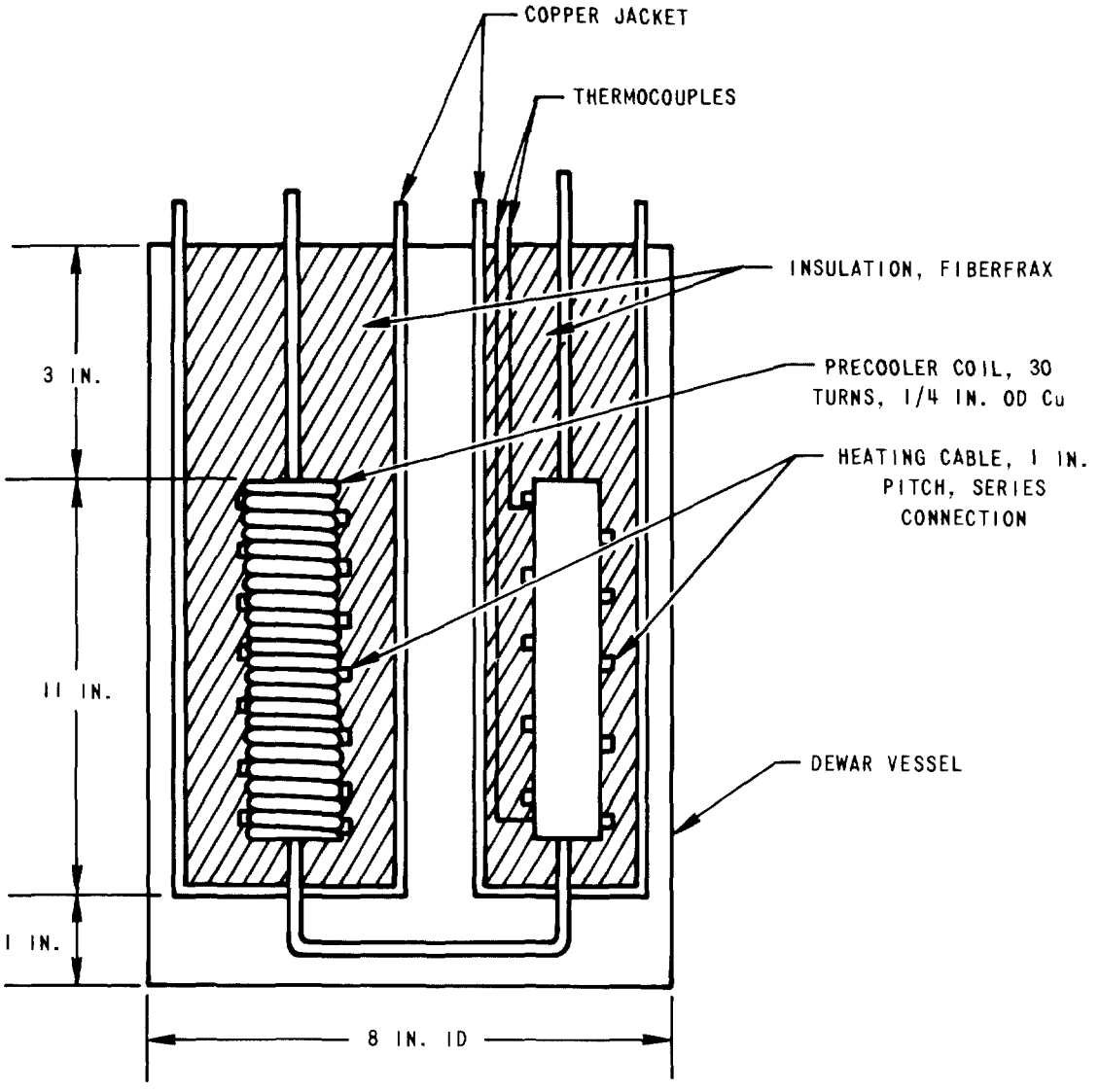

Figure 2. Precooler Coil and Charcoal Trap Arrangement in the Dewar Vessel

6502-2

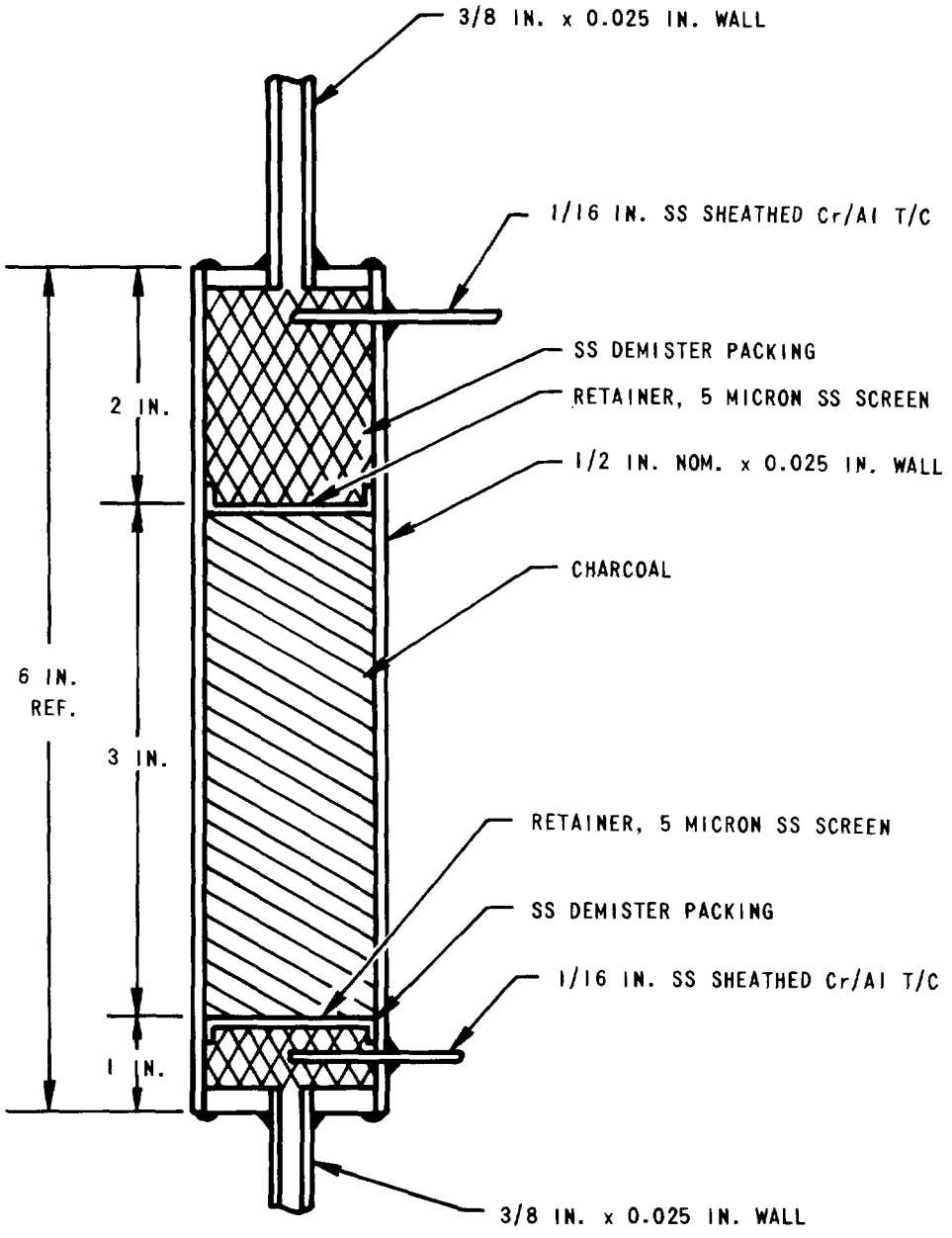

Figure 3. Charcoal Trap Details

6502-3

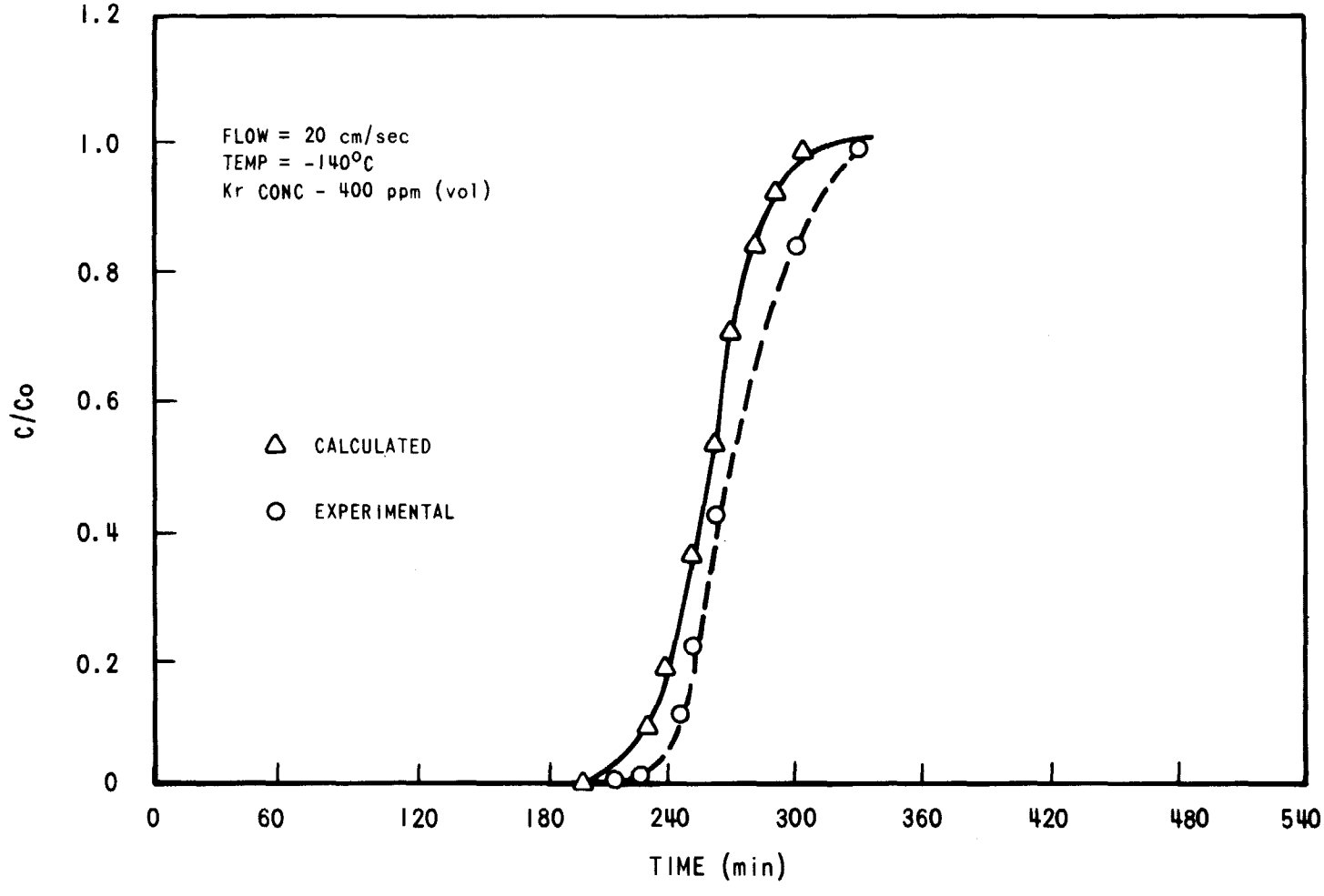

Figure 4. Comparison of Experimental Breakthrough Data With Calculated Curve for Run I-5

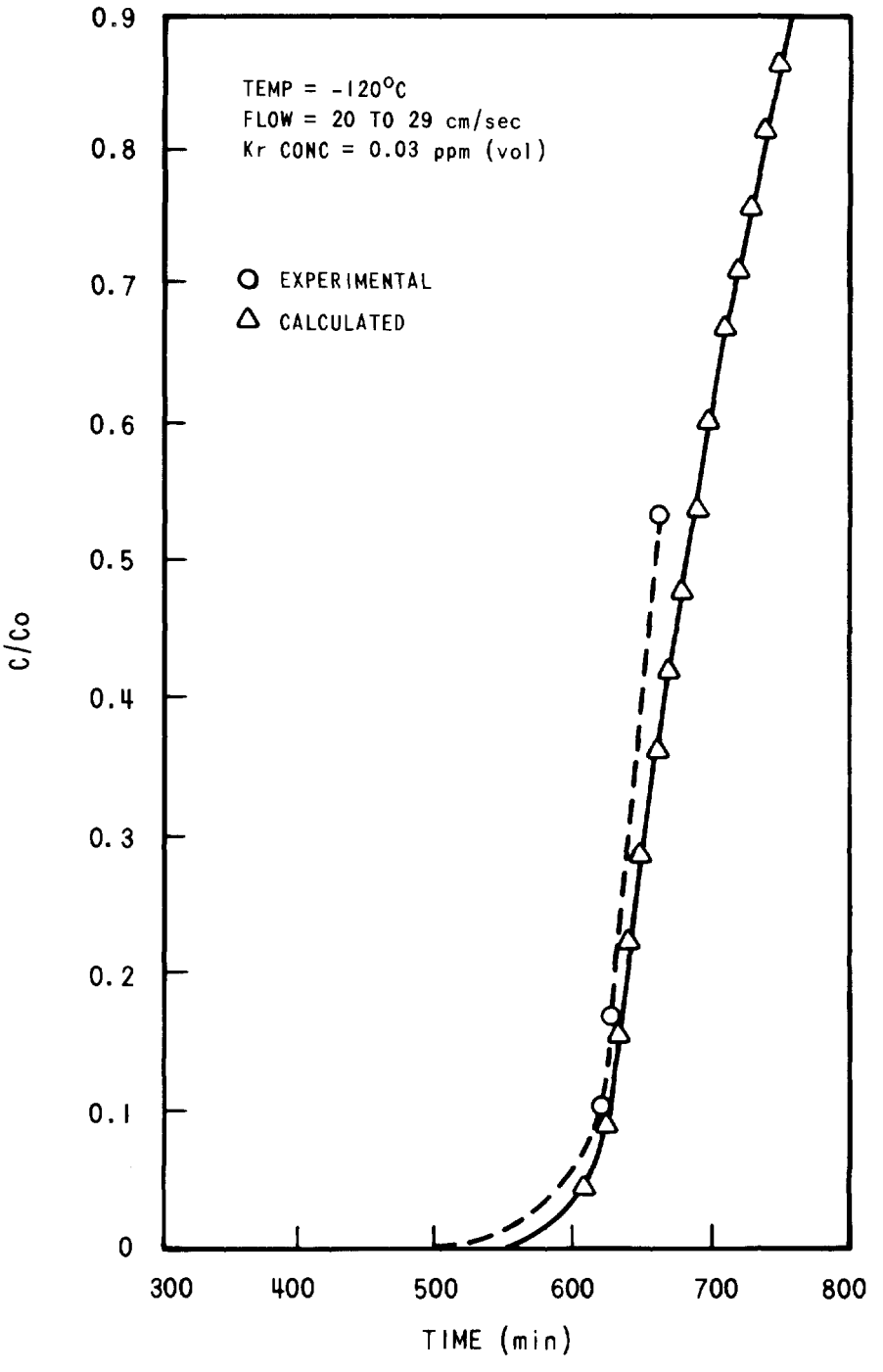

Figure 5. Comparison of Experimental Breakthrough Data With Calculated Curve for Run I-7

6502-1

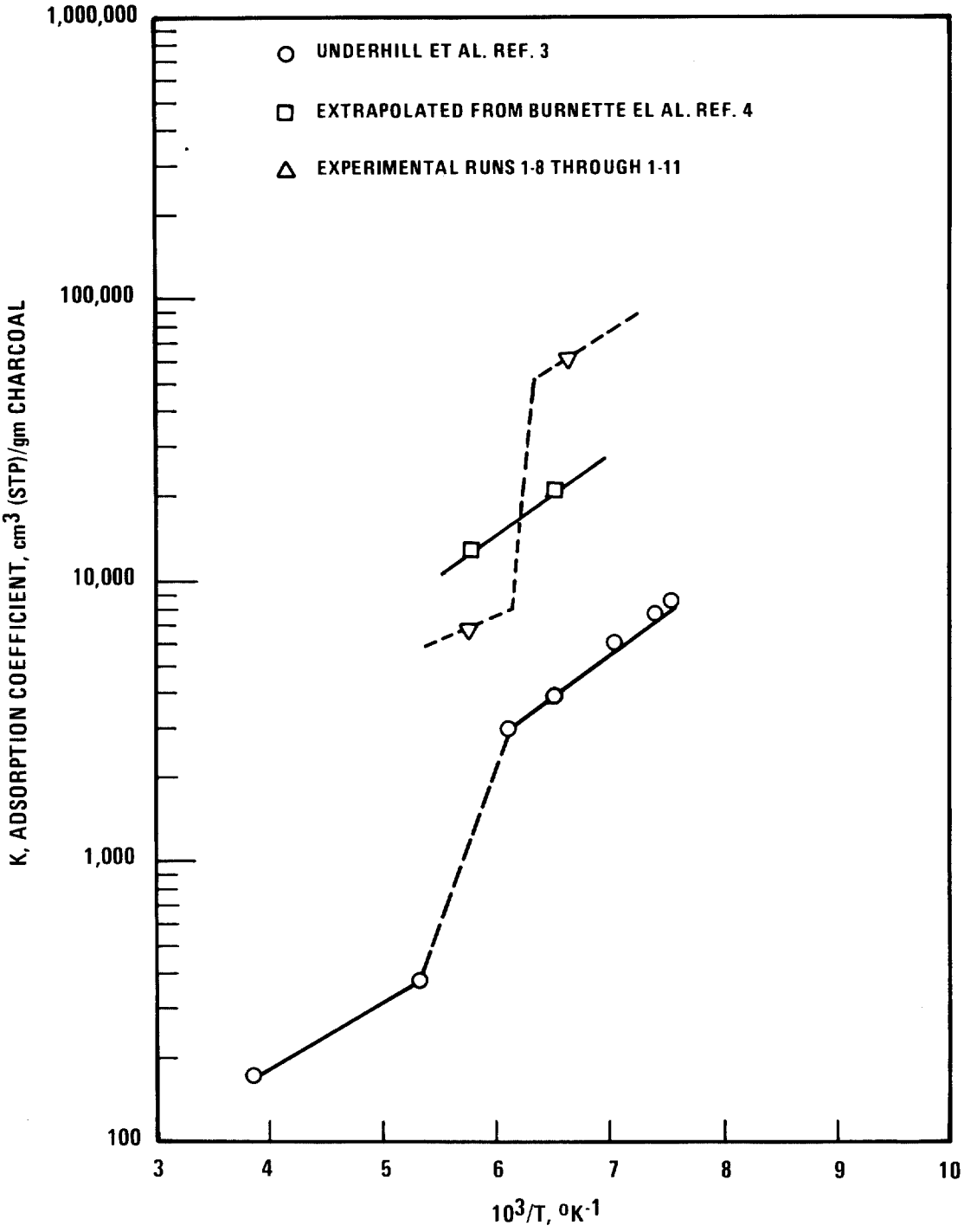

Figure 6. Adsorption Coefficient Versus Reciprocal Temperature

6502-6

DISCUSSION

BECK: I have two questions with regard to your regeneration scheme with helium. Did you investigate temperatures higher than 20 degrees centigrade?

COOPER: No, we did not.

BECK: On your vacuum regeneration scheme, I was wondering if you had any problems obtaining a five to ten micron range when pumping down your system. Would you anticipate problems doing so with a larger system?

COOPER: We did not have difficulty reaching that pressure with a small system. The problem with a large system may be time. When you have, as you must, a high integrity system, there's no reason why you couldn't obtain low pressures. It's a question of volume and pumping speeds.

MOELLER: You mentioned that you had designed your system with one percent failed fuel in mind. Have you looked ahead to the possibility of operating an LMFBR with vented fuel?

COOPER: Yes, we have. In the early days, we looked at that, but we have not updated the design. That concept is very far in the future and we are not expending any effort on it at this time. The emphasis is on completely sealed fuel now.

_____: Surface diffusion is extremely rapid and this is necessary to take advantage of the pore structure. Therefore, a complete model should take into account surface diffusion into pore structure.

COOPER: That is included in the pore diffusion term in the overall mass transfer coefficient. We found that a separate pore diffusion term is not required because it is so rapid, and it can be neglected. The process is gas phase transfer controlled. I think that one of the important things that came out of this work was that we could operate our beds at much higher superficial velocities, 5 to 30 cm/sec compared to the usual 1 cm/sec, and still show that gas phase mass transport was controlling. I don't think we want to limit our designs to low velocities.

SMITH: I was wondering if you could characterize your carbon in terms of such parameters as apparent density and carbon tetrachloride activity?

COOPER: The charcoal was Pittsburgh Activated Carbon Type PCB, 12 by 30. Data sheets are available from the manufacturer.

SMITH: Did you observe a functional relationship between pore diffusion and apparent density of the product?

COOPER: I don't have a comment on that.

JONAS: In your use of the adsorption coefficient, how do you differentiate between the adsorption capacity of the carbon and the rate of adsorption? Jonas and Sirrbely and Jonas and Rohrmann have used the Wheeler gas adsorption kinetics equation where the breakthrough time (t_b) for a gas penetrating a bed of carbon granules can be expressed by

$$t_b = \frac{We}{CoQ} W - \frac{\rho BQ \ln(C/Co)}{kv}$$

where W is the weight of carbon in the bed (g), We is the adsorption capacity (g/g) of the carbon for the gas, Co is the inlet concentration (g/cm^3), ρB is the bulk density of packing (g/cm^3), Q is the volumetric flowrate (cm^3/min), C is the exit concentration (g/cm^3), kv is the pseudo first order rate constant for adsorption (min^{-1}), and t_b is time in minutes. A plot of t_b versus W results in a straight line and from the slope and x-axis intercept, We and kv can be respectively calculated, thus separating the capacity and rate factors in a physical adsorption process. The equation assumes isothermal conditions. When the temperature of test is altered, the equation will apply when proper corrections are made. It must be recognized that a change of temperature will affect ten parameters in gas adsorption, namely, (1) adsorption rate constant, (2) adsorption capacity, (3) inlet concentration, (4) volume flowrate, (5) residence time of gas in the bed, (6) relative gas pressure, (7) adsorption potential, (8) desorption rate constant, (9)Langmirer type equilibrium constant relating the adsorption to the desorption rate constant, and (10) the resultant breakthrough time, t_b. It has been found, for example, in a study of the adsorption of dimethyl methylphosphonate vapor on a Pittsburgh activated carbon, that a rise in temperature from 25 C to 35 C produced a 20 minute decrease in breakthrough time, 87% of which was due to the decrease in the adsorption rate constant, 9% was due to a decrease in adsorption capacity, and 4% was due to associated effects. The temperature dependence of the adsorption rate constant was found to be nonlinear and can, as indicated above, be responsible for a major decrease in physical adsorption.

ENGINEERING SCALE TESTS OF AN FFTF FISSION GAS DELAY BED*

T. J. Kabele and A. P. Bohringer
Westinghouse-Hanford Company
P.O. Box 1970
Richland, Washington 99352

Abstract

The dynamic adsorption coefficient of ^{85}Kr on activated charcoal from a nitrogen carrier gas was measured at -80 and -120°C at pressures of zero and 30 psig. The effects of the presence of impurities in the nitrogen carrier gas (1% oxygen, and 100 vppm carbon dioxide) on the adsorption coefficient of ^{85}Kr were also measured.

The ^{85}Kr adsorption coefficient increased with decreasing temperature, and increased with increasing pressure. The presence of oxygen and carbon dioxide impurities in the nitrogen carrier gas had no discernible effect upon the adsorption coefficient. The adsorption coefficient for ^{85}Kr from nitrogen gas was lower than for adsorption of ^{85}Kr from an argon gas stream.

The work concluded a test program which provided design data for the fission gas delay beds which will be installed in the Fast Flux Test Facility (FFTF).

I. Introduction

The heart of both the FFTF Radioactive Argon Processing System (RAPS), which purifies primary argon cover gas, and the Cell Atmosphere Processing System (CAPS), which purifies nitrogen cover gas from inerted cells, is activated charcoal adsorption beds. These charcoal beds will delay noble fission gases long enough to allow the shorter lived isotopes of these gases to decay to a small fraction of their original activity. The delay is accomplished by the temporary adsorption of the fission gases, primarily the radioisotopes of xenon and krypton, on the charcoal. The small amounts of longer lived fission gases which complete a transit through the RAPS beds despite a long delay are subsequently removed from the primary argon cover gas stream by a gaseous fractional distillation process.

This paper contains the results of engineering scale tests of a prototypic FFTF charcoal bed. The test program was divided into two phases, adsorption from an argon carrier gas and adsorption from a nitrogen carrier gas. Results of the argon phase of the testing are presented in a topical report, HEDL-TME 73-26, dated May 1973.[1] Results of the tests using a nitrogen carrier gas are presented here.

---

* Work performed under USAEC Contract No. AT(45-1)-2170.

The primary objectives of the work presented in this paper were to measure the dynamic adsorption coefficient of ^{85}Kr on activated charcoal under prototypic CAPS conditions, and to determine if the coefficient was subject to scale-up effects, or the presence of gaseous impurities likely to be found in the CAPS nitrogen. The dynamic adsorption coefficients measured in these tests will be used in the design of the plant-scale adsorption beds to insure that adequate capacity is included in those plant units.

II. Test Description

The dynamic adsorption coefficients of ^{85}Kr for adsorption on activated charcoal from a nitrogen carrier gas stream were obtained using a pulse-tracer technique in which a pulse of radioactive gas was injected into a charcoal bed, and the resulting breakthrough curve analyzed by the method of statistical moments. [2] Scale up information was developed by comparing results from these tests with results from laboratory scale measurements made at the Harvard University School of Public Health and with literature data.

Test System

The apparatus constructed for these tests is shown schematically in Figure 1 and pictorially in Figure 2. The system consists of a charcoal bed, a pump for recirculating nitrogen gas through the bed, a well insulated, temperature controlled enclosure, a nitrogen gas supply, impurity and tracer addition stations, and valves, flowmeters, counting equipment, etc. for obtaining and recording data and for controlling the system. Nitrogen gas can be supplied to the bed either by recirculation of gas through the system using the pump with a small feed/bleed stream for pressure control, or by continuous addition of fresh nitrogen without recirculation. System gas pressure is maintained by addition of fresh nitrogen through a pressure regulator, with bleed streams to the counting chambers, chromatograph, and through a manual throttling valve to exhaust. Cooling for the system is provided by liquid nitrogen. A more detailed description of the major sub-systems follows.

Charcoal Bed and Charcoal. The charcoal bed is constructed from 8 inch Sch. 20, 304L-SS pipe and has a charcoal fill depth of 1.5 ft. The volume of charcoal is about one-half cubic foot. Gas flows downward through the vertically oriented bed at 1 scfm. Five thermocouples are located within the bed for monitoring and controlling the bed temperature.

The charcoal is Pittsburgh PCB 12 x 30 mesh, a coconut based activated carbon with a 0.45 g/cm^3 densely packed bulk density and a 50% void volume.

Charcoal Bed Refrigeration System. The refrigeration system for the charcoal bed is an insulated container using liquid nitrogen as coolant. The system is cooled by spraying liquid nitrogen into the vapor space near the charcoal bed. The inside of the refrigerated container is approximately three feet in diameter by six feet high with six inches of wall insulation. Three thermocouples are located

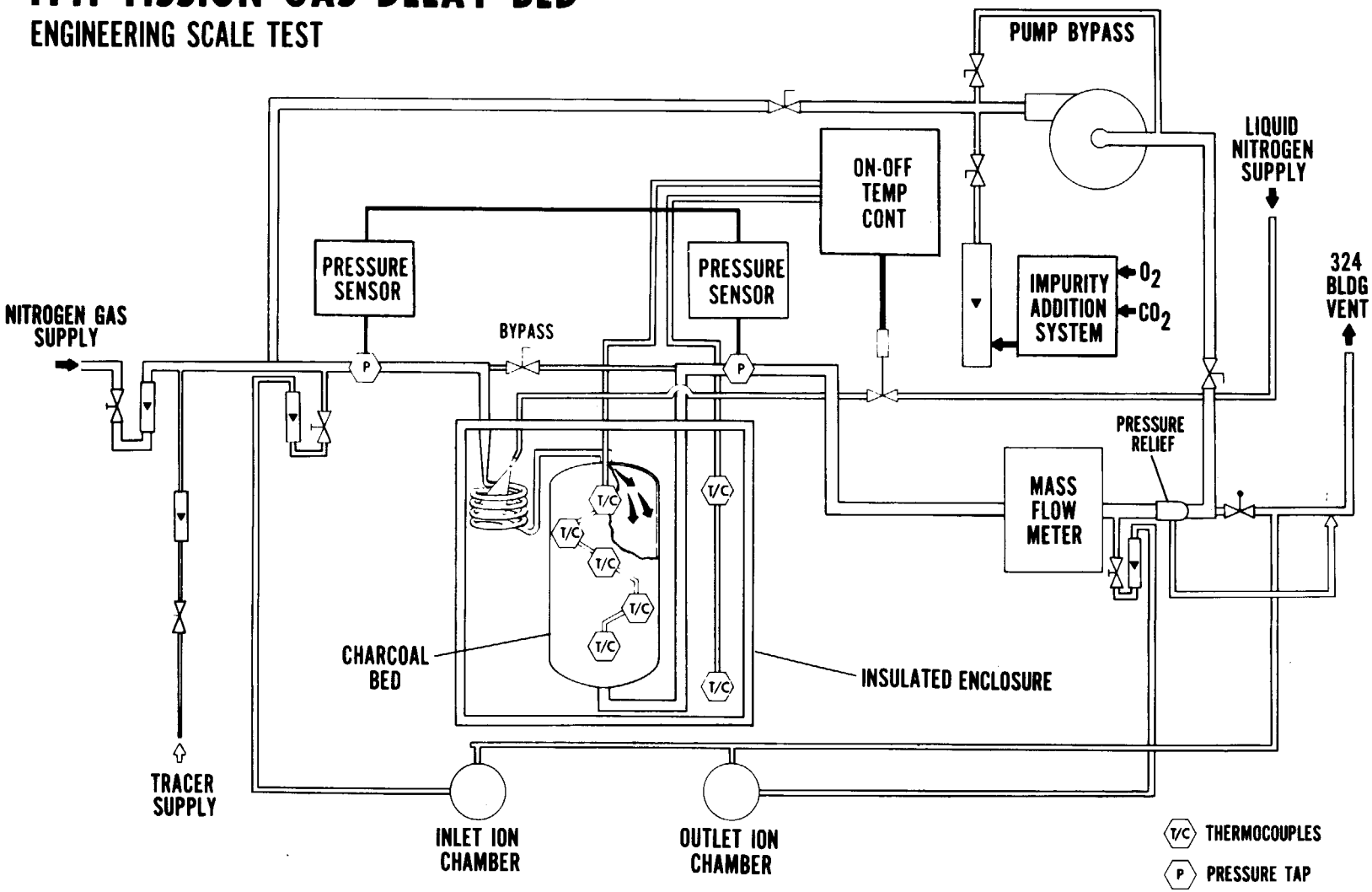

FIGURE 1. FLOW DIAGRAM OF TEST APPARATUS

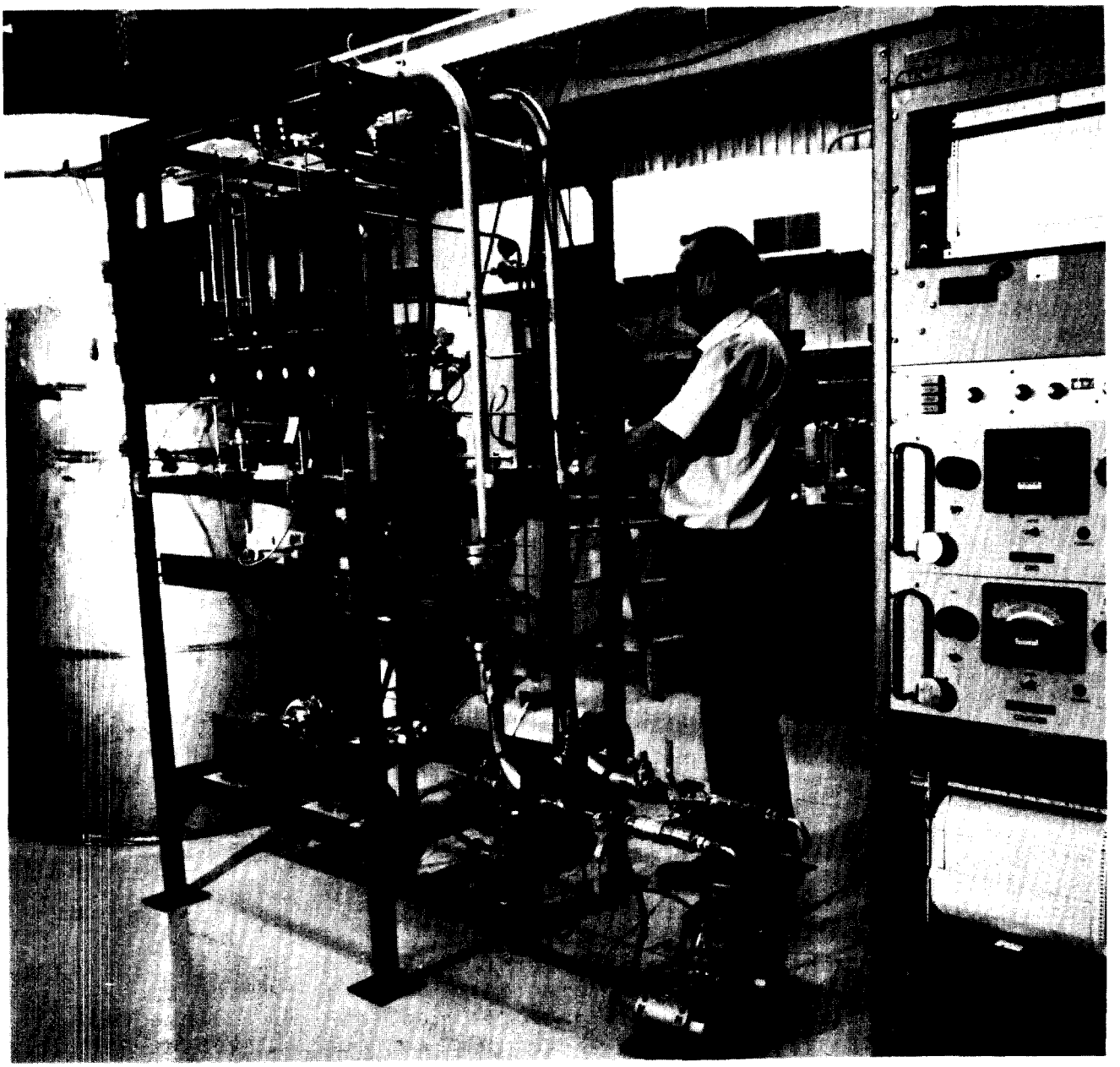

FIGURE 2. FISSION GAS DELAY BED TEST APPARATUS

within the insulated container to provide data on the cooling system performance.

Tracer Gas Addition Station. Tracer krypton-85 is added to the system by injection into the inlet gas line to the charcoal bed. The tracer is supplied from a pressurized gas cylinder and is injected into the inlet line through a manual, micrometer needle control valve. Injection flow rates are less than 0.1 scfm and last from twenty seconds to about two minutes. Addition of tracer is monitored by an inlet ion chamber and recorded. The krypton-85 was obtained from Oak Ridge.

Impurity Addition Station. Gaseous impurities (O_2, CO_2) can be added to the nitrogen gas stream to produce impurity levels anticipated in the FFTF nitrogen cover gas spaces. They can be added in either of two ways: from a pressurized gas cylinder, metered through the tracer addition micrometer valve or through a precision gas blending device also connected to the inlet gas line to the charcoal bed. This precision gas blending device consists of a modified Model 570 Precision Calibration System from Kin-Tek Laboratories which allows accurate blending of parts-per-million concentrations of several gases into a carrier gas stream. The blending is accomplished with calibrated permeation membranes and precise controls for the temperature, pressure, and flow rate of the several gas streams to be blended.

Tracer Monitoring and Data Log. Both the input tracer pulse and the concentration of tracer gas in the outlet line from the bed are monitored with 1000 cc flow-through ion chambers. The gas samples for these chambers are taken from taps on the inlet and outlet gas lines of the charcoal bed at nominal flow rates of approximately 500 cc/sec. The output signals from the ion chambers are recorded on a strip chart recorder.

Also recorded on strip-charts are the temperatures from the five thermocouples in the charcoal bed, the temperature of the refrigerated enclosure, the pressure drop across the bed, and the total system pressure. The total cumulative gas flow through the bed is also recorded.

Data Analysis

The dynamic adsorption coefficients of krypton-85 were calculated from the breakthrough curves by moment analysis[2]. These breakthrough curves were recorded on a strip-chart from the output signal of the outlet ion chamber. All of the breakthrough curves were nearly Gaussian in shape.

The mean holdup time of the tracer gas in the charcoal bed was calculated from the first moment of the breakthrough curves by:

$$t_1 = \frac{\int_0^\infty te^{\lambda t}c(t)dt}{\int_0^\infty e^{\lambda t}c(t)dt} \qquad (1)$$

where t_1 = mean holdup time

t = elapsed time from injection of tracer into bed inlet.

$c(t)$ = relative concentration of tracer in outlet gas line (from strip-chart recorder) as a function of time.

λ = decay constant for tracer gas.

The dynamic adsorption coefficient was calculated from the mean holdup time by

$$K = \frac{t_1 V}{m} \qquad (2)$$

where K = dynamic adsorption coefficient, cm^3 tracer gas/gm charcoal*

V = volume flow rate of carrier gas, cm^3/day

m = mass of charcoal in bed, gms

The actual computations were performed by computer. The strip-chart record of a breakthrough curve was transferred to punch cards, as was other pertinent data associated with the run (flow rate, temperatures, pressure, etc.), the computations were made, and a complete run data/results record was printed out for future reference. The integrations required in Equation (1) were done by the method of Simpson's Rule.

III. RESULTS AND DISCUSSION

The dynamic adsorption coefficients for ^{85}Kr adsorption from a nitrogen carrier gas are presented in Table 1. The ^{85}Kr coefficients were measured at -80 and -120°C and at pressures of zero and 30 psig. These conditions cover the expected ranges of temperature and pressure for the charcoal beds in the FFTF CAPS.

---

* The proper units of the dynamic adsorption coefficient are:

$\frac{cm^3 \text{ tracer gas}}{cm^3 \text{ carrier gas}} \times \frac{cm^3 \text{ carrier gas}}{gm \text{ charcoal}}$. The adsorption coefficient as presented here can be properly thought of as a partition coefficient.

TABLE 1

^{85}Kr ADSORPTION COEFFICIENT FROM NITROGEN COVER GASES

Test Conditions	Dynamic Adsorption Coefficient [cm^3(STP)/gm]		
	N_2	N_2,1%O_2	N_2, 100 ppm CO_2, 1%O_2
-80°C			
0 psig	1160	1190	1135
	1100	1170	1110
		1140	
30 psig	1570	1630	1580
	1540	1610	1570
		1630	
-120°C			
0 psig	4490	4570	4610
	4515	4830	4550
		4720	4500
30 psig	5720	5670	5420
	5810	5880	5420

First, the dynamic adsorption coefficient of ^{85}Kr was measured using a pure nitrogen carrier gas. This provided base-line data which could be compared with previous results obtained using an argon carrier gas and with measurements from a nitrogen carrier gas with selected impurities in it.

Next, the composition of the cover gas was changed to 1% oxygen and 99% nitrogen. The first set of determinations (same temperatures and pressures) was repeated. Lastly, a third constituent was added to the cover gas. Approximately 100 vppm of carbon dioxide, 1% oxygen, and the balance nitrogen was the composition of the cover gas for this third series of measurements. Again, the measurements were made at the same temperatures and pressures as the previous series. These concentrations of oxygen and carbon dioxide are the maximum anticipated for the nitrogen cover gas in FFTF inerted cells.

Effect of Impurities

The main conclusion to be drawn from these results is that neither oxygen nor carbon dioxide (at the concentrations tested) had a significant effect on the adsorption of ^{85}Kr from the nitrogen cover gas. Since these levels are at or above the concentrations expected in the nitrogen cover gases in FFTF, one can conclude that the presence of these gases will not adversely affect the performance of the CAPS charcoal beds.

This conclusion is subject to one important note of caution however. The operating temperatures of a large portion of the CAPS are well below the freezing point of carbon dioxide. Thus the potential exists for accumulating solid carbon dioxide on the charcoal and other cold surfaces of the system. This phenomenon was indirectly observed during our test program. The concentration of carbon dioxide in the inlet and outlet gas streams of the charcoal bed was periodically monitored. The inlet stream had a carbon dioxide concentration which normally ran between 90 and 100 ppm. No carbon dioxide was ever detected in the outlet gas stream. Thus carbon dioxide was continuously accumulating in the colder portions of the test system throughout the third series of measurements.

The accumulation of carbon dioxide in the CAPS, while not affecting system performance initially, may well become a problem if too much is allowed to build up. Two remedies are suggested: either remove the carbon dioxide before it reaches the cold charcoal beds or periodically allow portions of CAPS to warm up and release the frozen carbon dioxide. The former may require additional design, the latter can be handled in Operating Procedures.

Effects of Temperature and Pressure

The ^{85}Kr adsorption coefficients for adsorption from pure nitrogen at system pressures of zero and 30 psig are plotted as a function of reciprocal temperature in Figure 3. Included in the graph are results from the Harvard Air Cleaning Laboratory, obtained under similar conditions with laboratory scale equipment.[3] The agreement of our results with those from Harvard is excellent. Also included

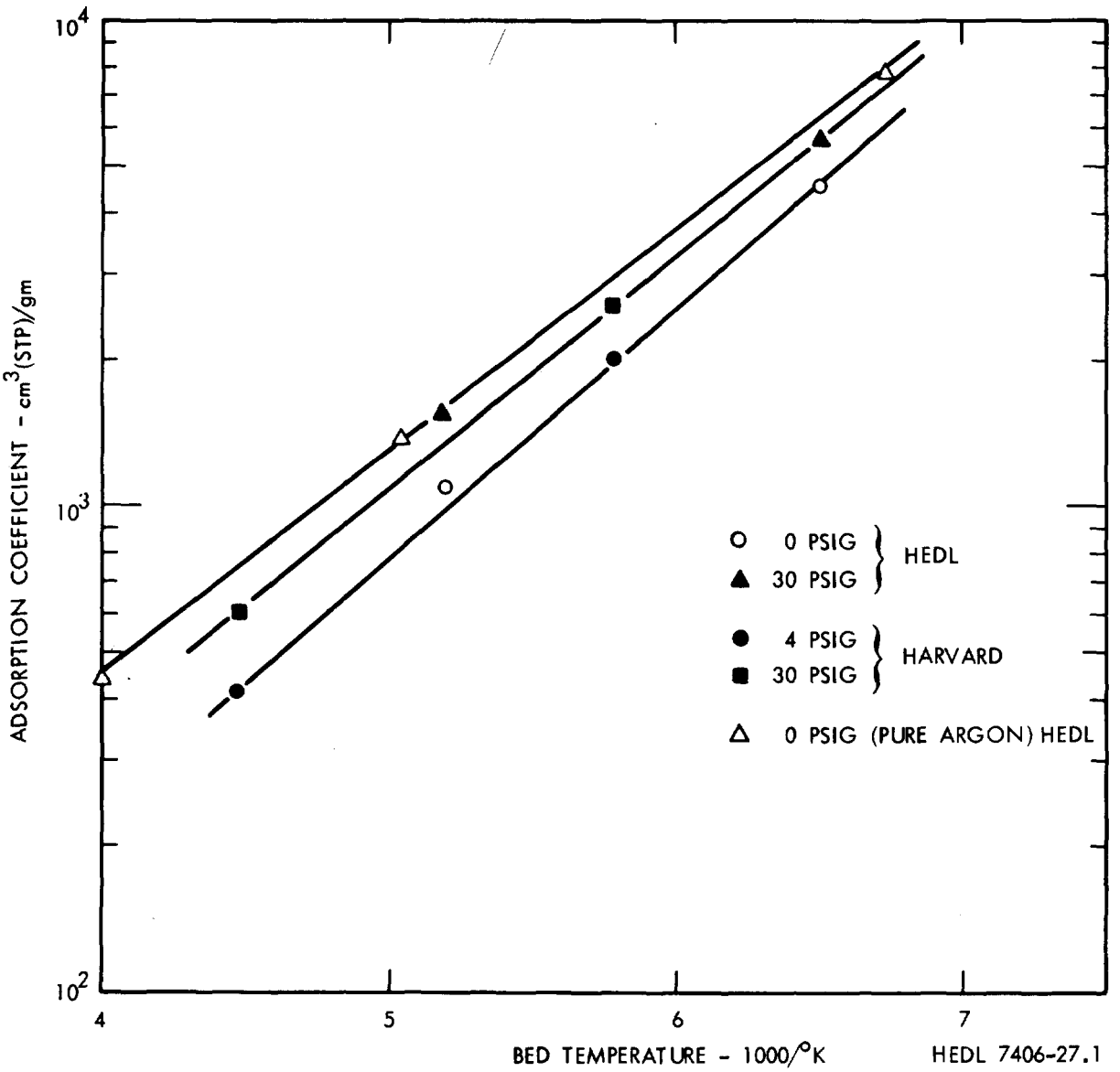

FIGURE 3. ^{85}Kr ADSORPTION COEFFICIENT FROM PURE NITROGEN

in Figure 3 for comparison purposes is the ^{85}Kr adsorption coefficient from argon gas at zero psig. (1)

As temperature decreases, the adsorption coefficient increases; as pressure increases, the adsorption coefficient also increases. This behavior is similar to that observed in this temperature/pressure range for ^{85}Kr adsorption from argon gas. (1)

The absolute magnitude of the coefficients for adsorption from nitrogen appears to be slightly lower than that for adsorption from argon. This difference would impact the planned use of the CAPS as a backup for the RAPS during the time when significant quantities of nitrogen carrier gas were present in the CAPS. However, since the difference in the magnitudes of the coefficients is less than a factor of two, the impact will probably be minimal.

Scale-Up

The excellent agreement of the adsorption coefficients measured in this work with those reported by Harvard(3) suggest that scale-up effects under these conditions are negligible. Most of the Harvard data was obtained with a charcoal bed only a few cubic inches in volume. Thus, this work represents a scale-up over their work of more than a factor of a thousand, without a significant change in the final results. This strongly indicates that scale-up from this work to the plant units can be accomplished without serious design risk. Care must be taken, however, to insure that pertinent design variables such as bed gas velocity, and L/D ratio, which affect flow and mass transfer, are properly scaled. The type and size of charcoal is also important. The charcoal used in these tests is the same type that will be used in FFTF.

IV. Conclusions

The major conclusions to be drawn from this work are:

- The maximum expected levels of gaseous impurities in the FFTF nitrogen atmospheres will not affect the adsorption of ^{85}Kr in the CAPS charcoal beds;
- Scale-up of the results of this work to plant-sized units should pose no serious design risk; and
- The adsorption coefficients for ^{85}Kr are less than a factor of two higher for adsorption from argon than for adsorption from nitrogen.

The tests run with oxygen and carbon dioxide in the nitrogen carrier gas strem produced results identical to those tests conducted using pure nitrogen. At the levels tested, there were no significant differences between ^{85}Kr adsorption coefficients measured in the presence of the impurities and those measured in pure nitrogen.

The excellent agreement of our results for ^{85}Kr adsorption from nitrogen with those of Harvard, despite the more than one thousand fold larger charcoal bed volume used in this work, suggests that using our adsorption coefficients as the basis for the design of the FFTF charcoal beds should present no scale-up problems. The FFTF

units will probably be about one hundred times the volume of the charcoal bed tested here, and thus represent a slightly smaller scale-up factor than already encountered between this work and Harvard's.

It is currently planned to use the CAPS as a back-up to the RAPS. The differences in the magnitude of the ^{85}Kr adsorption coefficients for adsorption from nitrogen and argon are less than a factor of two. With the large capacity built into the CAPS, this should present no serious problems in the event that the CAPS must be used temporarily as a back-up system to the RAPS.

The measurements of the ^{85}Kr adsorption coefficient using a nitrogen carrier gas were the last tests planned under our FFTF Fission Gas Delay Bed Test Program. No further tests are currently scheduled.

V. REFERENCES

1. T. J. Kabele, et al. "FFTF Fission Gas Delay Beds: Engineering Scale Test Report," HEDL-TME 73-26, May 1973, Westinghouse-Hanford Company Report prepared for USAEC-RRD.

2. D. W. Underhill, Nuclear Appl. and Tech., 8, 255-260 (1970).

3. A. S. Goldin and H. A. Trindale. "Adsorption of Fission Noble Gases on Activated Charcoal," Harvard Air Cleaning Laboratory, COO-3019-8. Semi-Annual Progress Report, January 1 - June 30, 1973 (issued December 1973).

Selective Adsorption-Desorption Method for the Enrichment of Krypton

Y. Yuasa, M. Ohta, A. Watanabe, A. Tani,

Nuclear Chemistry Section,

NAIG Nuclear Research Laboratory,

Nippon Atomic Industry Group Co., Ltd.

Kawasaki, Japan

and N. Takashima

Chemical System Engineering Section,

Atomic Power Division,

Tokyo Shibaura Electric Co., Ltd.

Tokyo, Japan

Abstract

Selective adsorption-desorption method has been developed as an effective means of enriching Krypton and Xenon gases. A series of laboratory scale tests were performed to provide some basic data of the method when applied to off gas streams of nuclear power plants. For the first step of the enrichment process of the experiments, Krypton was adsorbed on solid adsorbents from dilute mixtures with air at temperatures ranging from $-50^{\circ}C$ to $-170^{\circ}C$. After the complete breakthrough was obtained, the adsorption bed was evacuated at low temperature by a vacuum pump. By combining these two steps Krypton was highly enriched on the adsorbents, and the enrichment factor for Krypton was calculated as the product of individual enrichment factors of each steps. Two types of adsorbents, coconut charcoal and molecular sieves 5A, were used. Experimental results showed that the present method gave the greater enrichment factor than the conventional method which used selective adsorption step only.

I. Introduction

The adsorption of noble gases on solid adsorbents has been studies in order to investigate the feasibility of using it as a means of enriching radioactive Kr and Xe in off-gas streams of nuclear power plant. Generally, most of studies seemed to focus their attention on either a pressure swing adsorption technique or a thermal swing adsorption technique.

One cycle of the enrichment process of pressure swing adsorption technique is fundamentally composed of four steps; A) pressuizing step, B) Adsorption step under high pressure, C) pressure reducing step, and D) purge step. Krypton (Xenon) is enriched only at step B). The enrichment system using this method has an advantage that adsorption column does not need to be cooled, but has a disadvantage that step B) must be operated under high pressure and the enrichment factor of a single-stage adsorption bed is comparatively low. Kawazoe and Kawai gave data for the enrichment factors of Krypton in the same feed concentration as off gas of fuel reprocessing plant.[1)] They discussed the pressure swing adsorption technique on coconut charcoal adsorbents and showed the enrichment factors of $1.2 \sim 2.5$ for a single-stage operation.

In the case of thermal swing adsorption, one cycle of the enrichment process is fundamentally composed of three steps; A) cooling step, B) adsorption step at low temperature, and C) regeneration step. Krypton (Xenon) is enriched only at step B). This method gives higher enrichment factor than the pressure swing adsorption method without any operations under high pressure but needs the system cooling.

Wirsing, Hatch and Dodge measured the enrichment factors of Krypton on several solid adsorbents by thermal swing adsorption technique, and gave the factors of 20 ~ 128 for coconut charcoal adsorbents.[2)]

For the application of these methods to off gas streams of nuclear power plants, both method would require a multi-stage system. From the standpoint of enrichment factor, thermal swing adsorption method would need a fewer stages than pressure swing method. But on the other hand, the latter might be prefered from the standpoint of operation cost of the system since it has no thermal loss during the operation. We have not done the cost estimation yet and cannot discuss any more in this report about the applicability of both methods to the practical uses. At least, however, efforts to increase the enrichment factor itself in a single stage seems significant for both methods. Since both methods utilize only a selective adsorption, the combination of selective adsorption and selective desorption in a single stage seems to be one of practical answers for this purpose.

The objective of the present study was to develop the enrichment factor of noble gases by combining thermal swing adsorption method with selective desorption step. The process is described with four steps in order ; A) cooling, B) selective adsorption at low temperature, C) selective desorption under low pressure and low temperature, and D) regeneration of adsorbents by heating. Noble gases are enriched by successive steps B) and C). Enrichment factor obtained at step B) is the same as obtained by thermal swing adsortion method, and so the total enrichment factor is expected to increase by a factor obtained at step C).

A series of laboratory scale tests for Krypton were conducted to confirm that the enrichment factor of Krypton at step C) is greater than unity and at the same time the desorption rate of Krypton is acceptably small, and also to prove the applicability of the method to off gas clean up systems of BWR plant. Experimental procedures of the present study are shown in detail. Overall characteristics of the method are also discussed.

II. Selective adsorption-desorption method

A single stage operation of the enrichment process of this method is performed with two adsorption beds or preferably with three beds. As a basic concept for the enrichment process of a two beds-system is the same as that of a three beds-system, the process will be explained more easily with a two beds-system. A cyclic process of the system is shown schematically in Fig. 1. One cycle of the enrichment process is fundamentally composed of four steps as mentioned previously and that is shown in the figure.

One of two beds, the first bed, which has been filled with cleaned air, is first cooled to the desired temperature, which step is named as cooling step. Then the feed is passed through the bed untill the breakthrough for Krypton is detected. Krypton is enriched on adsorbents by the effect of the difference of the adsorption potential between Krypton and carrier gas, and this step is named as selective adsorption step. As soon as the Krypton in the effluent flow from the first bed becomes detectable, the feed flow is switched to another bed, the second adsorption bed, and the first bed is conducted to the next step. Of course, the second bed has to have been cooled by this time. At the next step, selective desorption step, the bed being kept at low temperature is evacuated to a desired pressure with a vacuum pump. Since Krypton is not desorbed so easily as carrier gas, as a result of the differences of the physical properties such as mass transfer resistance and adsorption potential between them, the ratio of the Krypton content to the carrier gas becomes greater in the bed. Although a little amount of Krypton is carried away with the exhaust

gas from the vacuum pump, Krypton release out of the system is prevented by returning the exhaust gas into the feed. For the last step, regeneration step, the bed is regenerated by heating. Several procedures could be used for regeneration, but with any procedures the trapped gas in the bed is desorbed anyhow and transfered either to a storage tank or to a secondary enrichment system. The regenerated bed is filled with cleaned effluent gas from the second bed and cooled to the desired temperature again. The cooled bed is kept waiting for the next cycle. So, while one bed is operated under adsorption step, another is operated under desorption, regeneration or cooling step.

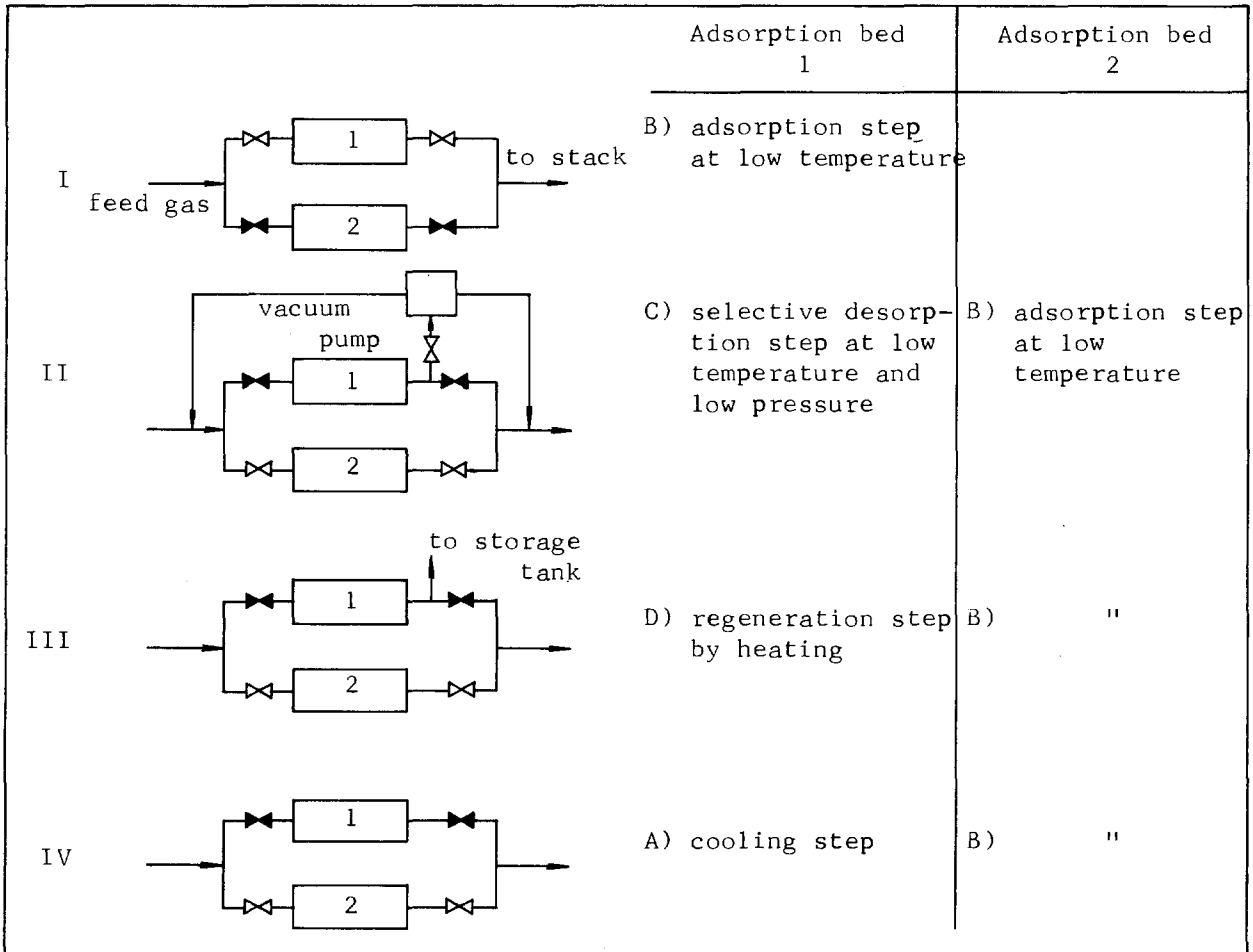

FIG I Selective adsorption - desorption cycle system.

It would be suggested that the three bed system is better than the two bed system to utilize the bed effectively at the adsorption step.[2] In this system, two beds are in the process of adsorption while the third one is to be under the successive either step of desorption, regeneration or cooling. When the upstream bed of the two has attained to a breaktrough level, the bed is conducted to the desorption step and the downstream bed of the two and the third one are placed under the adsorption step. In the two bed system, the breakthrough level must be selected as low as possible to decrease the release amount of Krypton carried away with the effluent stream. In comparison with this, the three bed system has an advantage that the breakthrough level of the upstream bed could be selected to be nearly complete breakthrough without noticeable Krypton release out of the system, since the downstream bed acts as the back-up adsorber.

It would be needed to explain the overall enrichment factor of Krypton which is devided to individual factors determined at each step.

We have defined the enrichment factor of Krypton as the ratio of Krypton content in the bed to in the feed. From this definition, total enrichment factor is described as follows,

$$\Psi = \frac{\text{Krypton/carrier gas (in the bed after the desorption step)}}{\text{Krypton/carrier gas (in the feed)}} \quad (1)$$

The enrichment factor at the adsorption step, Ψ_1, is the same value as given by the thermal swing adsorption method, and is presented as follows,

$$\Psi_1 = \frac{\text{Krypton/carrier gas (in the bed after the adsorption step)}}{\text{Krypton/carrier gas (in the feed)}} \quad (2)$$

The ratio of Krypton content to carrier gas in the bed increases with evacuating process at the desorption step, and so total enrichment

factor can be described as follows,

$$\Psi = \Psi_1 \cdot \Psi_3 \tag{3}$$

where

$$\Psi_3 = \frac{\text{Krypton/carrier gas (in the bed after the desorption step)}}{\text{Krypton/carrier gas (in the bed before the desorption step)}}$$

$$= \frac{\text{Krypton (in the bed after the desorption step)}}{\text{Krypton (in the bed before the desorption step)}} \cdot \frac{\text{carrier gas}}{\text{carrier gas}}$$

$$\frac{\text{(in the bed before the desorption step)}}{\text{(in the bed after the desorption step)}} \tag{4}$$

Let the first term in the equation (4) be replaced by η and the second term by Ψ_2, then

$$\Psi_3 = \Psi_2 \cdot \eta \tag{5}$$

From the equations (3) and (5), total enrichment factor is presented as follows,

$$\Psi = \Psi_1 \cdot \Psi_2 \cdot \eta \tag{6}$$

Ψ_2 represents the ratio of the amount of carrier gas in the bed before to after the desorption process, and therefore Ψ_2 is expressed as a function of pumping speed, as shown below,

$$\Psi_2 \cong \frac{Q_0}{Q_0 - \Phi} = \frac{1}{1 - \phi} \tag{7}$$

and $$\Phi \cong 5.34 \times 10^{-5} S \int_0^{\tau} p \, dt \tag{8}$$

where

Q_0 = the amount of carrier gas adsorbed at equilibrium, (mol)

Φ = the amount of carrier gas exhausted until time τ, (mol)

S = pumping speed at the temperature of $30^{\circ}C$, (l/min.)

P = pressure in the bed at time t, (Torr)

τ = evacuuating time at the step C). (min.)

η represents the ratio of Krypton content in the bed after to before the desorption process, and therefore η is expressed as a function of the desorption rate of Krypton, ξ , in the process, as shown below,

$$\eta = 1 - \xi \ . \tag{9}$$

III. Experimental

Apparatus and Method. A series of laboratory scale experiments were performed to provide some basic data for using the present enrichment method. The apparatus used is shown schematically in Fig. 2.

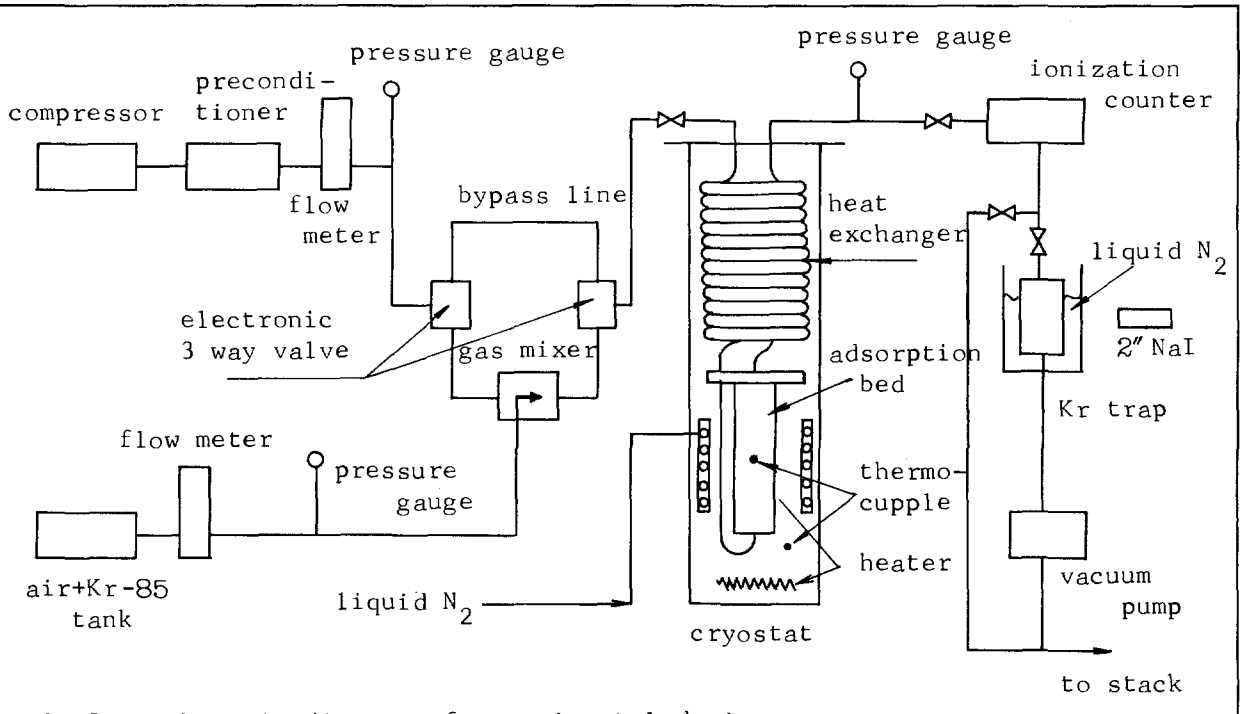

FIG II Schematic diagram of experimental device.

Adsorption experiment and desorption experiment were conducted departely in order to evaluate the individual enrichment factors and parameters which affect those factors.

The adsorption experiments were carried out by passing the feed through the adsorption bed, while the effluent was monitored with an ionization counter to measure the amount of Krypton breaking through with tagged ^{85}Kr. Following the adsorption experiments, the selective desorption experiments were conducted by evacuating the bed through a

Kr trap which was located in exhaust line and where ^{85}Kr was monitored with a scintillation counter to measure the amount of desorbed Kryton. An adsorption column which held the bed was placed in a cryostat, which was controlled over a range of temperature from -50°C to -170°C within ±1°C for the adsorption experiment and within ±5°C for the desorption experiment. The adsorption column was a cylinder with a diameter of 5 cm filled with adsorbents, of which some physical properties were shown in Table 1. The Kr trap was a glass cylinder which was about 3 cm in an effective length of 15 cm, filled with activated charcoal and immersed in liquid nitrogen.

Experimental Condition. Some of the experimental conditins are summarized as follows, and details are presented in Tables2 and 3.

Adsorbents: coconut base charcoal and molecular sieves-5A ,

Carrier gas: air,

Feed concentration: 1~5 ppm Kr, by volume, tagged with ^{85}Kr,

Temperature: -50°C to -170°C,

Pressure at the adsorption step: 0 kg/cm^2-G,

Bed size: 5 cm in diameter and 6 to 20 cm in length,

Air flow rate at the adsorption step: 1 cm/sec in superficial velocity,

Pumping speed at the desorption step: 5.7 l/min. to 22 l/min.

at the standard temperature of 30°C,

Ultimate pressure at the desorption step: nearly 10 Torr in most cases.

Enrichment Factors. In order to determine the enrichment factors under the specified conditions, it is needed to estimate the amount of carrier gas adsorbed as well as Krypton in the bed. For this purpose dry air was introduced into the bed, which had been evacuated to 10^{-2} Torr under the desired temperature, until the pressure arrived at

1 atmosphere in the bed. The net amount of adsorbed air was calculated from the amount introduced into the bed by subtracting a dead volume in the adsorption column and the associated tubing. The amount of Krypton adsorbed and the enrichment factor, Ψ_1 , were estimated by the equations (10) and (11) shown below, using the breakthrough curve obtained in the experiment.

$$Q_{Kr} \cong 0.045 f \cdot \tau (1 - \alpha) C_{Kr} \quad (10)$$

$$\Psi_1 \cong \frac{Q_{Kr} / Q_{air}}{C_{Kr}} \quad (11)$$

where

Q_{kr} = the amount of Kr adsorbed at breakthrough time τ , (mol)

Q_{air} = the amount of dry air adsorbed at equilibrium, (mol)

C_{kr} = Kr concentration in the feed, (mol /mol)

f = flow rate of the feed, (STP l/min.)

τ = breakthrough time, (min.)

α = integrated value of the breakthrough curve during the time, zero to τ .

In order to determine Ψ_2 and η , the pressure in the adsorption bed and the counting rate of ^{85}Kr collected in the Kr trap were recorded during the selective desorption experiment. After the bed was evacuated to a desired pressure, it was heated to 50°C and the amount of remained air in the bed was determined from the pressure and the volume of the column by correcting the air amounts on adsorbents at the temperature of 50°C. Then, the column was evacuated to 10^{-2} Torr through the Kr trap and the counting rate was recorded at the Kr

trap. Ψ_2 and η were estimated by the equations (12), (13), and (14) shown below,

$$\eta \cong 1 - A(t)/B \tag{12}$$

$$\Psi_2 \cong Q_{air}/Q'_{air} \tag{13}$$

$$Q'_{air} \cong 3.77 \times 10^{-5} V_d \cdot P + Q''_{air} \tag{14}$$

where

A(t) = the counting rate at the Kr trap, after the evacuation process to desired pressure, but before the bed heating to $50^{\circ}C$,

B = the counting rate at the Kr trap, after the bed was heated to $50^{\circ}C$ and evacuated to 10^{-2} Torr,

t = the evacuating time to desired pressure,

Q'_{air} = the amount of remained air in the bed after the selective desorption process, (mol),

Q''_{air} = the amount of air adsorbed at the temperature of $50^{\circ}C$ and the pressure of P, (mol),

Vd = the dead volume of the column, (cc),

P = the pressure in the column when the selective desorption process was completed and the column was heated to $50^{\circ}C$, (atm).

Φ in the equation (8) was estimated from the recorded pressure in selective desorption experiment. By substituting Φ into the equation (7), the dependency of Ψ_2 on the evacuating time was evaluated.

IV. Results and Discussion

The enrichment factor, Ψ_1, can be affected by parameters such as adsorbents, bed shape, temperature, gas flow rate and the breakthrough level.[2] In the present study, the effects of adsorbents and temperature were investigated while other parameters were held constant. The results are presented in Table 2 with the experimental conditions. The effect of temperature on Ψ_1 for coconut charcoal adsorbent is shown in Fig. 3 together with Ψ_2 and Ψ which will be explained later. Fig. 4 shows the same effect for molecular sieves-5A adsorbent. As is clear from Fig. 3 and 4, the higher Ψ_1 is obtain at the lower temperature for both adsorbents and coconut charcoal gives the higher Ψ_1 than molecular sieves-5A.

The factors Ψ_2 and η which have been defined in the equation (5) for the desorption process are affected by such parameters as pumping speed, evacuating time, ultimate pressure, temperature, bed shape and adsorbents. The experimental results for Ψ_2 and η obtained on the same conditions are presented in Table 3. Fig. 3 and 4 show the temperature effects on Ψ_2 and Fig. 5 shows the same effect on η .

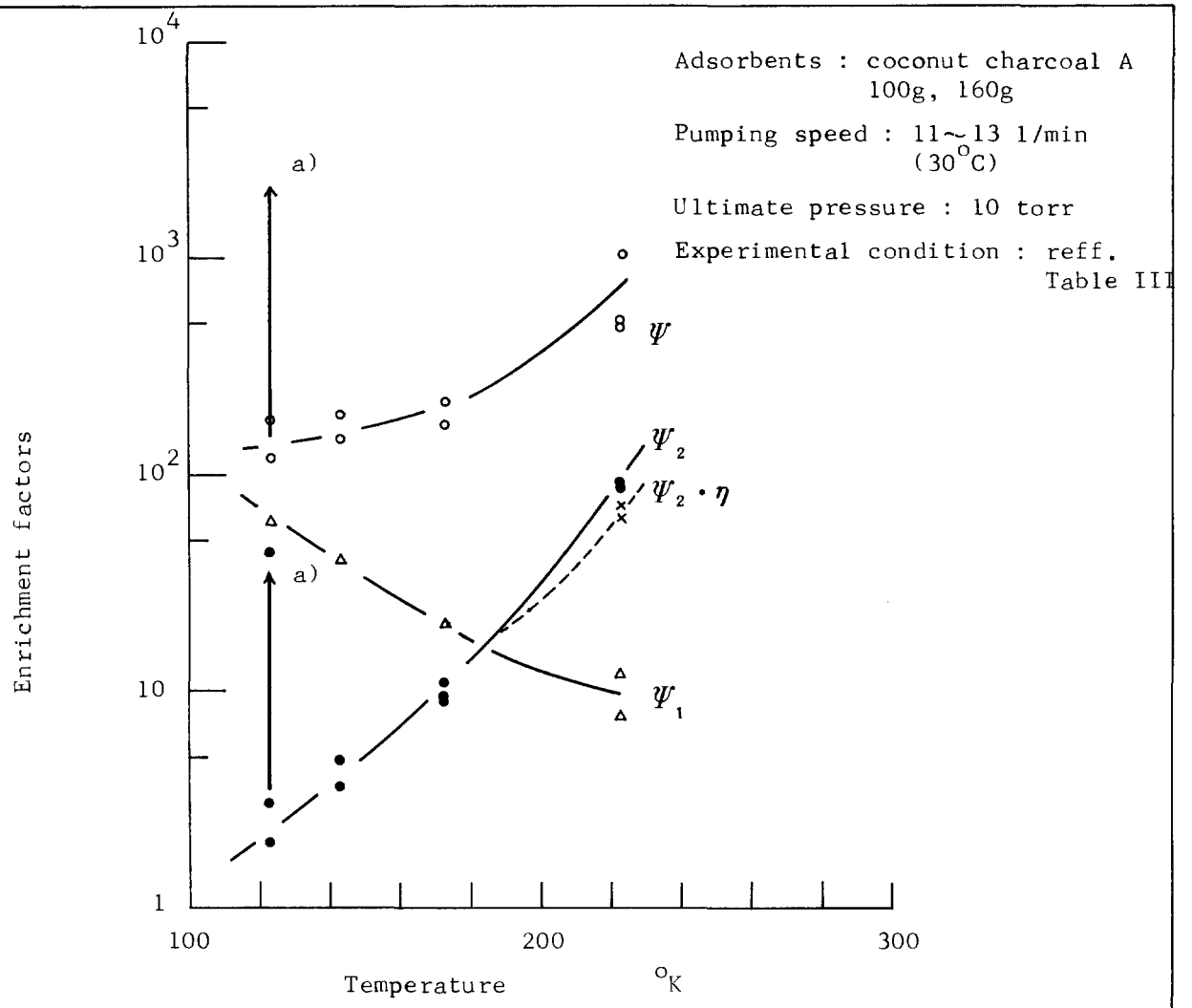

FIG III Enrichment factors versus temperature.

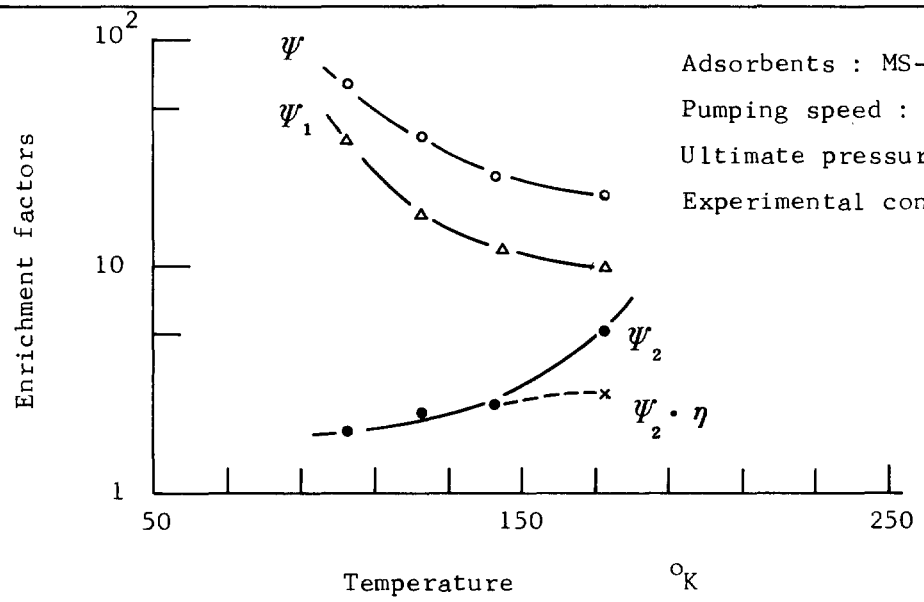

FIG IV Enrichment factors versus temperature.

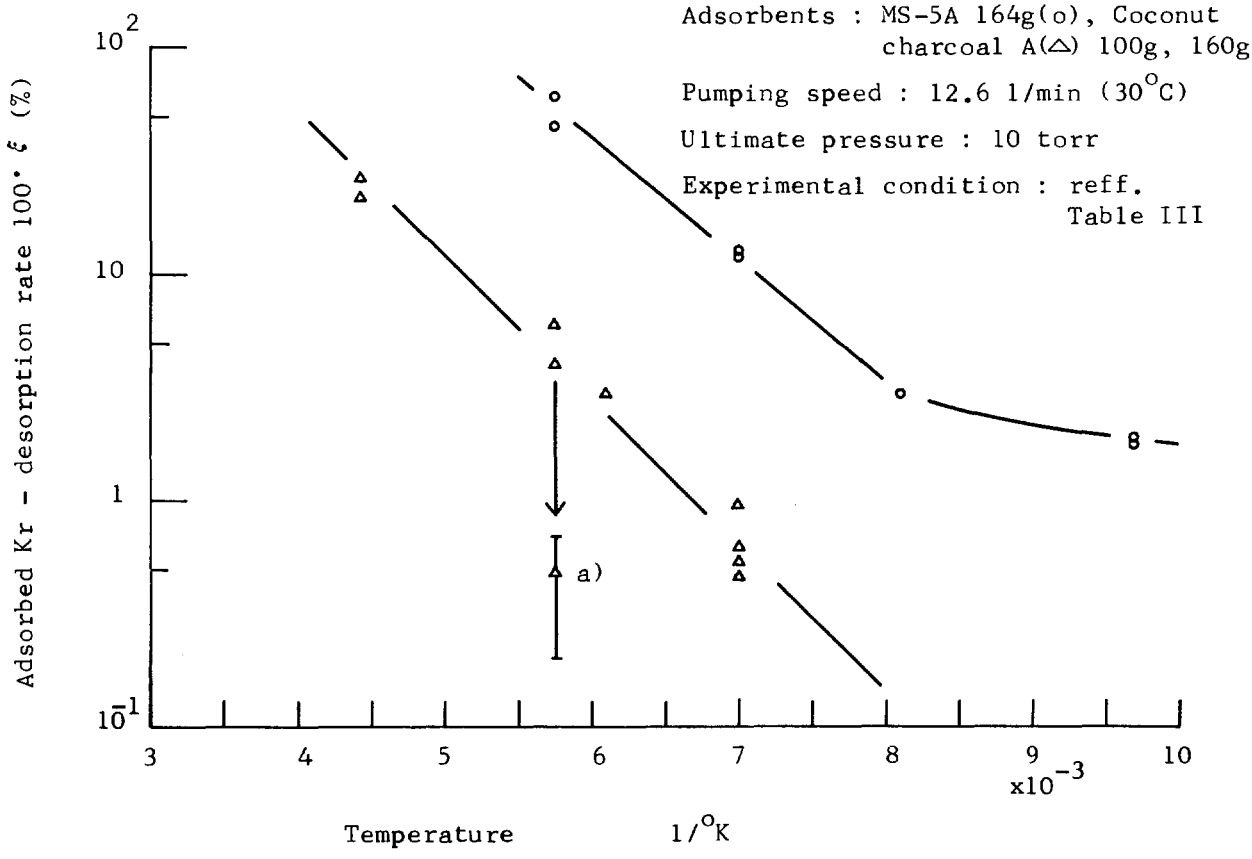

FIG V Adsorbed Kr - desorption rate versus temperature.

The total enrichment factor, Ψ , which was calculated from Ψ_1 , Ψ_2 , and η is shown also in Fig. 3 and 4. In these Figures it is clearly seen that the total enrichment factor, Ψ , has higher values than the enrichment factor, Ψ_1 , obtained from only the adsorption process. The evacuating time at the selective desorption process is so short in comparison with the period to breakthrough as seen in Tables 2 and 3 that the complete process of the enrichment cycle can be composed easily. It is also clear from the labelled points with a mark a) in Fig. 3 and 5 that Ψ is increased strongly without noticeable increase of Krypton desorption rate by evacuating the bed with increasing temperature, especially with coconut charcoal. Consequently the present method could offer an effective off gas clean-up system in place of the previous adsorption methods.

Fig. 6, 7 and 8 show the results of the selective desorption experiments which were performed to evaluate the effect of various parameters on the factors, ϕ $(= 1 - \frac{1}{\Psi_2})$ and ξ $(= 1 - \eta)$, described in equations(7) and (9). Fig. 6 shows the relation between the evacuating time and the factors, ϕ and ξ , on such a condition that the adsorption bed is evacuated at a fixed temperature. These factors approach to unity with increase of the evacuating time and the approaching rate becomes more rapid with the higher temperature of the bed as seen in the figures. The values of these factors are different from the values of the factors obtained on such a condition that the bed is evacuated with raising temperature.

	$\phi\ (=1-\frac{1}{\psi_2})$	$\xi\ (=1-\eta)$
fixed temperature of $-100^{\circ}C$	0.98 ~ 0.99	0.08 ~ 0.1
$-150^{\circ}C$	0.69	0.002
raising temperature		
from $-150^{\circ}C$ to $-100^{\circ}C$	0.98	0.002

where the pumping speed was 12.5 l/min. at $30^{\circ}C$, the evacuating time took about 70 min. and 160 grams of coconut charcoal was used as absorbents.

In the case of raising temperature, the factors, ϕ and ξ, are affected by the heating time as shown below,

heating time from $-150^{\circ}C$ to $-100^{\circ}C$	ϕ	ξ
20 min.	0.86	0.002
71 min.	0.98	0.007

where the pumping speed was 12.5 l/min. at $30^{\circ}C$ and 160 grams of coconut charcoal was used as adsorbents.

Fig. 7 and 8 show the effect of the pumping speed and of the adsorbent amount respectively on factors, ϕ and ξ, on the condition that the column is evacuated at fixed temperatures with fixed evacuating time of 5 minutes.

Adsorbents : Coconut charcoal A 160g

Pumping speed : 12.5～13.0 l/min (30°C)

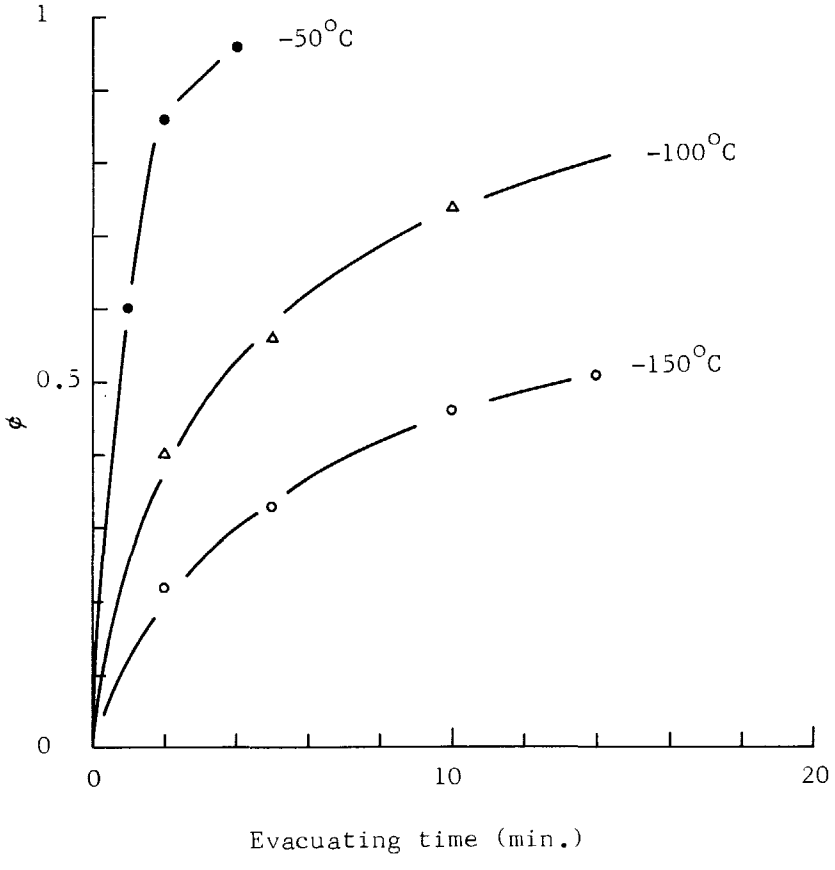

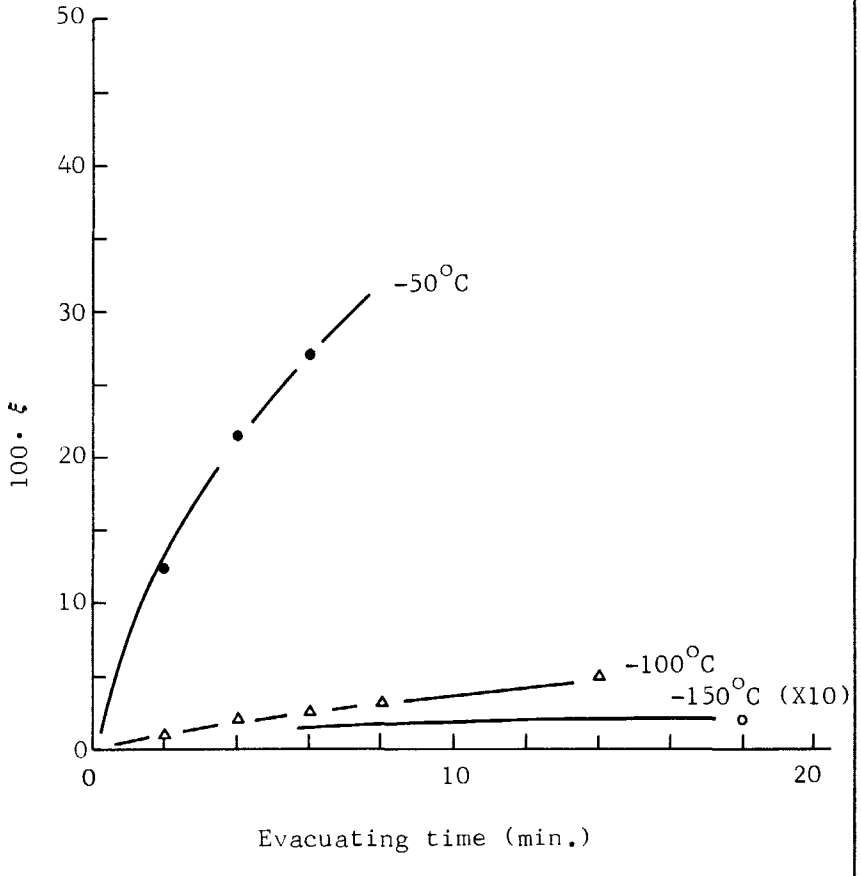

FIG VI Dependency of factors ϕ & ξ on evacuating time.

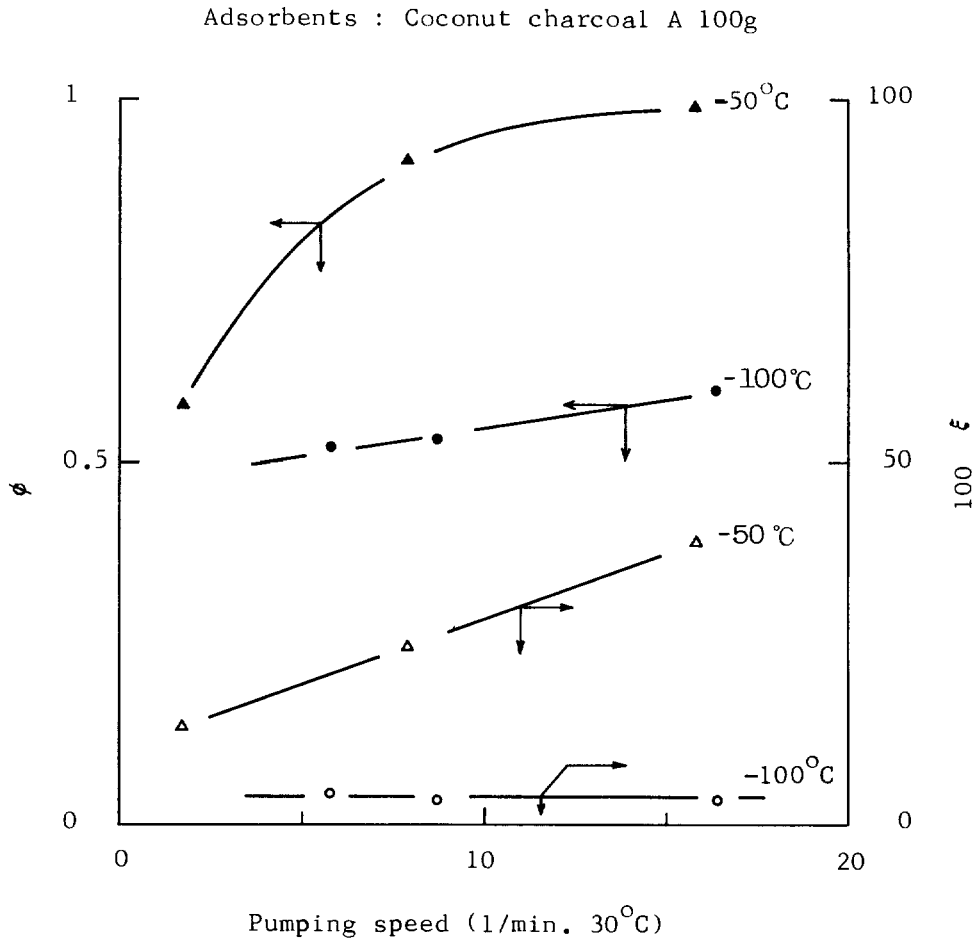

FIG VII Effect of pumping speed on ϕ & ξ

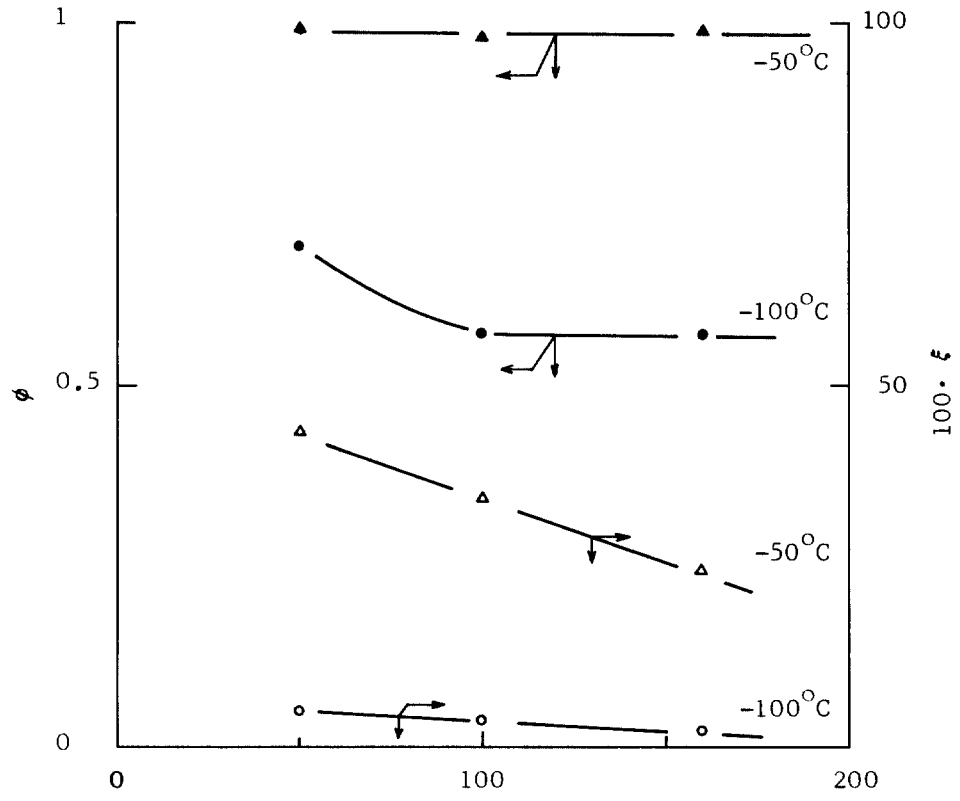

FIG VIII ϕ & ξ versus amount of adsorbents.

V. Conclusion

It was concluded that the present method gave greater enrichment factor for Krypton in dry air stream than conventional adsorption methods without any increase of Krypton release out of system. Consequently, the present method could be applied to off gas treatment system in nuclear power plant as an effective system. Coconut charcoal adsorbent was prefered for the present method to molecular sieves-5A adsorbent. Further investigation, however, is necessary to find more suitable adsorbents for the present method.

VI. Reference

1) K. Kawazoe and T. Kawai, "Concentration of Dilute Gases by Pressure-Swing Adsorption, Kagaku Kogaku, 37, 288-294, (1973)

2) E. Wirsing, Jr., L. P. Hatch, and B. F. Dodge, "Low-Temperature Adsorption of Krypton on Solid Adsorbents, BNL 50254 (T-586), (1970)

Table I Properties of adsorbents.

Adsorbents	Coconut charcoal A	Malecular sieves types 5A
Shape and Particle size	pellet 4.1 (±0.3) mm ϕ x 4 (±1) mm length	pellet 1/16" ϕ x 1/8" length
Packing density	0.42 g/cc	0.72 g/cc
Void fraction	0.38	0.32
Apparent density	0.68 g/cc	1.1 g/cc
Surface areas	1000 m^2/g	700 m^2/g

Table II Tabulation of adsorption experiments.

Adsorbents	Charcoal A	Charcoal A	Charcoal A
Packing weight (g)	160	160	160
Temperature (^{o}C)	-50	-100	-130
Superficial velocity (cm/sec)	1	1	1
Kr adsorbed at 100% breakthrough (STP cc/g)*	3.3×10^{-4}	2.4×10^{-3}	7×10^{-3}
100% breakthrough time (min)	58	330	790
Enrichment factor Ψ_1 at 100% breakthrough	7.4	21	40

Table II (continued)

Charcoal A	Charcoal A	Charcoal A	Charcoal A	Charcoal A	Charcoal A
160	100	100	100	50	50
-150	-50	-100	-150	-100	-150
1	1	1	1	1	1
1.5×10^{-2}	5.3×10^{-4}	2.2×10^{-3}	1.6×10^{-2}	2.4×10^{-3}	1.4×10^{-2}
1460	62	192	956	104	432
61	12	20	67	21	59

Table II (continued)

mol. sieves 5A	mol. sieves 5A	mol. sieves 5A	mol. sieves 5A
160	160	160	160
-100	-130	-150	-170
1	1	1	1
7.2×10^{-4}	1.2×10^{-3}	2.0×10^{-3}	4.2×10^{-3}
12.7	169	246	440
10	12	17	35

* Kr concentration in the feed is 1 ppm by volume.

Table III Tabulation of desorption experiments.

Adsorbent	Charcoal A	Charcoal A	Charcoal A
Packing weight (g)	160	160	160
Temperature (^{o}C) etc.	-50	-100	-130
Pumping speed at 30^{o}C, (l/min)	13.4	12.8	11.1
Pumping time,(min)	6	21	38
Ultimate pressure (Torr)	10	10	10
Ψ_2	84	11	4.8
η	0.73	0.94	0.991
Ψ	450	220	190
Reff. figure	FIG III, V	FIG III, V	FIG III, V

Table III (continued)

Charcoal A	Charcoal A			Charcoal A	Charcoal A	Charcoal A
160	160			100	100	100
-150	heating from -150 to -100			-50	-100	-150
12.5	11.8	11.5	12.5	12.7	16.4	11.0
45	20	65	71	4.0	14	35
10	10	10	10	10	10	10
2	7.0	43	45	90	8.7	3
0.999	0.998	0.995	0.993	0.785	0.96	0.999
120	430	2600	2700	520	170	180
FIG III, V	FIG III, V ; a)			FIG III, V	FIG III, V	FIG III, V

Table III (continued)

Charcoal A	mol. sieves 5A	mol. sieves 5A	mol. sieves 5A	mol. sieves 5A
100	160	160	160	160
heating from -150 to -100	-100	-130	-150	-170
11.2	11.2	12.0	12.5	12.5
45	15	15	15	15
10	10	10	10	10
43	5.2	2.4	2.3	1.9
0.995	0.40	0.87	0.970	0.982
2600	21	25	38	65
FIG III, V ; a)	FIG IV, V	FIG IV, V	FIG IV, V	FIG IV, V

PRESSURE-SWING SORPTION CONCENTRATION OF KRYPTON-85 FOR PERMANENT STORAGE

Joseph W. Ayers, Abraham S. Goldin, and Dwight W. Underhill
Harvard School of Public Health
665 Huntington Avenue
Boston, Massachusetts 02115

Abstract

The concentration of krypton-85 from the off-gas of a nuclear fuel reprocessing plant by pressure-swing adsorption-desorption is under investigation at the Harvard School of Public Health. System specifications include a decontamination factor of 10^4 for discharged gas and a concentration factor of 10^3 for the stored gas.

The basic system element is a bed moving countercurrent to the gas flow. In the high pressure leg, krypton is adsorbed by the activated carbon, providing a cleaned gas output. The carbon then passes through a depressurization zone into the low-pressure leg, purged of remaining krypton by a countercurrnet flow of clean gas, and then repressurized and reintroduced into the high pressure leg, The depressurization and purge streams constitute the krypton concentrate. The output of the high pressure leg, minus the purge and repressurization gas, represents the clean gas throughput. Overall concentration requirements are met by reflux and/or cascade of these elements.

Calculations of the quantity of charcoal and power required are presented for three different adsorbent flow rates, with given plant performance specifications. These calculations illustrate the effect of flow rate on the trade-off of size vs. power.

Introduction

Selective adsorption of krypton on activated carbon beds has often been recommended as a possible means of removal of fission gases from nuclear industry off-gas streams. This study examines through engineering calculations a process for removing and concentrating krypton-85 from nuclear fuel reprocessing by pressure-swing adsorption cycling(1) with moving activated carbon beds at room temperature. The calculations give information on the amount of active carbon required and on the power consumption, which are indicative respectively of capital and fixed costs. Use of moving beds allows the total volume of active carbon required for such a system to be very greatly reduced with respect to a system of similar separating power with fixed beds. This advantage of a moving bed system allows a room temperature system to be considered in competition with other presently proposed fission gas removal systems(2,3).

Similar moving bed active carbon adsorption systems, not involving pressure swings, have been described by Berg(4), and subjected to

both analytic and numerical analysis[5,6]. The generic system similarities shared by the system element described below and liquid extraction systems[3,7] are noteworthy.

I. System Element

Figure 1 shows schematically the basic system elements of a krypton removal plant based on the proposed process. It consists of four parts - a high-pressure air-cleaning bed, a low-pressure purging bed, a pressurizing zone, and a depressurizing zone. The high pressure gas stream enters the adsorbent bed, which is moving countercurrent to the gas flow with a velocity such that the krypton front remains stationary. A volume of adsorbent free of krypton entering the upper column at point B moves continuously towards point A in rodlike flow encountering and dynamically equilibrating with gas containing progressively more krypton until it reaches point A, where it is in dynamic equilibrium with the element feed gas. The krypton-loaded adsorbent then exits at point A and is depressurized, releasing air and some krypton. The volume of adsorbent then enters the low pressure bed at point C, and moves at the same rate towards point D. A portion of the cleaned air output of the high pressure bed flows from D towards C, purging the low pressure bed so that the volume of active carbon reaching point D is free of krypton. At point D, the regenerated volume of charcoal is repressurized and reintroduced to the high pressure bed at point B.

The net effluent from the high pressure bed, i.e. the total air output less that air used to pressurize the active carbon entering at point B and that air used to purge the low pressure bed represents the system clean air throughput. The quantity of krypton which entered the high pressure bed in the high pressure stream will now be confined to the stream removed from the process as a result of the depressurization of adsorbent at the input end of the high pressure bed plus the air stream used for stripping of the low pressure bed.

This basic system element may be used with reflux and/or in cascade to attain greater concentrations than are possible with a single pass process.

System Element Characteristics

Characterization of the elements of Figure 1 is required to facilitate conceptual plant design. Some design parameters are determined by the adsorbent material and others by the choice of operating parameters.

Adsorbent Determined Properties

System characteristics determined by adsorbent properties, and hence only partially within engineering control, are:

1) Ratio of mobilities of krypton and air as a function of pressure.

2) Effect of pressure on carrier gas capacity.

3) The intraparticle mass transfer resistance as a function of

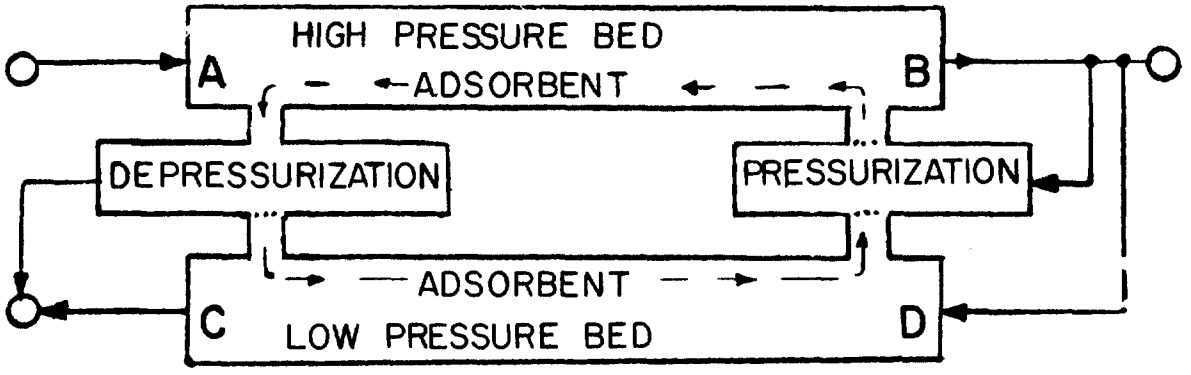

FIGURE 1 SYSTEM ELEMENTS

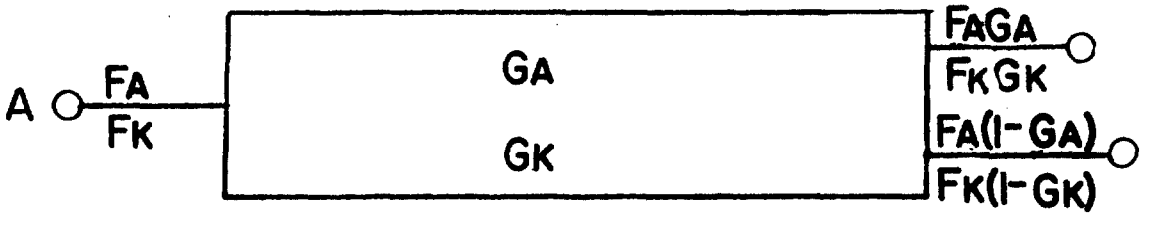

FIGURE 2 SYSTEM ELEMENTS CHARACTERIZED BY PARTITION FRACTIONS

pressure.

4) The effect of pressure on krypton: air desorption and adsorption.

Design Determined Properties

In the following calculations, the "allowed" parameters are those that can be incorporated in a practical plant design. Additional simplifying assumptions used in these calculations are:

1) The process is isothermal.

2) Air is treated as a single component.

3) The krypton adsorption isotherm is linear.

4) HETP at rapid flow rates is limiting by intraparticle mass transfer resistance.

For overall system calculations, the system element of Figure 1 may be considered as a three port "black box", the characteristics of which are primarily dependent on:

1) Upper and lower pressure limits.

2) Material parameters of the adsorbent.

3) The relative flow rates of gas and adsorbent.

Figure 2 shows the system element as a three port component characterized by two partition fractions, G_A and G_K, which specify respectively the routing of the air flow F_A and the krypton flow F_K from the input port A to the output port B. Overall material balance is required, thus specifying the flows to the output port C. The material flow relations are included in Figure 2. The mixture is assumed to be very dilute so that subsequently, the absolute flow volume is treated as being due entirely to air flow.

There is no "best" system independent of economic considerations. Separation may be maintained constant with smaller masses of activated carbon by increasing the adsorbent flow rate. However, with larger adsorbent flows, more of the cleaned air must be used for repressurization and purging with a resultant decrease in concentration factor. Accordingly, there are infinite families of system solutions, giving the same decontamination and concentration. Systems which require small volumes of activated carbon have a higher power consumption.

Material

Pittsburgh Type PCB activated carbon is the adsorbent material

chosen for conceptual plant design. The physical properties of this carbon are given in Table I.

Table I

PHYSICAL PROPERTIES OF PCB ACTIVATED CARBON[8]

Total Surface Area (N_2, BET Method), m^2/g	1150-1250
Apparent Density (Bulk Density, dense packing), g/cc	0.44
Particle Density (Hg Displacement), g/cc	0.850
Real Density (He Displacement), g/cc	2.2
Pore Volume (Within Particle), cc/g	0.72
Voids in Dense Packed Column, %	50.0
Specific Heat at 100°C	0.25

Figures 3,4, and 5 present respectively for this charcoal at room temperature

1) Effect of pressure on ratio of krypton mobility to air mobility.
2) Effect of pressure on air adsorption.
3) HETP (Height Equivalent of a Theoretical Plate) as a function of flow for two particle diameters at 20 atmospheres and 1.0 atmosphere absolute pressure.

These data have been determined experimentally in this laboratory. A report of the experimental procedure is in preparation.

II. Conceptual Plant

The system chosen for evaluation consists of two elements with extensive reflux. Upper and lower pressure limits chosen for the system are 20 atmospheres and one atmosphere. At 20 atmospheres and room temperature, the bed is close to its maximum krypton capacity for a dilute krypton-air mixture ($\sim$ 160STP cc/cc charcoal). Specification of one atmosphere as the lower pressure limit is based largely on the convenience of using the atmosphere as a reference pressure source for bed depressurization. An improved limiting performance would be expected at very low pressures, but lack of knowledge of behavior at these pressures precludes their use in these calculations. Practically, the need for high capacity vacuum pumps in addition to mechanical compressors, argues against this choice. The system flow diagram is shown in Figure 6. The two system elements are here characterized as three port active devices each with two partition fractions which specify the routing of air and krypton respectively from the input ports to the two output ports. The overall plant material partition fractions $G_{A,p}$ and $G_{K,p}$ are fixed at 0.999 and 10^{-4}, respectively.

Calculation Procedure

The series of calculations required is quite involved and periodically requires engineering judgment to select indeterminant

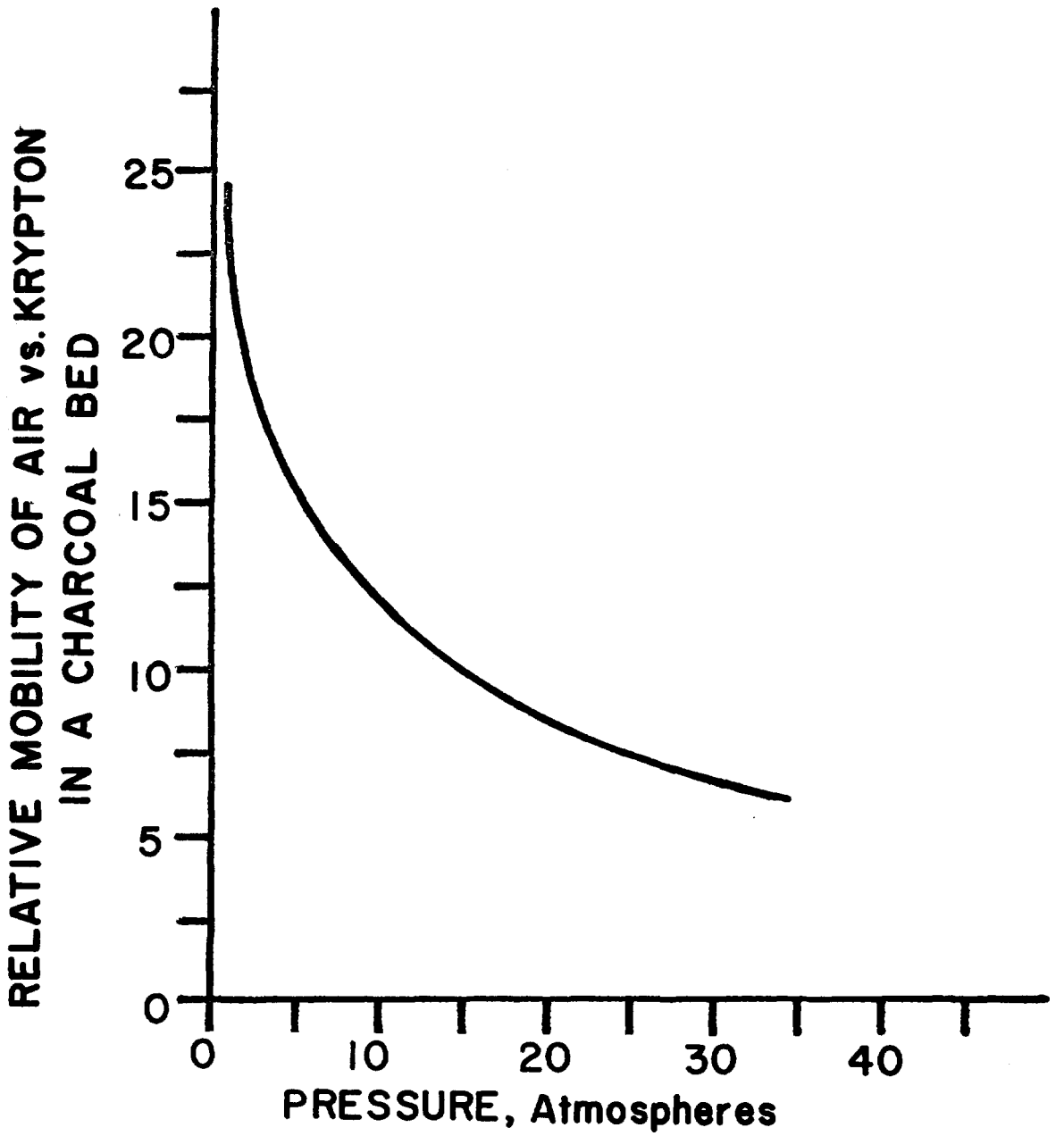

FIGURE 3 EFFECT OF PRESSURE ON THE RATIO OF THE MOBILITIES FOR AIR AND KRYPTON IN A CHARCOAL BED.

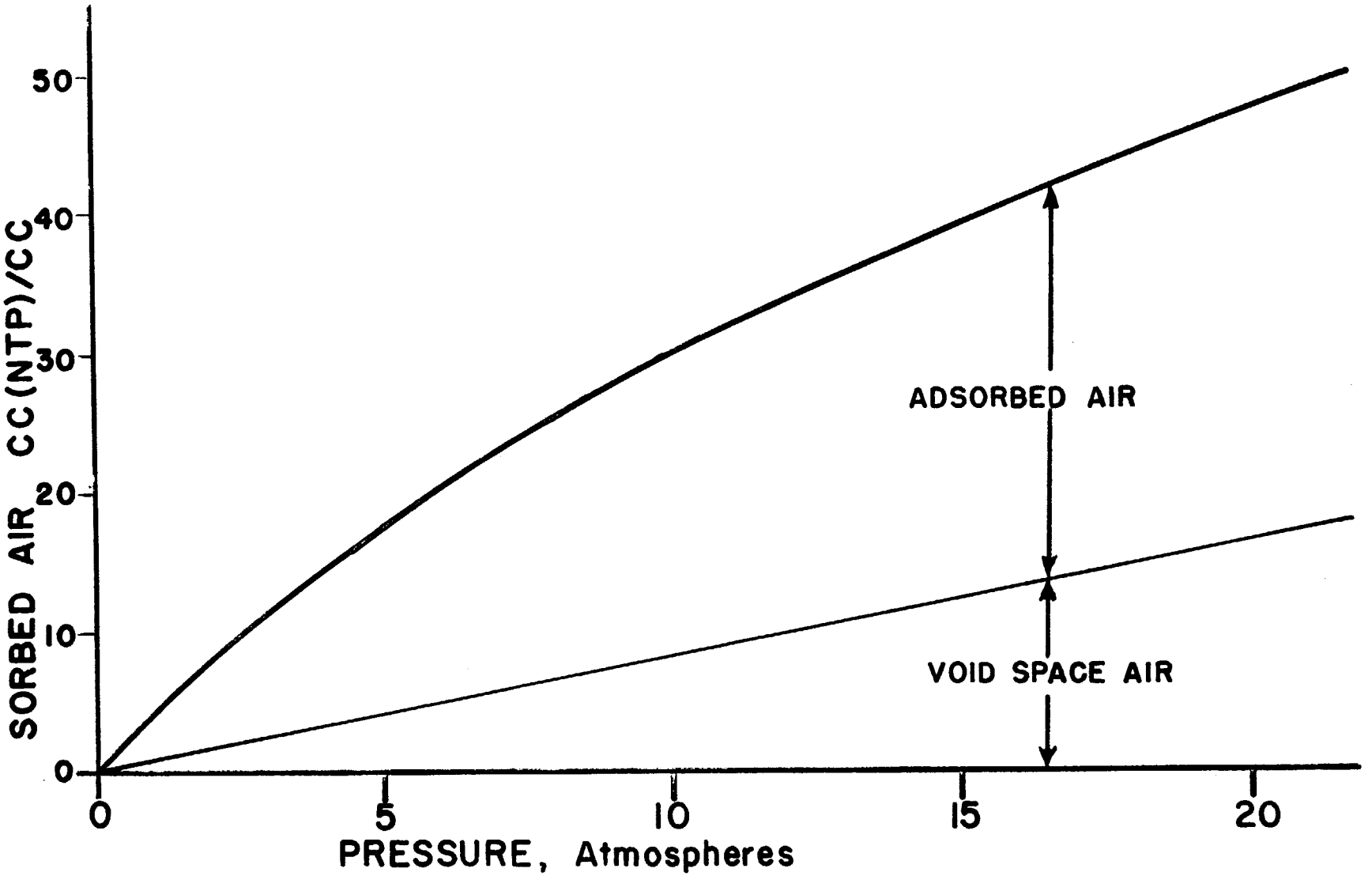

FIGURE 4 EFFECT OF PRESSURE ON AIR BY CHARCOAL

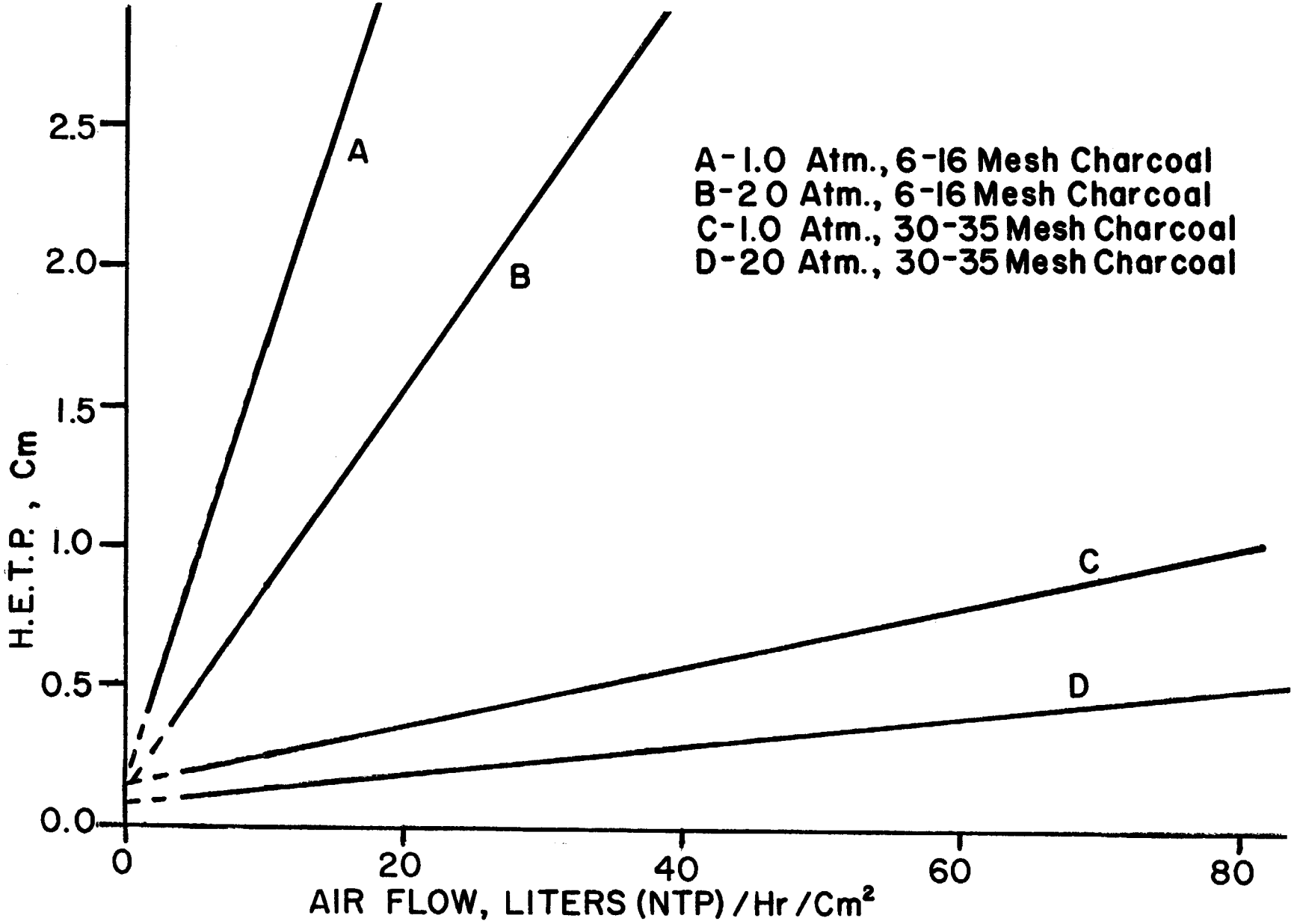

FIGURE 5 EFFECT OF FLOW RATE AND VELOCITY OF AIR ON H.E.T.P.

parameters. Approximations likely to result in serious error are identified when recognized. Calculation steps are:

1. Determine sets of $G_{A,1}$, $G_{A,2}$, $G_{K,1}$, $G_{K,2}$ for the flow sheet of Figure 6 which satisfy overall system $G_{A,p}$, $G_{K,p}$ requirements.

2. Correlate G_A's, G_K's with relative feed gas and adsorbent flows, using air:krypton mobility ratio vs. pressure and bed air capacity vs. pressure data.

3. Determine krypton:air desorption and adsorption during depressurization and pressurization.

4. Using set of values from above steps, determine krypton concentrations at column ends.

5. Using concentrations, flows, and krypton:air mobility data, calculate required number of theoretical plates for columns.

6. Using number of plates, flows, HETP vs. flow, and adsorbent permeability data, calculate bed length which satisfies a pressure drop constraint and required number of plates simultaneously.

Determination of Partition Fractions

Partition fractions were determined using mass balance equations from the flow diagram of Figure 6. The pertinent mass balance equations are:

$$[F_{A,3}(1-G_{A,1}) + F_{A,5}] (1-G_{A,2}) = F_{A,5} + F_{A,1}(1-G_{A,p}) \quad (1)$$

$$[F_{A,3}(1-G_{A,1}) + F_{A,5}] G_{A,2} + F_{A,1} = F_{A,3} \quad (2)$$

$$F_{K,5} = F_{K,1}(1-G_{K,p})/n \quad (3)$$

$$\left[\frac{(1-G_{K,p})}{n} + \frac{1-G_{K,1}}{G_{K,1}} (G_{K,p}) \right] (1-G_{K,2}) = \frac{n+1}{n} (1-G_{K,p}) \quad (4)$$

$$\left(\frac{n+1}{n}\right)(1-G_{K,p}) G_{K,2} / (1-G_{K,2}) = \frac{F_{K,2}}{F_{K,1}} \quad (5)$$

The quantity, n, of equations 3, 4, and 5 is defined as:

$$n = \frac{F_{A,1} (1-G_{A,p})}{F_{A,5}} \quad (6)$$

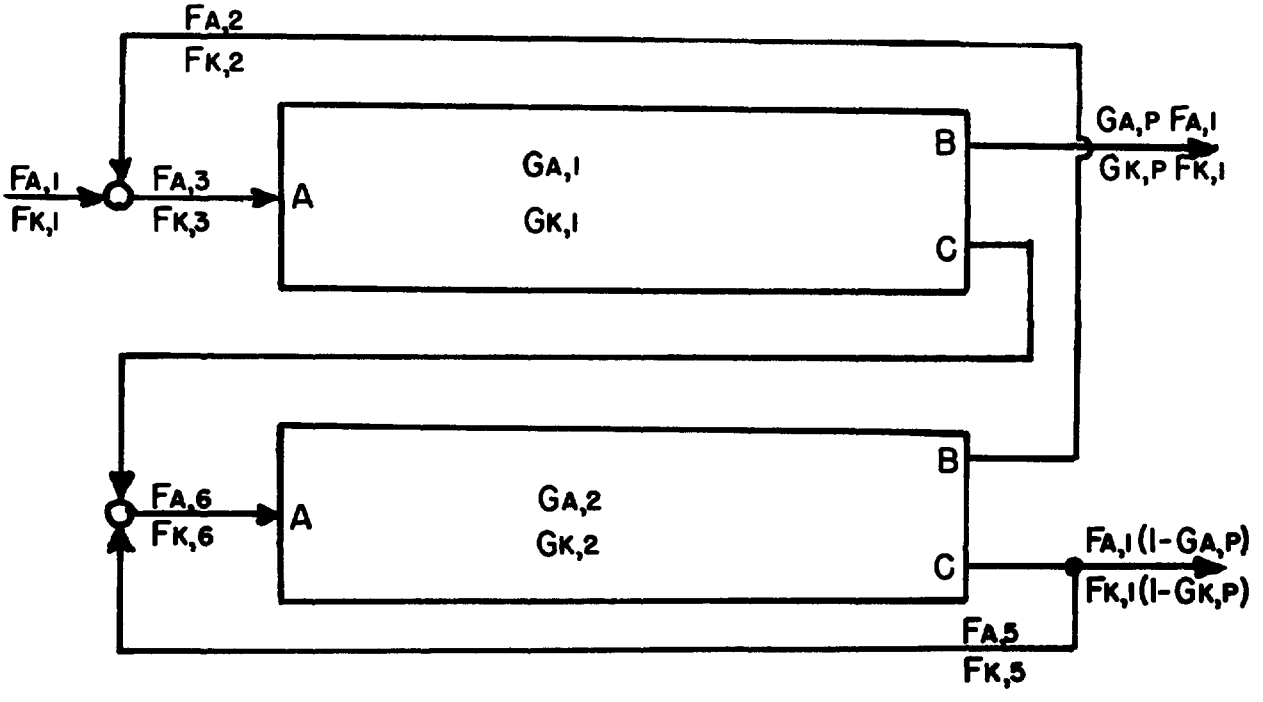

FIGURE 6 SYSTEM FLOW DIAGRAM

The five equations are indeterminate and the following constraints were used to obtain solutions:

$$(a)\quad G_{A,1} = G_{A,2} \tag{7}$$

$$(b)\quad \frac{1}{1-G_{A,1}} \leq 2.5 \tag{8}$$

$$(c)\quad \frac{G_{A,1}}{G_{K,1}} = \frac{G_{A,2}}{G_{K,2}} \tag{9}$$

These constraints were based on the following engineering reasoning. The first criterion is based essentially on the second which limits $G_{A,1} \leq 0.6$. Since air throughputs were similar, it seemed reasonable to simplify matters by letting the G_A's be equal.

The second criterion is a limitation of the properties of activated carbon operated within the pressure limits of 20 atmospheres and one atmosphere. This quantity corresponds to Kawazoe and Kawai's Z or enrichment ratio[1] and has very nearly the same value. The same Z value of 2.5 to 2.6 would be expected as an upper limit at ambient temperature for other activated carbons whose adsorption properties are characterized by a predominance of micropores (Dubinin's[9] First Structural Type).

The third constraint amounts to making the work of fractionation, which is measured by G_A/G_K, the same for each half of the plant. Intuitively, this should be near the most efficient mode of operation of the plant.

With these constraints and with the specific selection of the values 2.5, 2.2, and 2.0 for $1/1-G_A$, the corresponding G_K's were obtained for further calculation.

Correlation of Partition Fractions With Flow

For ideal mass transfer there is an activated carbon velocity, v_c^*, which will keep a krypton front stationary in the column for any given superficial feed gas velocity. The feed gas velocity for this stationary front is M(P) times the activated carbon velocity. M(P) is the ratio of the mobilities of air and krypton in a dilute mixture at a specified pressure (Figure 3), where $M(P) = v_A^*(P)/v_c^*(P)$. With non-ideal mass transfer, front breakthrough will be determined by the length of the bed and by the height equivalent of a theoretical plate(HETP). To control the level of breakthrough with a given bed, the velocities of adsorbent may be either increased or decreased with respect to v_c^*.

The arbitrary constraint is applied, that the cross sections of high and low pressure columns are equal, making adsorbent velocity identical in both columns. Then, expressing flows on a one atmosphere basis and designating high and low pressures by P1 and P2, we set in the high pressure column for unit cross section an air flow

$$F_1 = v_A P1 = M(P1)\, v_c\,(P1)\, P1 \tag{10}$$

and adsorbent flow

$$v_c = v_c^*(1+\Delta) \tag{11}$$

i.e. an adsorbent flow greater (or less) than that required to maintain an ideal front stationary by a factor $(1+\Delta)$. In the lower column, the ideal air flow required to maintain an ideal stationary front is,

$$F_2^* = M(P2)\, v_c^*(P2)\, (1+\Delta)P2 \tag{12}$$

This flow is increased by the same factor that adsorbent flow was increased in the high pressure column to counteract zone spreading, giving

$$F_2 = M(P2)\, v_c^*(P2)\, (1+\Delta)^2\, P2 \tag{13}$$

Depressurization and pressurization volumes are identical and are

$$F_3 = v_c^*\,(1+\Delta) \cdot [c(P1) - c(P2)] \tag{14}$$

where c(P) is adsorbent capacity on a one atmosphere basis, per unit volume of bed.

Now, referring to the system element as a three port device,

$$\frac{1}{1-G_A} = \frac{F_1}{F_2+F_3} \tag{15}$$

$$= M(P1)P1 / \left\{ M(P2)P2(1+\Delta)^2 + [c(P1)-c(P2)](1+\Delta) \right\} \tag{16}$$

Equation (16) relates system element partition fractions with adsorbent and air flows. The arbitrary increase of both adsorbent, in the upper column, and air, in the lower column, flows by the same amount, Δ, beyond that necessary to maintain stationary an ideal front is again based on the principle that equally dividing the task of overcoming effects of irreversibilities should approximately optimize the system.

Krypton Loss During Depressurization

The total fraction of krypton lost during depressurization, both by desorption and from void volume, must be established in order to determine column end concentrations which are, in turn, required for column length calculations.

These assumptions are made:

1) Release is isothermal.

2) Released krypton is very dilute.

3) There is no backdiffusion from the gas into the particles. This is equivalent to an assumption of continual outward motion of gas from particles - i.e. rapid depressurization.

Under these conditions, the particle surfaces will lose gas by desorption to the gas in the internal and external void volumes until the amount of adsorbed gas reaches a new equilibrium with the low pressure limit established by depressurization.

Since M(P) is the relative probability of desorbing an air "molecule" as compared to a krypton molecule, it expresses the relative rate of loss of air and krypton during depressurization from the initial quantities of air and krypton adsorbed. As the gas is almost entirely air, the pressure end-point for desorption is determined by air desorption alone. As air is desorbed, the ratio E(P) of the initial adsorbed quantity of krypton to the remaining adsorbed quantity of air, will increase. The product of 1/M(P) and E(P) then expresses the rate of loss of krypton from the initial quantity.

E(P) is obtained graphically from Figure 4, which is adsorbed air per unit volume of bed at room temperature. The fraction of krypton desorbed, f_K, has been determined by graphical integration. The fraction lost from the void volume is determined by subtracting from the quantity initially in the void volume, the quantity in the void volume after the new equilibrium is established. This omits a mixing correction which should be small since the total air mass flow during depressurization is about forty times the final mass retained. The final krypton concentration in the void volume is nearly $E(P2)/M(P2) \cdot C_o$ where C_o is initial krypton concentration in void volume, so that the fraction of krypton lost from the void volume is

$$f_v = (P1\ C_o - P2\frac{E(P)}{M(P2)}\ C_o)/P1\ C_o \qquad (17)$$

The original division of krypton between void volume and charcoal surface is determined by M(P1) and the bed void fraction (for PCB charcoal $\approx .81$), and is

$$\text{fraction adsorbed} = \frac{M(P1) - \varepsilon}{M(P1)} \qquad (18)$$

$$\text{fraction in void} = \frac{\varepsilon}{M(P)} \qquad (19)$$

Then total krypton fraction released, f_T, is

$$f_T = f_K(\frac{M(P1) - \varepsilon}{M(P1)}) + f_V(\frac{\varepsilon}{M(P1)}) = .1855 \qquad (20)$$

for the system we considered.

Calculation of Concentrations at Column Ends

At this point in the calculations, air mass flows throughout have been determined, as have G_A's, G_K's, Δ, and krypton depressurization flow. These give the krypton mass flows so that the krypton concentrations x_i in the gas can be readily established at all column ends, relative to the input krypton concentration.

The krypton concentrations y_i in the adsorbent are not uniquely determined. An arbitrary choice was made to select (by trial and error) y_4 such that y_4 and y_3 would be equally displaced from their respective equilibrium lines. Refer to Figure 7 for nomenclature. This choice balances the concentration gradient causing krypton to desorb into the low pressure purge stream and the concentration gradient causing krypton to adsorb from the high-pressure stream, at their respective (right-hand) column ends. y_3 and y_4 are related by the simple equation:

$$(E_1)y_4 = (E_1)y_3 + R_4x_4 \qquad (21)$$

where E_1 is the adsorbent flow rate and R_4 is the repressurization air flow rate. All the y's are simply related, and once one is selected, the rest are determined.

Calculation of Number of Plates

From the concentrations x_i and y_i and the values of mobility M(P) at the upper and lower pressure limits, the required number of theoretical plates for the fractionation can be calculated. For this calculation, the Kremser equations[10], appropriately modified for adsorption, may be used:

$$N_p = \frac{\log \left[\frac{x_B-(y_T/M)}{x_T-(y_T/M)}\,(1-A) + A\right]}{\log 1/A} \qquad (22)$$

$$A = \frac{\text{gas flow (1 atm)}}{\text{pressure}/M(P)(ET)} \qquad (23)$$

Subscripts B and T refer to input and output column ends, respectively, and the other symbols are as previously used, all in consistent units.

The above equation is for krypton sorption from air. For desorption:

$$N_p = \frac{\log \left[\frac{y_T-Mx_B}{y_B-Mx_B}\,(1-1/A) + 1/A\right]}{\log A} \qquad (24)$$

Calculation of Column Size

From the required number of plates, concentrations, flows, and HETP (Figure 5), the column length can be calculated for flow regions where intraparticle mass transfer resistance controls HETP, i.e. for flows large in comparison to that for minimum HETP. Column permeability and associated pressure drop then becomes important, especially in the high pressure columns.

For the high pressure columns, we have constrained the pressure drop across the column to be 5% of applied pressure, allowing the use of constant plate height. Calculation of column size with 5% pressure drop constraint requires simultaneous solution of equations for column length as a function of flow and pressure drop and column length as a function of the number of plates and HETP at a given flow.

Pressure drop per unit bed length at the high pressure limit was determined by transforming the manufacturer's published one-atmosphere flow data for 6-16 mesh activated carbon to 20 atmospheres and 30-35 mesh particles through Ergun's equation[11] re-written as

$$\frac{\Delta P}{Z} = \left(\frac{dp_1}{dp_2}\right)^2 a_1 v + \left(\frac{dp_1}{dp_2}\right)^2 b_1 \rho v^2 \qquad (25)$$

where dp_1, dp_2 = particle diameters for 6-16 and 30-35 mesh respectively

a_1, b_1 = values obtained from manufacturer's data

ρ = gas density

v = superficial velocity

All plant calculations performed were based on use of 30-35 mesh adsorbent. Viscosity of the gas is assumed to be unchanged from its 1.0 atmosphere value.

In the low pressure column, superficial velocities are on the order of three times those in the high pressure column, resulting in a significant pressure drop. Accordingly, characteristics of the low pressure column cannot be simply calculated since from point to point in the column, pressure, superficial flow velocity, turbulence, and relative adsorption mobilities for both air and krypton vary significantly. Calculation of an overall system would be greatly simplified by constraining pressure drop in the low pressure column to 5%, but this would result in greatly overestimating the quantity of charcoal required for fabrication of the plant. In principle, it is certainly possible to numerically simulate this column, although the practical problems of doing so accurately are significant. Accordingly, we have chosen to calculate the low pressure column based on its 1.0 atmosphere pressure characteristics.

Power Requirements

The total volume of gas requiring compression is assumed to be 1) the plant feed, plus 2) the feed to the second system element. Two stage compression with a polytrophic exponent (n) of 1.35 is assumed. The formula used is:

$$kw = .056313 \frac{n}{n-1} \cdot P1\ V_1 \left[\left(\frac{P2}{P1}\right)^{\frac{(n-1)}{2n}} - 1 \right] \qquad (26)$$

where P is in atmospheres, V in m^3/hr.

III. Results

The calculations outlined above have been performed for a model plant based on the flow diagram of Figure 6, using adsorbent flows which correspond to $1/1-G_A = 2.0$ (Figure 7), $1/1-G_A = 2.2$ (Figure 8), and $1/1-G_A = 2.5$ (Figure 9). Overall specified decontamination of cleaned air by a factor of 10^4 and concentration of krypton by a factor of 10^3 were basic calculation parameters. Flow, adsorbent mass, etc., are based on an assumed feed gas flow of 1,000 m^3/hr at room temperature and one atmosphere.

In figures 7, 8, and 9 the air flow rate (at one atmosphere) and krypton concentration of each stream is shown on that particular stream. Flow rates, designated by R, are in m^3/hr. Krypton concentrations in gas streams, designated by x, are normalized to an input krypton concentration of 10^{-4}. The plant input is R_1 (1000 m^3/hr, $x = 10^{-4}$). The clean air output is R_7 (999 m^3/hr, $x = 10^{-8}$); the output to storage is R_{14} (1 m^3/hr, $x = 0.1$).

In addition to the R and x values on the streams, the krypton concentrations per cc of charcoal, designated by y_1 through y_8, are given for the column ends, again normalized to a feed krypton concentration of 10^{-4}. The countercurrent activated carbon flows E_1 and E_2, in m^3/hr, are also given.

For each column, the following parameters are listed:

number of theoretical plates, N_p
total cross-sectional area, cm^2
length, cm
mass of activated carbon needed, kg

For each plant, the total activated carbon requirement and the total power requirements for compression of gas streams has been calculated. These values are listed in Table II. It is apparent from this Table that the activated carbon requirement is fairly sensitive to the value of the "enrichment ratio"[1], $1/1-G_A$. The required quantity decreases for small values of this parameter, perhaps in contradiction to the expectation that a higher enrichment ratio produces a better plant. It must be noted that the decrease in plant size is obtained at the expense of an increase in power requirements.

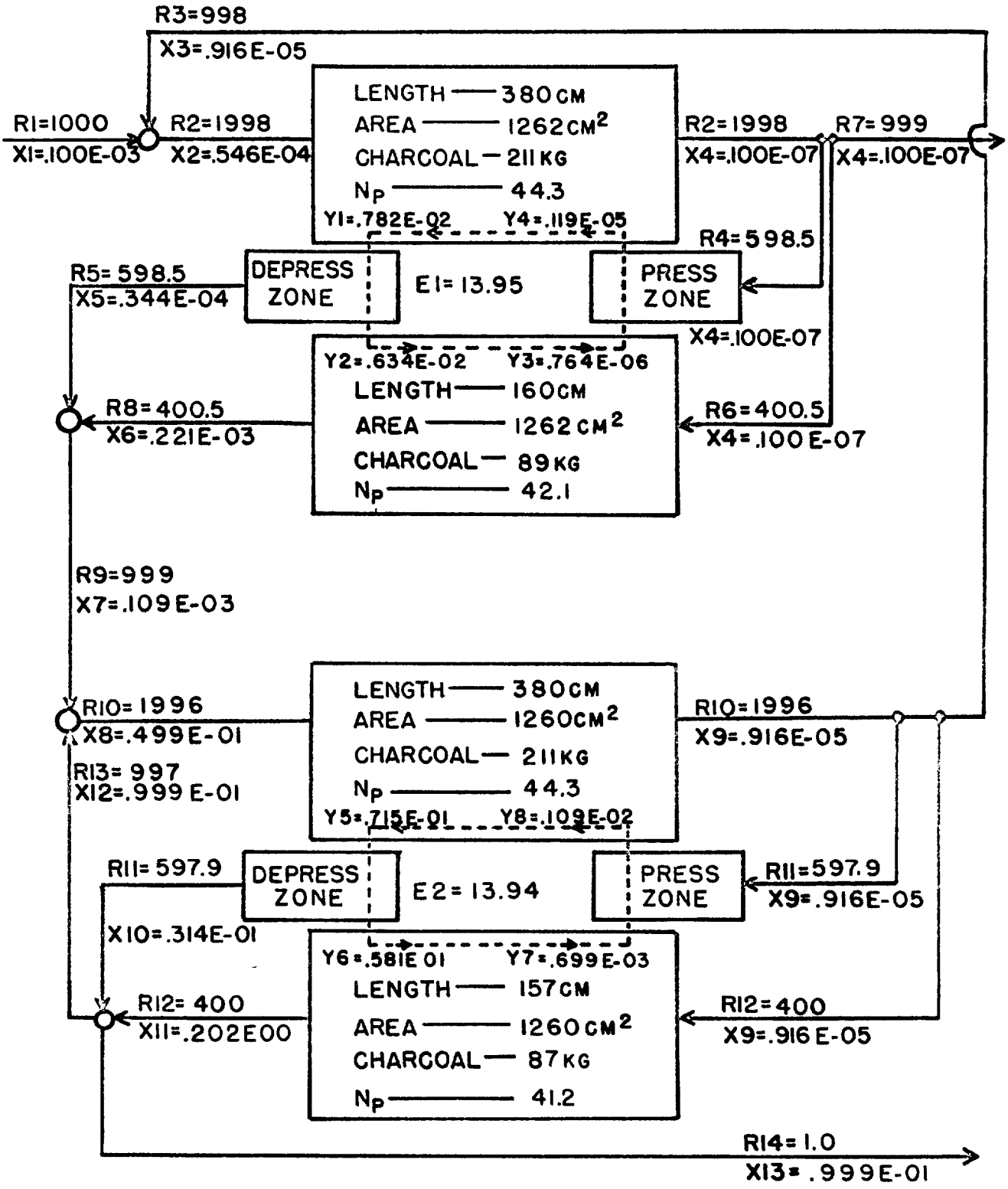

Figure 7. Calculated Parameters for Two Element Moving Bed Plant, η_A = 0.500

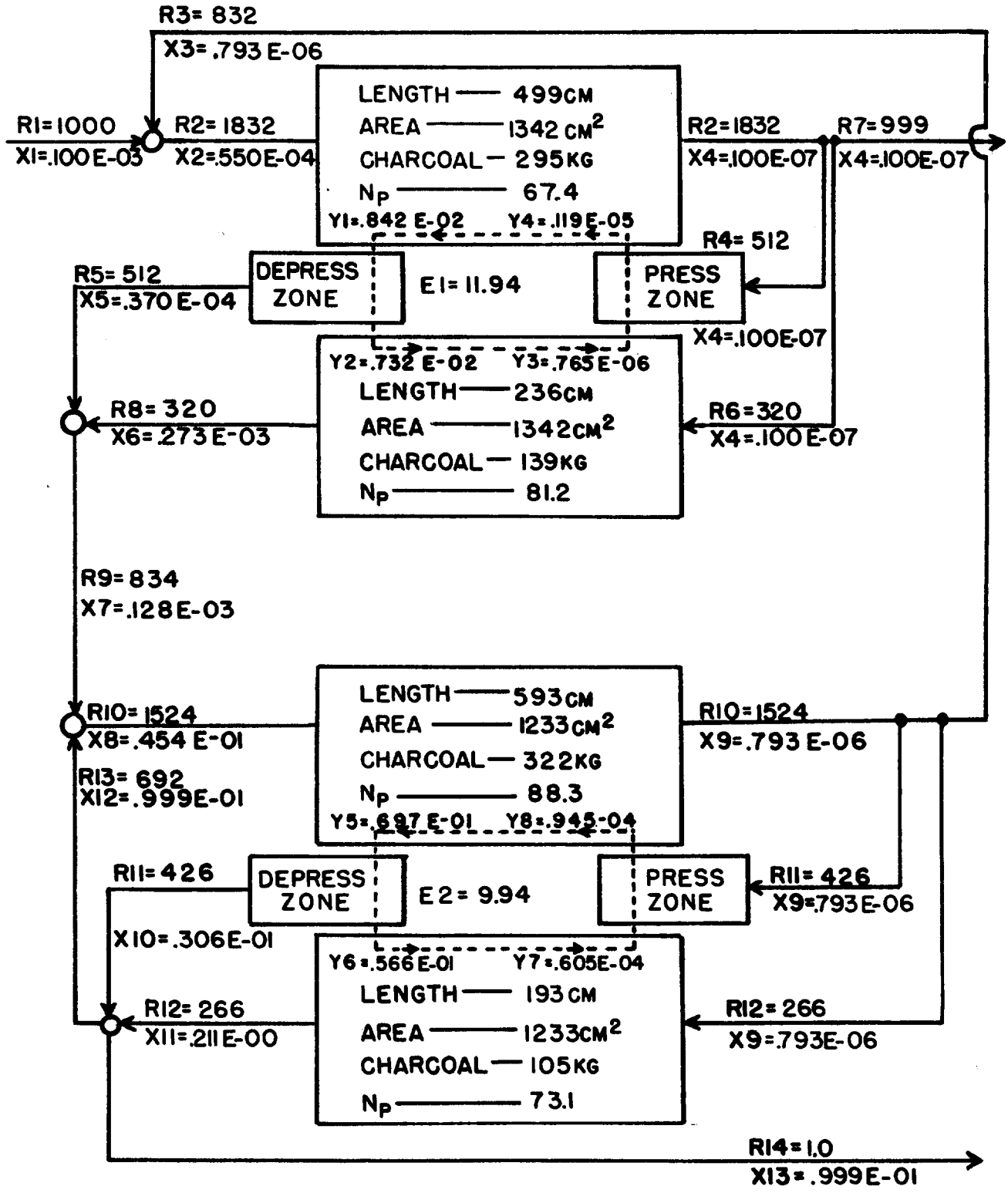

Figure 8. Calculated Parameters for Two Element Moving Bed Plant, G_A = 0.545

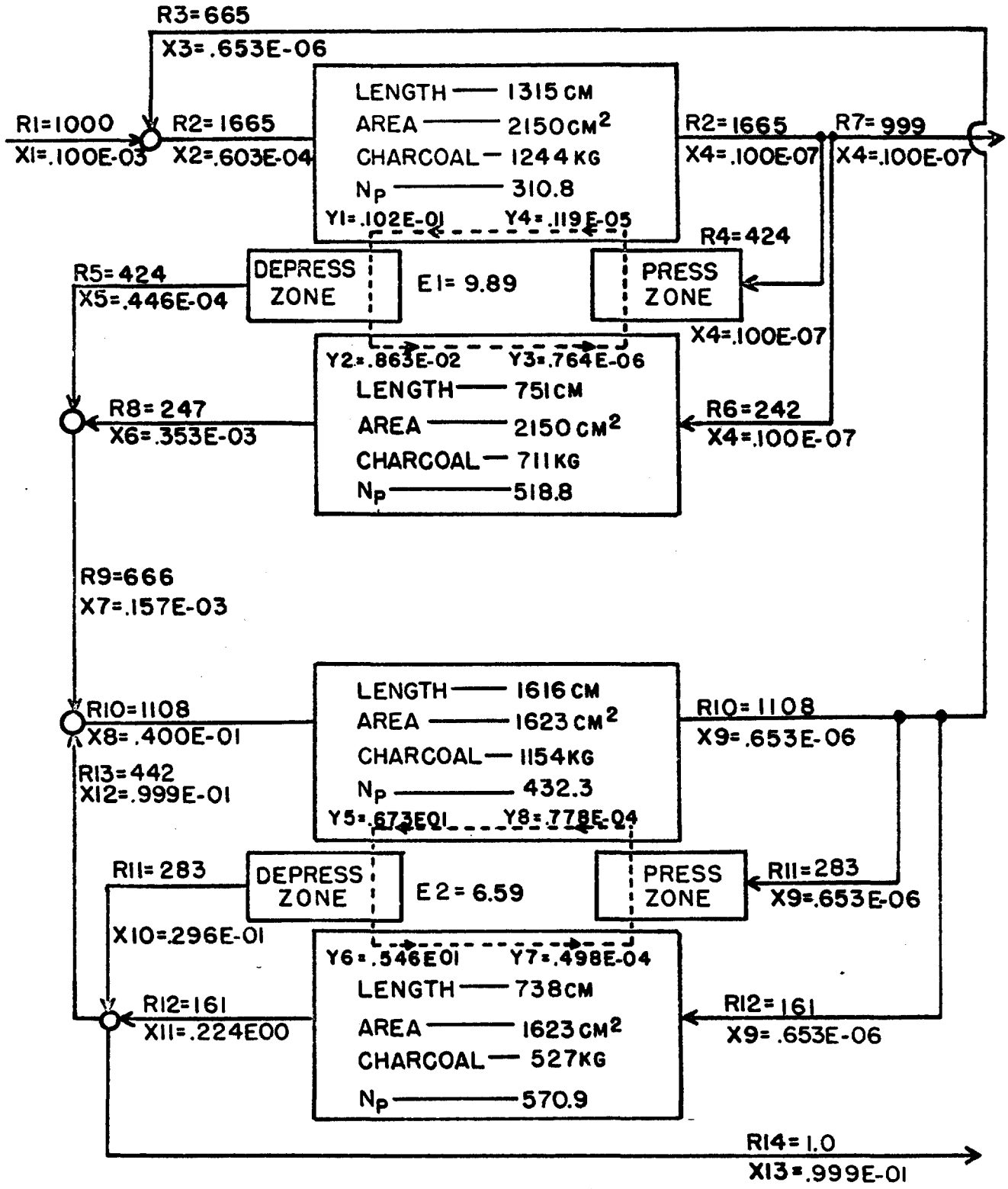

Figure 9. Calculated Parameters for Two Element Moving Bed Plant, G_A = 0.600

Table II

SUMMARY OF CALCULATIONS BASED ON 1000 m^3/hr FEED, 20.0 ATMOSPHERES AND 1.0 ATMOSPHERE PRESSURE LIMITS

	G_A	$1/1-G_A$	Adsorbent Mass, kg	Power Required, kw
Plant 1	.500	2.00	598	308.4
Plant 2	.545	2.20	861	259.8
Plant 3	.600	2.50	3636	217.0

IV. Discussion

Plant Implementation

The above calculations indicate that a moving bed, pressure swing cycle plant would be of practical size and power consumption and hence economically feasible. Implementation of the conceptual design in total would necessitate design and fabrication of a charcoal circulation mechanism operating in synchronism with pressure locks. Such a mechanical design does not present insurmountable difficulties; most of the problem has already been solved in development of the Hypersorption process. However, most of the advantages of the continuously moving bed may be obtained by moving the bed in increments; this may be accomplished in practice by dividing the bed(s) into segments and changing the points at which gas is introduced. This would correspond to a relative incremental bed motion. Such a compromise would simplify mechanical design, eliminate activated carbon attrition as a result of mechanical abrasion, improve equipment reliability and maintainability, and simplify design of equipment safeguards to minimize fission gas loss in case of accident causing bed rupture. A segmented, step-motion bed would result in a performance degradation in comparison to a continuously moving bed in inverse proportion to the number of segments into which the bed is divided.

For a practical plant, we would, at this point in conceptual design, consider a two-element configuration subdivided into at least ten identical units per element. Of these ten, one would be depressurizing, another repressurizing, and the remainder divided into high and low pressure beds in a manner to approximate the calculated length of each section. This configuration has the advantage of providing independent areas and carbon flow rates in the two elements. Storage may be provided in the inter-element lines to accommodate surges and removal of interferences may be provided on side streams.

Interferences

The question of interferences has not been considered at any length pending establishment of the viability of the basic process. It appears almost certain that impurities less strongly adsorbed than

krypton would pass through the plant and be discharged with the cleaned air.

More strongly adsorbed interferences could present a greater problem. They would move "down" the plant and tend to accumulate in the krypton concentrate streams. If left unchecked, such a process might change the nature of the gas or lead to blockage of virtually all the activated carbon sites. Water, iodine, nitrogen oxides, and xenon would be expected to be more strongly adsorbed than krypton. The first three of these could probably best be handled by removal from a concentrated stream, such as those indicated by R_{11}, R_{12}, and R_{13}. The removal would be facilitated by the increased concentration of the impurity. Xenon, because of its chemical inertness and its close similarity to krypton would be more difficult to remove. It may be that this element may simply be left to accumulate in the krypton product.

Deviations from Equilibrium

An activated carbon surface can be considered to consist of a continuum of fixed sites of all positive adsorption energies. Some preliminary experimental data in this laboratory is consistent with an approximately Gaussian distribution, analogous to that noted by Dubinin and Raduskevich[9]. They are also in qualitative agreement with Glueckauf's calculations for binary mixture adsorption, based on an exponential site distribution[12]. Effectively, these findings indicate that trace krypton can compete only for the highest energy sites occupied at a given total pressure. At sufficiently high total pressure or low temperature, all available sites will be occupied by air, thus forcing off or displacing krypton adsorbed at lower pressure. This accounts for anomalous adsorption curves[13] and also for the pressure dependence of relative mobility M(P). The krypton will also be present in general on higher energy sites, where it is less firmly held. Accordingly, at high pressures, the krypton makes fewer and shorter stops on its random walk through the adsorption bed. The mechanism of zone spreading, and thus the height equivalent of a theoretical plate, may thus be expected to be profoundly affected by large changes in total pressure.

Adsorbent Material

Adsorbent volume could be reduced if a better adsorbent were available. Suitability depends on the relative mobilities at the pressure limits of interest and over the concentration ranges of interest, on the magnitude of intraparticle mass transfer resistance, and on the bulk air adsorption coefficient change between the pressure limits. Relatively little data is available on adsorption of binary mixtures at different pressures on different adsorbents. For charcoals, the assumption that the surface is affine for krypton and the gases in air and that the distribution of adsorption sites as a function of energy is similar for different charcoals should, if valid, preclude drastic improvements as a result of improved air-krypton mobility ratios and/or decreased air adsorption. Intraparticle mass transfer resistance has been found to vary significantly among activated carbons. Particle size is an important parameter in the flow region of interest.

Size and shape of macropores relative to the overall particle dimension appear to determine the particle size at which intraparticle mass transfer resistance begins its transition from micropore to macropore diffusion as the rate limiting step.

V. Summary

The pressure-swing adsorption-desorption cycle for concentrating krypton from air has been combined with a moving bed concept. The combination can be applied to a continuous krypton separation for nuclear fuel reprocessing plant off-gases. The plants may be approximated without an actual moving bed by suitable control of the gas streams.

The basic system element contains a cyclic flow of adsorbent moving from a high pressure loading leg to a depressurization zone to a low pressure purge leg to a repressurization zone and back into the high pressure leg. The flow of gas is countercurrent to the adsorbent, contaminated gas being introduced into the high pressure leg and decontaminated gas being used for repressurization and purge.

Calculations have been made for three two-element plants utilizing activated carbon with pressure limits of 20 atmospheres and 1 atmosphere. Specifications for each plant were 1) decontamination factor of 10^4 for discharged air stream, 2) concentration factor of 10^3 for krypton concentrate stream, and 3) feed stream of 1000 m^3/hr. Activated carbon requirements for the three plants were from 598 kg to 3636 kg, with corresponding compressive power requirements from 308 kw to 217 kw. Such plants in concept seem to compare favorably with krypton removal systems based on other processes.

Acknowledgement

The authors wish to acknowledge their indebtedness to Mr. John M. Price. Mr. Yosuke Mishiro performed the programming and calculations. We are grateful also to the Atomic Energy Commission, Division of Waste Management and Transportation, for support under Contract Number AT(11-1)3049.

References

1. Kawazoe, K., and Kawai, T., "Concentration of Dilute Gases by Pressure Swing Adsorption", Kagaku Kogaku, 37, 288-294 (1973).

2. Slansky, C. M., "Separation Processes for Noble Gas Fission Products for the Off-gas of Fuel Reprocessing Plants", Atomic Energy Review, 9, 423-40 (1971).

3. Merriman, J. R., Pashley, J. H., Habiger, K. E., Stephenson, M. J., and Anderson, L. W., "Concentration and Collection of Krypton and Xenon by Selective Absorption in Fluorocarbon Solvents", in "Treatment of Airborne Radioactive Wastes", International Atomic Energy Agency, Vienna, 1968 (STI/PUB/195) pp 303-313.

4. Berg, C., "Hypersorption Design", Chem. Eng. Progress, 47, 585-91 (1951).

5. Kasten, P. R., and Amundson, N. R., "Analytical Solution for Simple Systems in Moving Bed Adsorbers", Ind. and Eng. Chem., 44, 1704-11 (1952).

6. Pollock, A. W., Brown, M. F., and Dempsey, C. W., "Machine Solution of a Boundary Value Problem for a Continuous Arosorb Process", Ind. and Eng. Chem., 50, 725-29 (1958).

7. Steinberg, M., and Manowitz, B., "Recovery of Fission Product Noble Gases", Ind. and Eng. Chem., 51, 47-50 (1959).

8. Calgon Corporation, Pittsburgh Activated Carbon Division, Technical Bulletin 23-108 (undated).

9. Dubinin, M. M., and Radushkevich, E. D., Zhur. fiz. khim. 23, 469 (1969) reported in "Active Carbon", Smisek,M. and Cerny,S. Eds., Elsevier, Amsterdam, 1970, p. 116.

10. Kremser, A., National Petroleum News, 22, 42 (1930); reported in "Mass Transfer Operations", 2nd ed., Treybal, R. E., McGraw Hill, New York, 1968, p. 115.

11. Ergun, S., Chem. Eng. Progress, 48, 89 (1952); reported in "Mass Transfer Operations", 1st ed., Treybal, R. E., McGraw Hill, New York, 1955, p. 142.

12. Glueckauf, E., "Monolayer Adsorption of Two Species on Non-Uniform Surfaces", Transactions of Faraday Society, 49, 1066-79 (1953).

13. Underhill, D. W., Hall, R. R., Gold, A., Goldin, A., First, M. W., Moeller, D. W., "Semiannual Progress Report, Harvard Air Cleaning Laboratory", September 1, 1972-December 31, 1972, Report No. COO-3019-4, p. 2-1, 2-15 (Issued February, 1973).

14. Richardson, L. B., and Woodhouse, J. C., "The Adsorption of Mixed Gases by Charcoal I., CO_2 and NO", J. Amer. Chem. Soc. 45, 2638-53 (1923).

15. Harvard Air Cleaning Laboratory (In preparation).

16. Damkohler, G. Z., "A Statistical Derivation of the Adsorption Isotherm of Binary Gas Mixtures", Z. Physik Chem. B23, 58-68 (1933); reported in "Physical Adsorption of Gases", Young, D. M. and Crowell, A. D., Butterworth, Washington, D. C. 1962, p. 397.

DISCUSSION

DEMPSEY: You mentioned in the course of the talk that some of this technology has been used in the petroleum industry. I wonder if the equipment involved is pretty well advanced and adaptable to nuclear purposes as it stands?

GOLDIN: I can't say that definitely. The equipment has been used in the petroleum industry for about 20 years, I think. The papers mentioned in references four, five, and six, I think date from 1951 or 1954. The petroleum industry does not use pressure cycling, they use thermal cycling and they move the carbon beds. Except that we ran out of time, I would have said our idea for implementing this would not be to move the carbon beds (although that could be done) but to subdivide each system element into a number of small columns, probably ten or thereabouts. Two would be used for the pressurization and depressurization zones, the remainder would be in the high pressure and low pressure columns in proportion to the required length. By switching the gas flow from one bed to another, you get the equivalent of incrementally moving the bed rather than continuously moving it. This, we feel, would lead to somewhat simpler design, would eliminate any attrition of the carbon, although reported attrition of the carbon in the oil plants is rather small. There would be reduction in performance. I think the 600 kilogram plant is small enough and cheap enough that you could double its size to allow for degraded performance without running into substantial troubles.

COOPER: Have you investigated the application of the pressure swing system to a low through-put LMFBR type covergas system. If you did not, how would you evaluate its practicability?

GOLDIN: Ayer, a coauthor, is not here. He thinks that this moving bed system would give you the equivalent of a very small holdup. We talked, for example, in terms of making systems small enough so that welders could make their own oxygen from ambient air. On my own, I can't answer the question. We certainly have not done an investigation except to read the chemical engineering literature on moving beds. It seems it should be adaptable.

ELIKAN: It seems to me after looking at the pressure swing system proposed, even with your modification to eliminate carbon transport, that it's kind of a pipefitter's nightmare. How do you compare this system to a thermal swing in terms of its complexity?

GOLDIN: I think the piping is more complicated than a thermal swing system. I read the thermal swing system paper rather hurridly and I just have not got this much familiarity with it. The implementation of either one of them is rather advanced, beyond where we stand today. I can see problems with the valving but I am not an engineer and I don't know much about piping. We conceive of this unit running somewhat like a distributor, i.e., an input is continually switched to different contact points.

BLANCO: I would like to make an observation and ask a question. The use of charcoal to treat the off gases from a fuel reprocessing plant must be evaluated in terms of operability and safety. The off gases can contain nitrogen oxide, which can react with the charcoal. Have you studied this problem? This safety problem has been an objection to the use of charcoal in past designs.

GOLDIN: We have looked at it in two ways. One way is to consider the use of molecular sieves. We tried one sieve which turned out to be unsatisfactory. The data on other sieves indicated they would be unsatisfactory as well. We haven't gotten to considering impurities experimentally. Impurities that hold less firmly than krypton would be expected to pass out with the air to be discharged to the stack. To the extent that they are not radioactive and not toxic, that's all to the good. The impurities which are more strongly held than krypton (among these I would include nitrogen oxides, iodine , xenon , and water) would probably tend to move down the plant and concentrate in the product. We contemplate that the system would be installed downstream of the iodine and nitrogen oxide scrubbers, with probably more impurity removal and certainly moisture separation. In addition, we consider that there would have to be a side stream take-off after some concentration for continuous removal of nitrogen oxide, etc. to keep these substances from concentrating. Otherwise, the gas flow would eventually wind up being nitrogen oxide rather than air. We have not gone into that in detail but it would have to be handled in some such manner.

GENERAL ATOMIC'S RADIOACTIVE GAS RECOVERY SYSTEM

J. A. Mahn and C. A. Perry
General Atomic Company
San Diego, California

Abstract

General Atomic Company has developed a Radioactive Gas Recovery System for the HTGR which separates, for purposes of retention, the radioactive components from the non-radioactive reactor plant waste gases. This provides the capability for reducing to an insignificant level the amount of radioactivity released from the gas waste system to the atmosphere--a most significant improvement in reducing total activity release to the environment.

I. Introduction

General Atomic Company has long maintained a continuing effort to further improve the already uniquely low activity releases from its High-Temperature Gas-Cooled Reactor (HTGR) nuclear power plants. As a result of this effort, a Radioactive Gas Recovery System has been developed for the HTGR which separates, for purposes of retention, the radioactive components from the non-radioactive reactor plant waste gases. The system utilizes a chromatographic adsorption process which provides a mechanism for separating a gas mixture into its constituents.

II. Background

The HTGR is a helium-cooled, graphite-moderated nuclear reactor which utilizes a prestressed concrete reactor vessel (PCRV) for the primary containment. During normal operation a fraction of the circulating primary coolant helium is continuously diverted to a helium purification system for removal of chemical and radioactive impurities. Periodically, a purification train low-temperature adsorber is regenerated, with the gas waste being transferred to the radioactive gas waste system for temporary storage and radioactive decay. These impurities (in a helium carrier gas) are subsequently processed in the radioactive gas recovery system and separated into three streams: (1) a stream containing hydrogen, helium, and tritium, which is returned to the PCRV, where the hydrogen and tritium are subsequently cleaned up by the purification system hydrogen getter unit; (2) a stream containing krypton, xenon, and helium, which is returned to the PCRV for retention within the reactor plant; and (3) a stream containing the activity-free residual gases O_2, N_2, and CO, which is first monitored to confirm that it is activity-free and then vented to the atmosphere.

III. System Design

The system consists of a pretreatment section which removes oil, CO_2, and H_2O from the charge gas, a chromatographic adsorption section which provides the mechanism for separating the gas mixture into its constituents, a compressor section which returns the radioactive gases to the PCRV, a vacuum pump which removes the non-radioactive residual gases, following separation, for subsequent radiation monitoring and release, and a chilled brine refrigeration unit which provides cooling to the chromatographic adsorption section.

Gas waste from a gas waste system storage tank is introduced at the inlet of the radioactive gas recovery system at 14.6 atm (200 psig) and a maximum temperature of 93.4°C (200°F). The process stream first passes through an oil adsorber, where any oil which might have been introduced by the gas waste system compressor is removed by adsorption on activated charcoal. The stream is then saturated with water vapor in the saturator in preparation for CO_2 removal. CO_2 is removed from the process stream by chemical reaction with a suitable reactant, such as "Sodasorb," in the CO_2 absorber. Water vapor is then condensed and removed by chilling the gas stream to about 4.45°C (40°F) in a heat exchanger employing chilled brine. The condensed water is removed by means of a knockout pot in the heat exchanger. Any remaining water vapor is then removed by adsorption on molecular sieve in a dryer. At this point, the process stream is ready for the separation of the remaining radioactive and non-radioactive constituents.

The heart of the system is the chromatographic adsorption section, which consists of two activated charcoal adsorber columns, each cooled to 4.45°C (40°F) by chilled brine. The separation of the process stream into its constituent species is based on the dynamic adsorption of gases on activated charcoal and results from the fact that the more volatile species, such as helium and hydrogen, migrate through the charcoal faster than the less volatile species, such as krypton and xenon, which migrate through the charcoal very slowly as they pile up on the front end of the column. The other constituent impurities lie between these two cases in their adsorption characteristics and make up the third stream in the separation process.

The actual separation process consists of five phases. In Phase 1 (the charging step), gas flows through the two adsorber columns in series until krypton is detected at the middle sample point within the first column, or until any of the chemical impurities (CO, O_2, N_2) are detected at the outlet of the first column. Termination of gas flow is automatic. Flow is also terminated if CO_2 is detected at the outlet of the CO_2 absorber or if H_2O is detected at the outlet of the dryer. During this phase, the effluent gas from the second adsorber column is compressed to about 49.3 atm (725 psia) by the gas recovery compressor and routed to the PCRV. This gas consists only of helium, hydrogen, and tritium.

In Phase 2, a flow of purified helium, supplied at 14.6 atm (200 psig) from the helium storage system, is introduced at the inlet of the first adsorber column and again passes through the two columns in series. Flow is continued until the effluent from the first adsorber is free of oxygen, nitrogen, and carbon monoxide and until the effluent from the second adsorber is free of hydrogen and tritium. Flow is also terminated if krypton is detected at the lower sample point within the first column (approximately 90% of the distance through the column). During this phase, the effluent from the second column (helium, hydrogen, and tritium) is also compressed and routed to the PCRV. Upon completion of this phase, the separation is complete. All of the hydrogen and tritium has been purged from the two adsorber columns and routed to the PCRV, all of the krypton and xenon remains in the first adsorber, and the chemical impurities are on the second adsorber.

In Phase 3, the two adsorber columns are isolated from each other by means of an isolation valve between the columns. A stream of purified helium from helium storage is introduced at the outlet of the first column, flowing through the adsorber in the reverse direction, until all of the krypton and xenon has been purged from the bed. Flow is in the reverse direction as most of the krypton and xenon will have accumulated on the front end of the bed. This stream is compressed by the gas recovery compressor and routed to the PCRV. In Phase 4, the second adsorber column is depressurized and then evacuated with a vacuum pump. The effluent is discharged to the plant vent after passing through an oil adsorber to

remove any oil introduced by the vacuum pump and after appropriate activity monitoring in the radioactive gas waste system. In Phase 5, the second adsorber column is repressurized to 14.6 atm (200 psig) with purified helium from helium storage, the isolation valve between the columns is opened, and the system is ready to receive another batch of gas for processing.

The system operates batchwise, with the operation repeated as many times as necessary to process the inventory of gas from the radioactive gas waste system.

Chilled brine for the chiller and for the jackets of the adsorber columns is provided by a refrigeration unit which is included as part of the system.

The oil adsorbers, the CO_2 absorber, and the dryer are cartridge-type units. Spent cartridges are purged with helium and disposed of as solid radwaste.

The system is normally operated during periods when the PCRV is pressurized to power operating levels, and gas is discharged to the PCRV by means of the compressor. If the PCRV is depressurized, however, such as during reactor refueling, the system is operated in the same manner but at a reduced flow rate and with the gas discharged to the PCRV through a flow control valve downstream of the compressor.

System operability is not essential for start-up, operation, or shutdown of the reactor, nor for the operation of any other auxiliary system. In the event of a system malfunction, the system is removed from service. Any contained gaseous activity is then removed by venting and purging to the radioactive gas waste system, following which the system is repaired and returned to service. Thus, no spare components are required in the system.

Sample lines for monitoring chemical impurities and radiation are located at appropriate points to determine breakthrough of the beds and when to change from one phase of the chromatographic separation to the next.

DISCUSSION

COOPER: From your description of the system, it appears that you are recycling tritium into the reactor system and then purifying it from there. Can you comment on what the daily or annual release of tritium would be, due to leakage or other releases from the plant?

MAHN: The only anticipated release of gaseous tritium would be from leakage and I can't tell you what it would be for a plant. Tritium resides in the helium purification system and the radioactive waste and gas recovery systems for various periods of time. What one needs to do, is sit down and go through a residence time analysis based on the design leakage from these systems. It is extremely small. First of all, we have an equilibrium level of tritium in the primary coolant of a 3,000 megawatt (thermal) plant of approximately five and a half curies. The ultimate disposal of tritium and hydrogen comes about by adsorption on the titanium sponge in the helium purification system. The tritium and hydrogen are then treated as solid wastes. The reason we get tritium in the gas waste systems is due to the fact that the low temperature adsorber in the purification system amounts to a delay bed for the tritium and hydrogen and upon regeneration of this bed the hydrogen and tritium adsorbed on the bed are transferred to the gas waste system. As far as releases from the plant of gaseous tritium are concerned, there are none except for minor system leakages.

DEVELOPMENT OF THE KRYPTON ABSORPTION IN LIQUID CARBON DIOXIDE (KALC) PROCESS FOR HTGR OFF-GAS REPROCESSING*

R. W. Glass, H. W. R. Beaujean,† H. D. Cochran, Jr., P. A. Haas, D. M. Levins,‡ W. M. Woods

Oak Ridge National Laboratory
Oak Ridge, Tennessee

Abstract

Reprocessing of High-Temperature Gas-Cooled Reactor (HTGR) fuel involves burning of the graphite-matrix elements to release the fuel for recovery purposes. The resulting off-gas is primarily CO_2 with residual amounts of N_2, O_2, and CO, together with fission products. Trace quantities of krypton-85 must be recovered in a concentrated form from the gas stream, but processes commonly employed for rare gas removal and concentration are not suitable for use with off-gas from graphite burning. The KALC (Krypton Absorption in Liquid CO_2) process employs liquid CO_2 as a volatile solvent for the krypton and is, therefore, uniquely suited to the task.

Engineering development of the KALC process is currently under way at the Oak Ridge National Laboratory (ORNL) and the Oak Ridge Gaseous Diffusion Plant (ORGDP). The ORNL system is designed for close study of the individual separation operations involved in the KALC process, while the ORGDP system provides a complete pilot facility for demonstrating combined operations on a somewhat larger scale. Packed column performance and process control procedures have been of prime importance in the initial studies.

Computer programs have been prepared to analyze and model operational performance of the KALC studies, and special sampling and in-line monitoring systems have been developed for use in the experimental facilities.

Introduction

Development of the KALC process is proceeding with the goal of providing a viable means of removing in a concentrated form radioactive krypton released during the reprocessing of spent HTGR fuel. A comprehensive review[1] of the process concept was presented at the 12th USAEC Air Cleaning Conference, so that only a brief recounting is presented here.

---

*Research sponsored by the U. S. Atomic Energy Commission under contract with Union Carbide Corporation Nuclear Division.

†Guest scientist, KFA, Julich, West Germany.

‡Guest scientist, Australian Atomic Energy Commission, Research Establishment, Lucas Heights, N.S.W., Australia.

Feed will be provided in gaseous form to the KALC process as a result of burning the HTGR graphite fuel matrix to expose the fuel particles for further reprocessing. An estimated analysis of the gas stream after filtration is given in Table I. For a 1-metric ton/day plant the given numbers would be multiplied by 100 since 100 blocks would be processed per day. Iodine and tritium will be removed by processing steps prior to introducing the off-gas to the KALC system.

The KALC process operates at about 20 atm pressure and at temperatures from about -15°C to -40°C. A simplified flowsheet is given as Figure 1. Before being fed into the system, the filtered and pretreated off-gas is compressed and chilled so that part of the CO_2 is condensed. In the absorption stage virtually all of the Kr is selectively absorbed in the liquid phase. All gas components with solubilities less than Kr (viz., O_2, N_2, and CO) are returned by the fractionation stage to the absorber for final discharge from the top of the absorber. Gases more soluble than Kr (viz., Xe) follow the liquid CO_2 to the stripper stage where Kr is removed overhead and concentrated. Xenon may either be allowed to accumulate in the CO_2 to the point where it is eventually discharged from the top of the absorber, or it may be removed by a separate distillation operation on the recycle CO_2 stream.

Program and Objectives

Two experimental facilities are being used in the development of the KALC process. At ORNL, the Experimental Engineering Section Off-Gas Decontamination Facility (EES-ODF) is being used primarily to obtain fluid dynamics and basic mass transfer data for the various individual processing steps. Sequentially, at the Oak Ridge Gaseous Diffusion Plant, the ORGDP LMFBR-HTGR Fuel Reprocessing Off-Gas Decontamination Pilot Plant is being used to demonstrate the integrated operation of all KALC processing steps.

Facility Description

The EES-ODF is shown schematically in Figure 2, and will operate essentially as a gas-liquid flow system in which gas containing ^{85}Kr contaminant is passed countercurrent to a liquid scrub stream which absorbs the contaminant selectively. The liquid containing the tracer-level contaminant is then distilled to produce both a concentrated contaminant product gas and a purified liquid scrub stream.

The decontaminated gas from the absorption operation and the concentrated contaminant product gas are recombined and introduced into the absorption column to allow continuous operation via complete recycle of process fluids. Similarly, the purified liquid scrub produced in the distillation or "stripping" operation is recycled to the absorption column.

By simultaneously operating the absorption and stripping portions of the facility, with each portion providing feed to the other, the total system material is held captive, and the results of selected operating conditions may be investigated in a "steady-state" mode.

Major system components include packed towers for the absorption and stripping operations, pumps for moving the liquid streams, and gas compressors for transport and pressurization of the gas streams. Assorted surge and hold tanks are used as necessary for smooth operation and shutdown. Electric heaters are used to boil or "distill" the contaminant gases from the liquid, and condensers are employed to liquefy portions of the gas streams and provide reflux for the distillation operations. Gas and liquid sampling and tracer monitoring are important parts of the

Table I. Estimated burner off-gas analysis[a]

Major Component	lb	scf	Mole Fraction
CO_2	1223	9976	0.897
O_2	75	846	0.075
N_2	24	312	0.028
Contaminant	**ppm (Total)**	**ppm (radioactive)**	**Curies**
Krypton	16	1.2	572.0
Tritium	2.4×10^{-2}	2.4×10^{-2}	9.8
Iodine	3	9.2×10^{-7}	0.2
Xenon	61	---	---

[a]For head-end reprocessing of one FSVR fuel block; 6-year exposure, 150-day cooling.

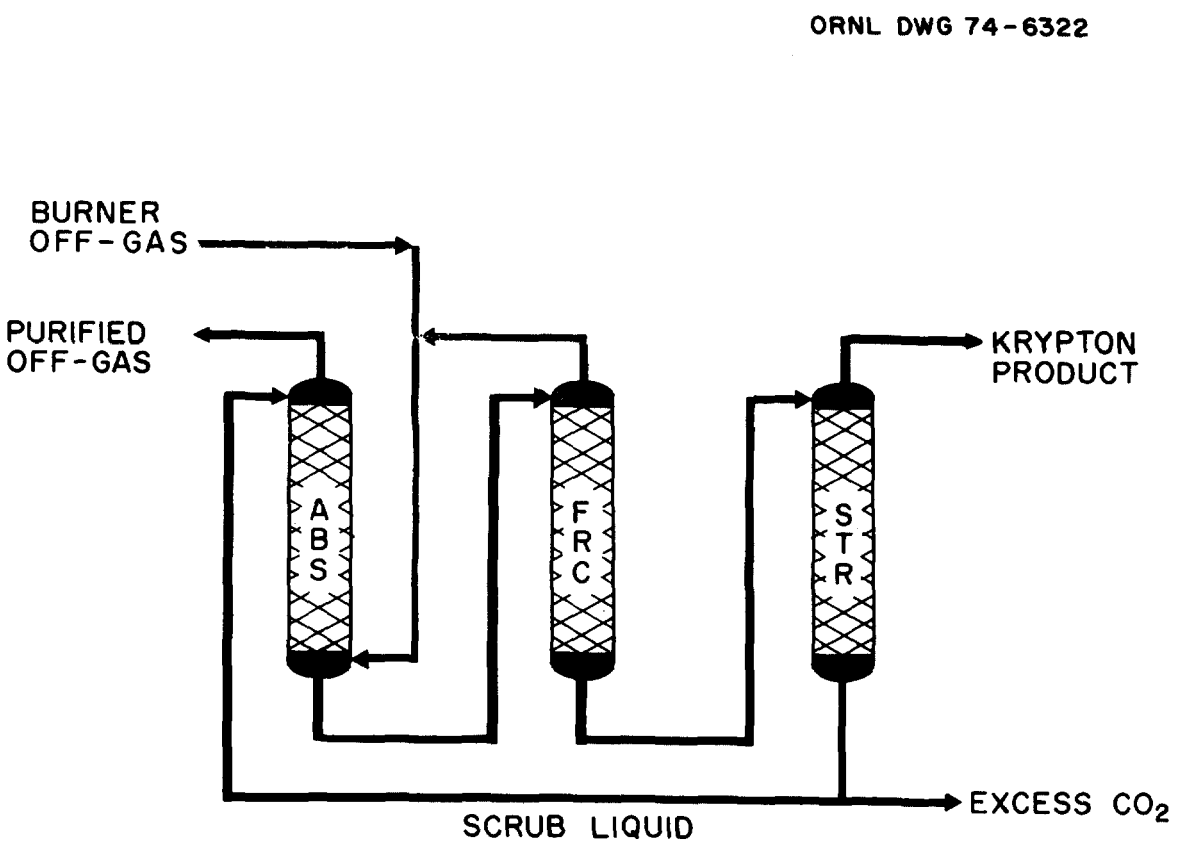

Figure 1. Basic KALC System Flowsheet.

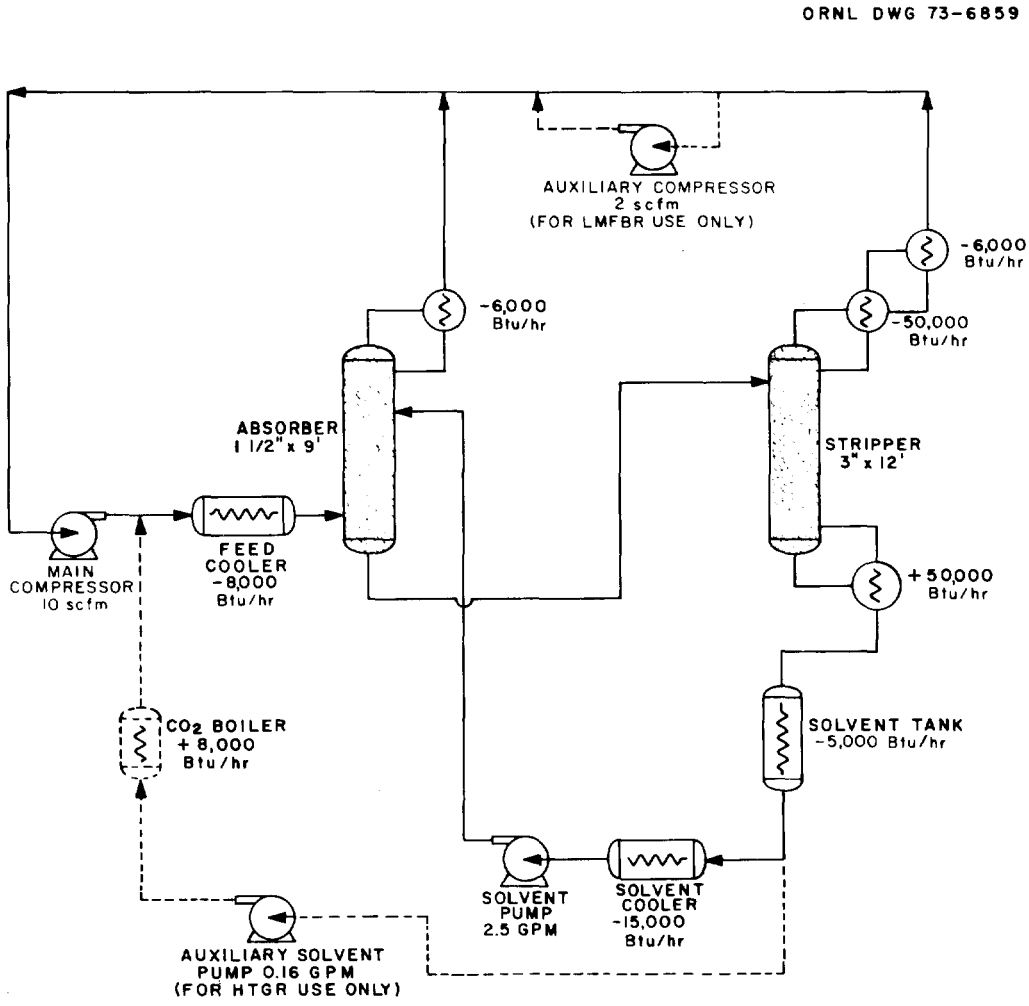

Figure 2. Experimental Engineering Section Off-Gas Decontamination Facility.

EES-ODF operations. Figure 3 presents the various sample and monitor points allowed for in the system. All sampling is effected from a central station using electrically activated values. Figure 4 illustrates a portion of the sampling hardware as it pertains to the absorber column.

Operating conditions vary, depending on which reprocessing off-gas is being investigated, but typical conditions for the absorption operations are in the temperature range of -15°C to -40°C at a nominal pressure of 20 atm. Stripping conditions for the HTGR off-gas study are similar to the absorption conditions, except for differing liquid-to-vapor ratios. Typical flow rates for the various streams range from 5 to 10 scfm for the gas and from 1 to 2 gpm for the liquid.

The ORGDP Pilot Plant is similar in operational aspects to the EES-ODF. In addition to the absorber and stripper columns present in the EES-ODF, the pilot plant employs a fractionator to separate lighter gases coabsorbed with the krypton during the absorption step prior to stripping the krypton from the liquid CO_2 stream. The basic flowsheet for the pilot plant is similar to that depicted in Figure 1 with the various streams combined for total recycle operation. The size of the pilot plant is approximately 2 to 3 times that of the EES-ODF.

Scheduled Objectives

Presently, the combined schedule for HTGR studies in both facilities allows for two campaigns in the EES-ODF followed by one campaign in the pilot plant during the next 12 months. The first EES-ODF campaign is scheduled for completion by September 30, 1974, and the primary objective will be to complete fluid dynamics studies with special emphasis on packed column performance relating specifically to the woven-wire mesh packing currently in use. Peculiarities in the packing performance were observed in the earlier operation of the EES-ODF and subsequently confirmed by special testing at the ORGDP Pilot Plant. An understanding of the packing performance, viz., flooding, pressure drop, etc., is so fundamental to subsequent design and operations efforts that resolution of the observed discrepancy between actual and predicted performance is considered top priority. During the fluid dynamic studies, final shakedown, testing, and calibration of Kr monitoring equipment, fluid sampling components, and fluid analysis equipment will proceed simultaneously. All systems should be ready during the latter part of the first campaign for acquisition of preliminary dynamic distribution data. As indicated, these data will be preliminary insofar as the primary objective in the latter portion of Campaign 1 will be to provide a totally operable system for Campaign 2.

Campaign 2 for the EES-ODF is scheduled for completion in the latter part of February 1974. At that time the facility should be ready for a major effort to collect mass transfer and dynamic distribution data on Kr-light gas-CO_2 systems. Details of operating conditions will have been established throughout Campaign 1 in line with observed mechanical and fluid dynamic capabilities. Campaign 2 will focus on selected operation of the absorption column for absorption-related data and on selected operation of the stripper column for fractionation and stripping-related data. Both the absorption and stripping portions of the EES-ODF will be operated simultaneously, but only limited data will be available from one system while the other system is being studied in detail, since operating conditions for one system are prescribed by default once particular conditions are selected for the other.

The single campaign scheduled for KALC studies in the ORGDP Pilot Plant will commence shortly after Campaign 2 is completed in the EES-ODF, and will generally involve a restricted range of variables based on favorable conditions derived from

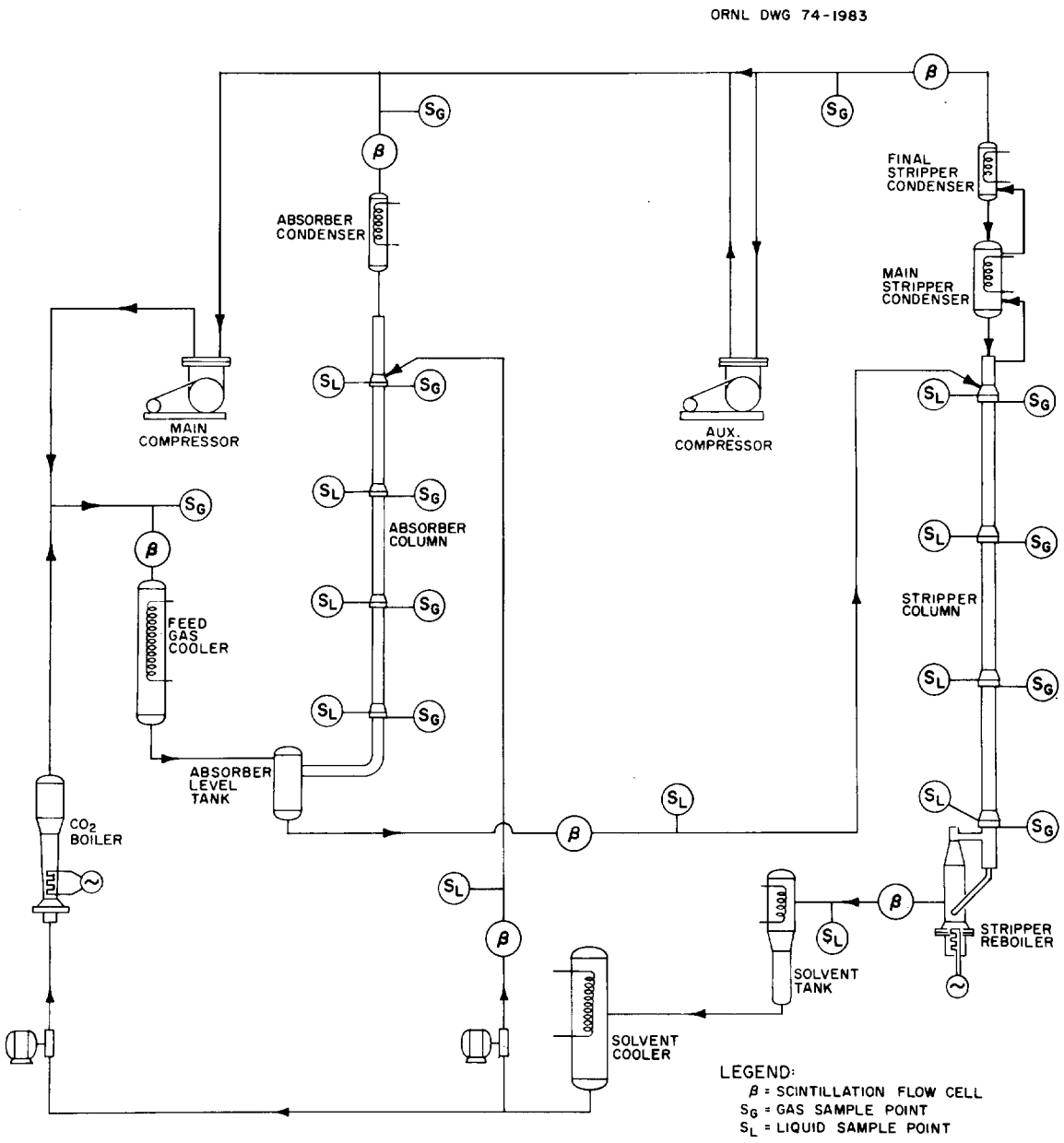

Figure 3. Sample and Monitor Points in the EES-ODF.

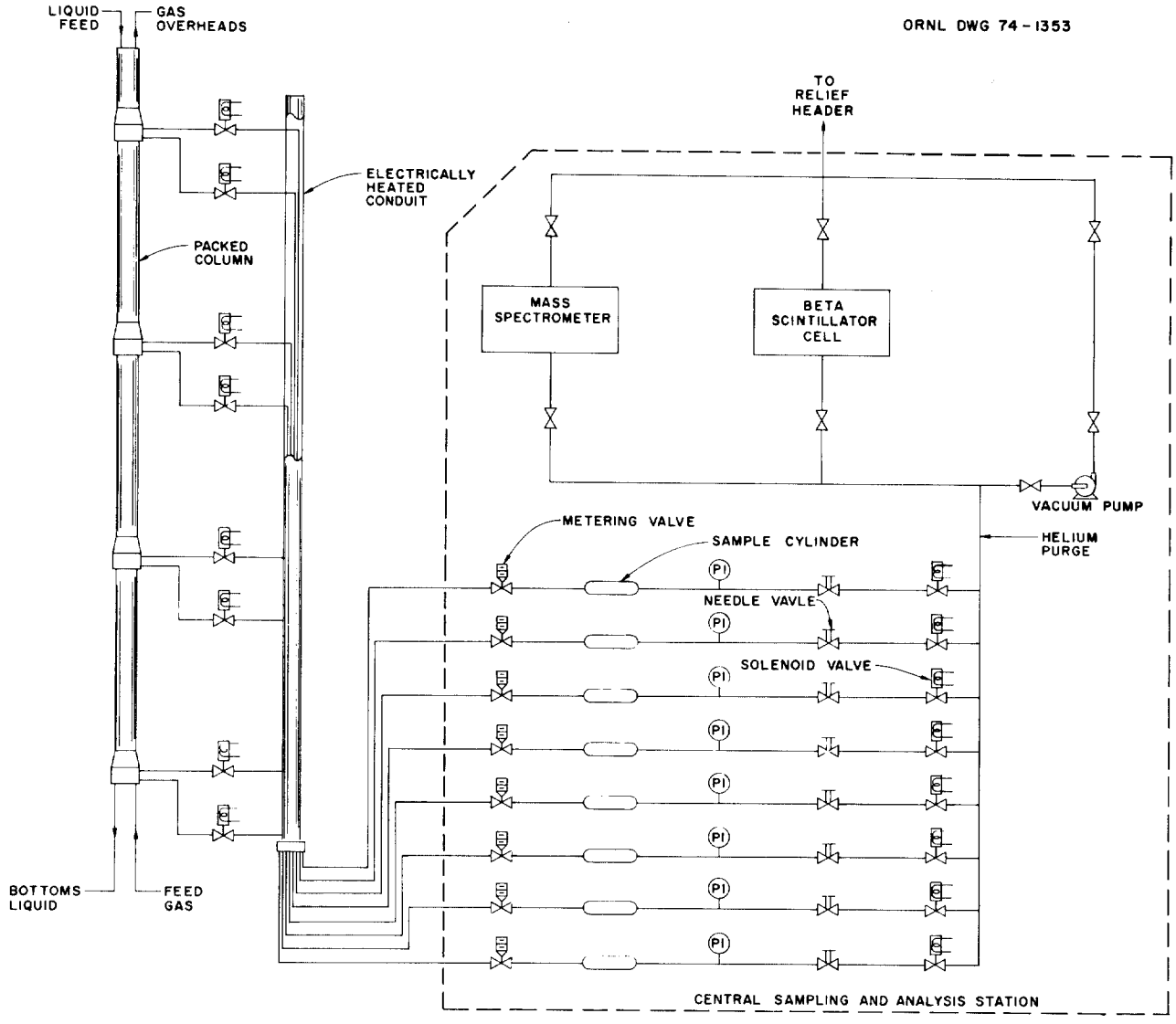

Figure 4. Absorber Column Sampling System Schematic.

operations of the EES-ODF. Any troublesome aspects of semi-long-term pilot plant operations will be subsequently given closer attention in the smaller-scale EES-ODF. Overall objectives for the pilot plant activities will include confirmation of individual absorption, stripping, etc. studies conducted in the EES-ODF in an integrated operations fashion.

Preliminary Experimental Results

Feasibility studies of the basic KALC process were conducted on an engineering scale in November and December of 1971. The experiments were conducted in the former ORGDP Selective Absorption Pilot Plant and demonstrated both the operability and potential efficiency of the basic process.

Since the early studies, the ORGDP Selective Absorption Pilot Plant has been replaced with an upgraded system to accommodate the present off-gas studies. Additionally the design, fabrication, and installation of the EES-ODF have been completed at ORNL. Both systems have undergone most of the shakedown tests and have, to a limited extent, operated as scheduled for short-term tests.

The bulk of early testing in the EES-ODF has centered around fluid dynamics studies of the packed columns. Figure 5 indicates the findings to date for observed flooding vs. predicted.* Other tests indicate a significant amount of influence by column samplers so that packing performance alone cannot account for the lowered flooding velocities. Samplers are presently being removed, and additional testing will provide unequivocal flooding information relating directly to the packing.

A single early campaign at the ORGDP Pilot Plant has confirmed the flooding data observed in the EES-ODF. Primarily, this initial campaign was designed to realistically shake down the newly constructed plant under expected KALC processing conditions. Krypton tracer was not used for the initial campaign, and O_2-CO_2 system performance data are being analyzed now. It appears that no significant deviations from past experience or general theory will result from the data analysis.

Determination of the krypton decontamination factor and the krypton concentration factor will depend on the ability of monitoring equipment to resolve extremely low concentrations of ^{85}Kr. In-line beta cells are being developed to take advantage of the predominant beta radiation from the ^{85}Kr isotope. Figure 6 illustrates the early version of the beta cell. Background considerations are practically eliminated with beta counting, and the amount of scintillation material can be varied to accommodate the expected concentrations. Figures 7 and 8 indicate the observed performance of the beta cell chamber during background and density effect testing. Observed counting effectiveness for the cell is approximately 80% based on a measured efficiency of 13.3% relative to a calculated (theoretical) efficiency of 16%.

Discussion

Development of the KALC process is proceeding on a timely schedule and will provide important information within the next few months. Resolution of typical development problems such as flooding performance, monitoring techniques, general system operability, etc., are receiving the priority effort which they must have during the early stages of development.

---

*Prediction based on vendor-supplied design information for Goodloe Packing; Packed Column Co., a division of Metex Corp., Edison, N. J.

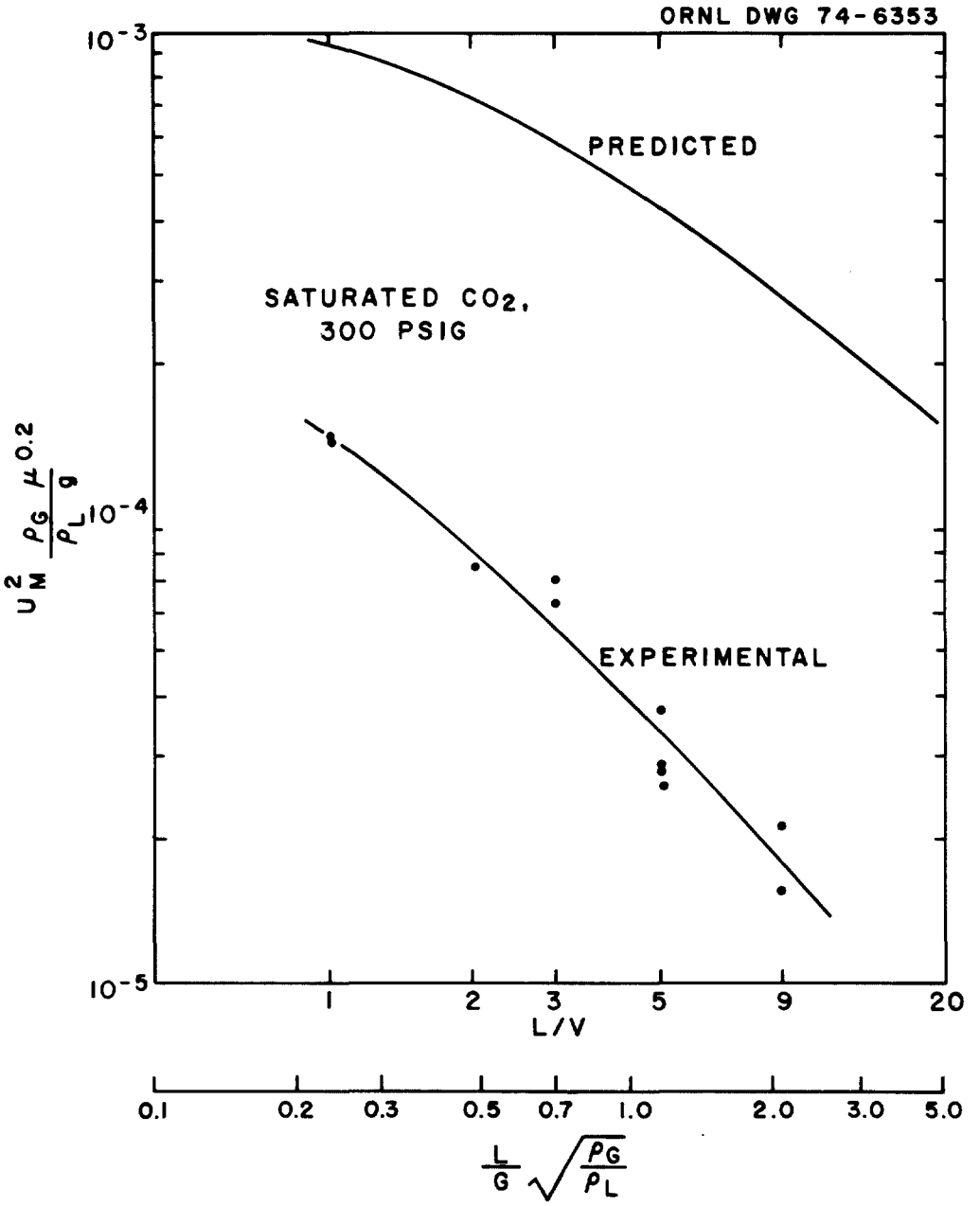

Figure 5. Flooding Curves for the EES-ODF Stripper Column.

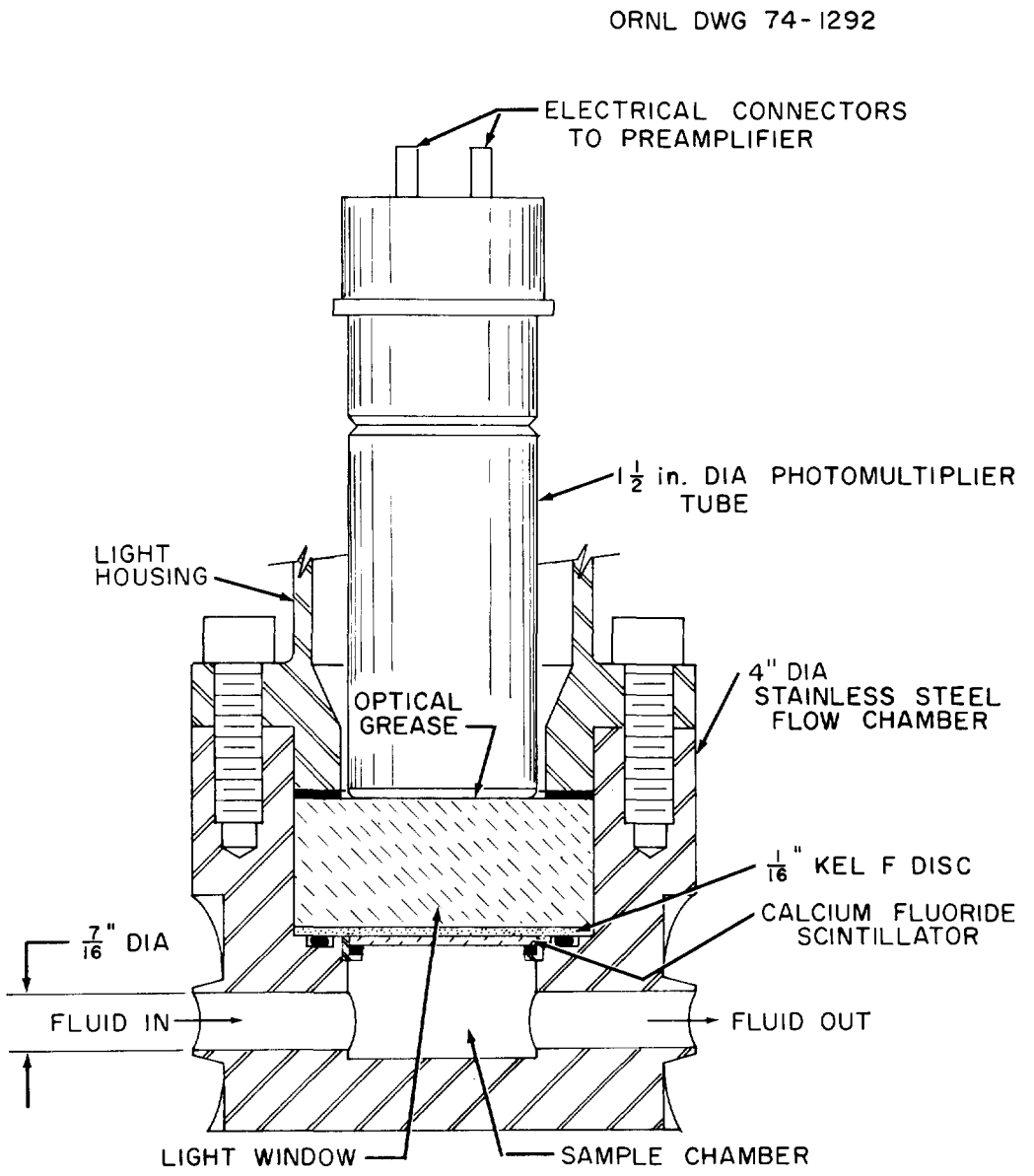

Figure 6. Beta Scintillation Flow Cell Detector.

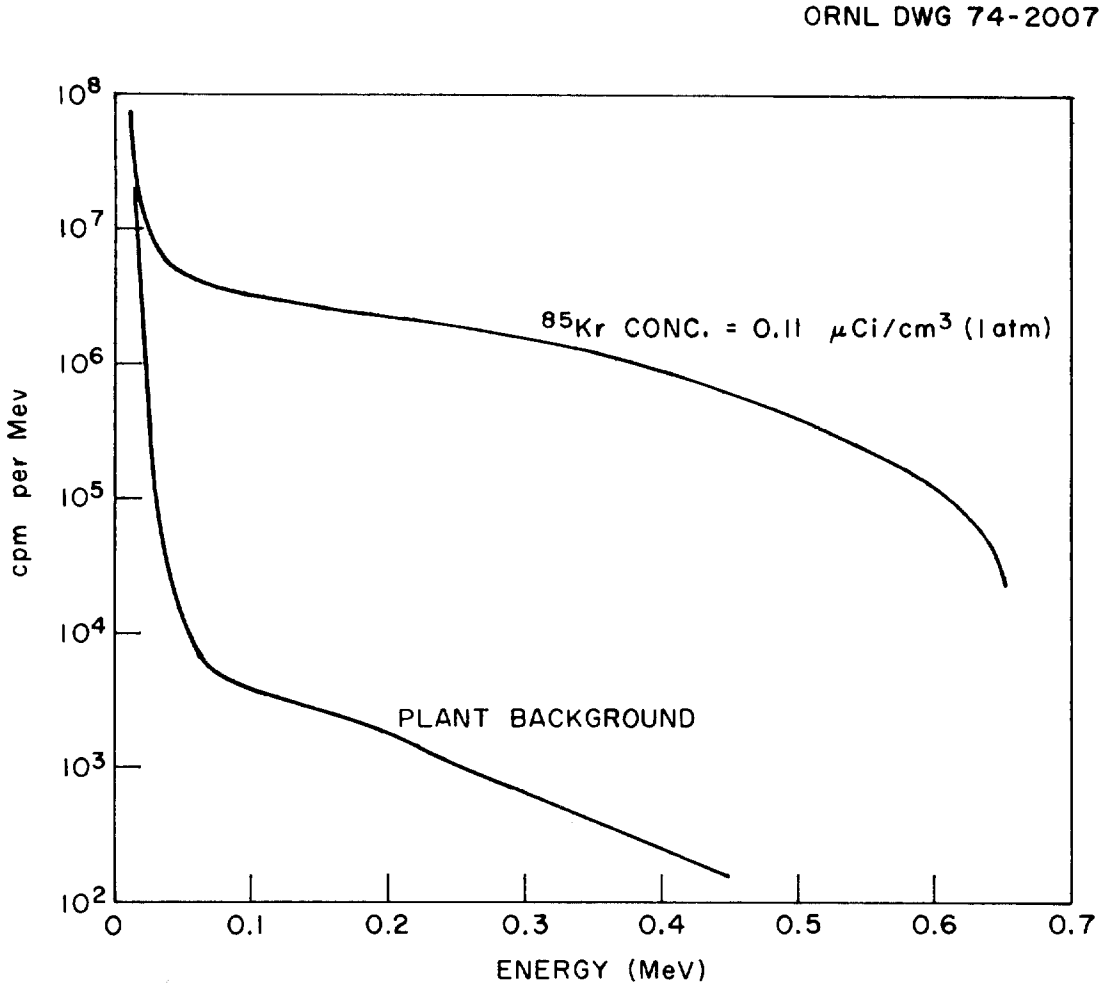

Figure 7. ^{85}Kr Energy Spectra for the Beta Flow Cell Detector.

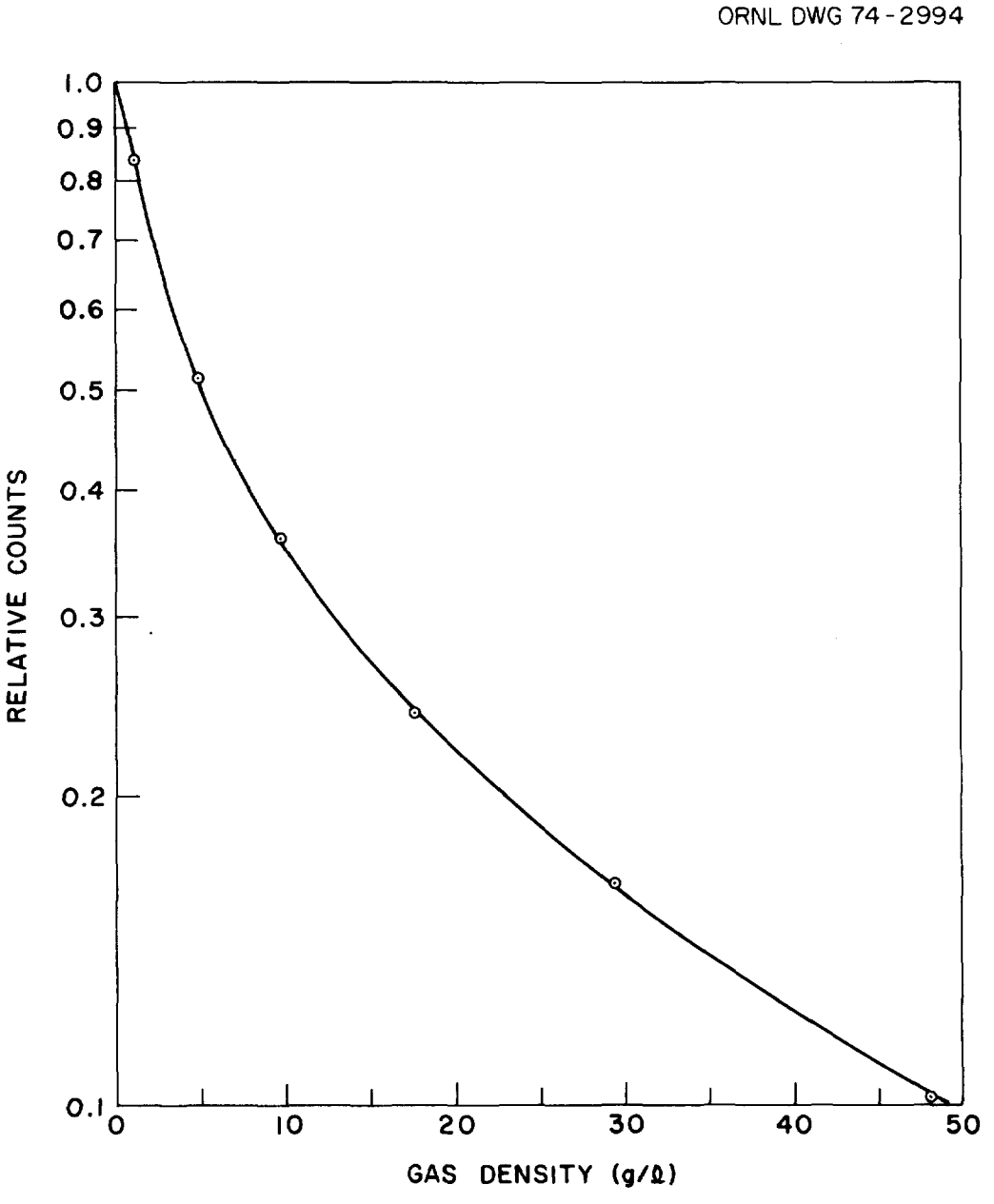

Figure 8. Effect of Density on the Count Rate (Fixed Quantity of ^{85}Kr) in the Beta Scintillation Flow Cell.

References

1. M. E. Whatley, R. W. Glass, P. A. Haas, A. B. Meservey, and K. J. Notz, "Decontamination of HTGR Reprocessing Off-Gases," Proceedings of the 12th AEC Air Cleaning Conference, August 28-31, 1972, pp. 86-99.

DISCUSSION

BENDIXSEN: Would you care to comment on the relative composition of the krypton - xenon product, in the waste products, particularly with reference to the oxygen and carbon monoxide concentration?

GLASS: The xenon problem has not been quantified yet simply because xenon is not present in large amounts and it is non-radioactive. The concentration of it in any stream would, of course, depend on desired operation of a column. One could operate to produce in the krypton stream as much or as little of the xenon as one desired. The concentration of lighter gases, carbon monoxide, etc., in various streams will depend on what is transpiring upstream of the process; namely, conversion of CO to CO_2, or oxygen to CO_2. The compositions in the various streams would be affected by the length of the column, which is, in large part, the goal of the basic studies that we are conducting now.

KOVACH: Are you postulating iodine in the pathways through the system or are you postulating that the iodine would be removed prior to the gas entering the system? A second question; because I was given a very hard time in the near past about operating a system at 100 PSI, I would like to get your opinion on operating at 300

GLASS: For the first question concerning iodine, the effect has been idicated in various conceptual and other flow sheets and is treated as a separate item. Tritium is treated as well prior to the count process. We are also aware that there has been some investigation of iodine-CO_2 equilibria, which indicates, and to some extent is based on,the fact that some amount of iodine may be presumed to be present. If there were no prior processing steps, we would be able to concentrate the iodine from the liquid stream leaving the process. It is hoped that if this particular additional process is not developed along with the basic CO_2 system that we will continue to receive the necessary priority to be functional when the hot demonstration pilot plant is used. We would want iodine removal to occur prior to CO_2 and to be able to study iodine behavior in the CO_2 system itself. We believe that iodine will go with the liquid CO_2. Regarding 300 PSI, we are not using a high pressure system. Standard schedule 40 pipe handles our pressures quite easily and we have had no major problems. Once we find a leak, we tighten it up and it's fixed. I think high pressure operations, 60 atmospheres, for example, might be a problem, but we don't see problems from using 300 PSI.

AKUT - A PROCESS FOR THE SEPARATION OF AEROSOLS, KRYPTON, AND TRITIUM FROM BURNER OFF-GAS IN HTR-FUEL REPROCESSING

M. Laser, H. Barnert-Wiemer, H. Beaujean, E. Merz and H. Vygen

Institute for Chemical Technology
Kernforschungsanlage Jülich GmbH
517 Jülich / Germany

Abstract

The AKUT-process consists of the following process steps:
- aerosol retention by an electrostatic separator followed by HEPA filters,
- oxidation of CO with O_2 or reaction of excess O_2 with CO, respectively,
- compression,
- scrubbing and/or liquefaction,
- separation of krypton by distillation,
- separation of tritiated water and iodine by adsorption or chemical reaction.

Liquefied off-gas with low permanent gas content resulting from graphite burning with oxygen may be distilled at ambient temperature. Off-gas with higher permanent gas content from burning with oxygen enriched air must be processed at lower temperature. The ambient temperature flowsheet is preferable from economic as well as safety point of view.

Introduction

Reprocessing plants are the most important sources of radioactive releases into the atmosphere. Presently these plants emit krypton and tritium quantitatively. Other isotopes are discharged to a higher or smaller extent. The radiation burden to the public in the neighbourhood of such plants resulting from these releases are relatively small as long as the plant size is small and the decay time of the depleted fuel elements is high. Economic considerations, however, call for a plant size which serves for approximately 50,000 MWe installed electric power and about 150 days decay time for LWR and HTR fuel elements. Using the present state of the art the resulting radiation burden may be well above the radiation limits recommended by several national authorities which are more restrictive than the ICRP radiation limits (1). The German Atomic Energy Commission, for instance, has recommended to limit the radiation dose outside a nuclear plant area to no more than 30 mrem/a from gaseous effluents.

Improvement of the currently applied technique can only reduce the radiation burden to a small extent, for instance in the case of iodine or aerosols. Further reduction requires new processes for the separation of krypton and tritium. From a practical as well as an economic point of view, however, it is necessary to develop an off-gas cleaning system which considers all the important isotopes.

Special tasks arise from reprocessing of HTR fuel elements

because of the high burner off-gas volume.

Off-gas Purification in HTR Reprocessing Plants

Most of the radioactivity released during reprocessing of HTR fuel elements is liberated during the burning of the graphite matrix and the following dissolution of the heavy metal ash.

The total amount of radioactive isotopes and the calculated radiation dose outside a 50,000 MWe HTR fuel reprocessing plant with an annual throughput of about 365 t of heavy metal using the present state of the art are given in table I. The data show very clearly the order of the problem:

- ^{14}C cannot be separated by achievable means. The radiation burden can be reduced only by higher atmospheric dilution, for instance by increasing the stack hight, or by choosing a plant site which is not used by farming.
- ^{3}H, ^{85}Kr, and ^{129}I should be retained to more than 99%.
- ^{131}I retention must be improved by a factor of 100.
- aerosol retention should also be improved by a factor of 10.

The relative amount of liberation during the respective process steps strongly depends on the type of the fuel elements. With carbide fuels nearly 100% of the noble fission gases, iodine, and tritium are volatilized during the burning step. The aerosol content is relatively high. From oxide fuel elements however only about 10% krypton, 10 to 50% tritium and small amounts of iodine and aerosols are found in the burner off-gas.

For an effective off-gas cleaning process an unnecessary dilution should be prevented and special purification processes should be applied for the several off-gas types. Following this philosophy we are developing separate off-gas purification systems for burner and dissolver off-gas:

- the AKUT process for the separation of aerosols, krypton, and tritium as well as iodine from burner off-gas, and
- the CRYOSEP process for the separation of noble gases from the dissolver off-gas (2).

In special cases however it may be expedient to combine both off-gas streams before off-gas cleaning (Figure 1).

AKUT Flow Sheet

The AKUT process consists of the following steps:

- aerosol retention by an electrostatic separator followed by HEPA filters,
- oxidation of carbon monoxide with oxygen or reaction of excess oxygen with carbon monoxide, respectively,
- compression,
- scrubbing and/or liquefaction,
- separation of krypton by distillation,
- separation of tritiated water and iodine by adsorption or chemical reaction.

Table I Calculated annual radioactive release with gaseous effluents from a 50,000 MWe HTR reprocessing plant

Reactor Type		HTR						
Burn-up	MWd/t	100,000						
Throughput	t/yr	365						
	t/d	1.2						
Decay Time	d	150						
		^{3}H	^{14}C	^{85}Kr	^{129}I	^{131}I	Aerosol β	Aerosol α
Throughput	Ci/yr	$1.6 \cdot 10^{6}$	$5.0 \cdot 10^{3}$	$2.5 \cdot 10^{7}$	50	$1.4 \cdot 10^{3}$	$3.75 \cdot 10^{9}$	$2.7 \cdot 10^{7}$
Fractional Release		1	1	1	0.01	0.01	10^{8}	10^{-8}
Emission	Ci/yr	$1.6 \cdot 10^{6}$	$5.0 \cdot 10^{3}$	$2.5 \cdot 10^{7}$	0.5	14	38	0.3
Concentration	Ci/m^3	$5.1 \cdot 10^{-9}$	$1.6 \cdot 10^{-11}$	$8.0 \cdot 10^{-8}$	$1.6 \cdot 10^{-15}$	$4.5 \cdot 10^{-14}$	$1.2 \cdot 10^{-13}$	$0.9 \cdot 10^{-15}$
Mat.Conc./Fallout	Ci/m^3	$4 \cdot 10^{-14}$	$1.1 \cdot 10^{-12}$	$1.5 \cdot 10^{-11}$	$1 \cdot 10^{-18}$		$01-2 \cdot 10^{-12}$	
Inhalation Dose	mrem	12.8	0.3		0.3	1.5	4	14
Submersion-β-Dose	mrem	0.3	0.01	185				
Submersion-γ-Dose	mrem			9				
Ingestion Dose	mrem	70	20		230	365	15	
Total	mrem	83	20	194	230	365	19	14

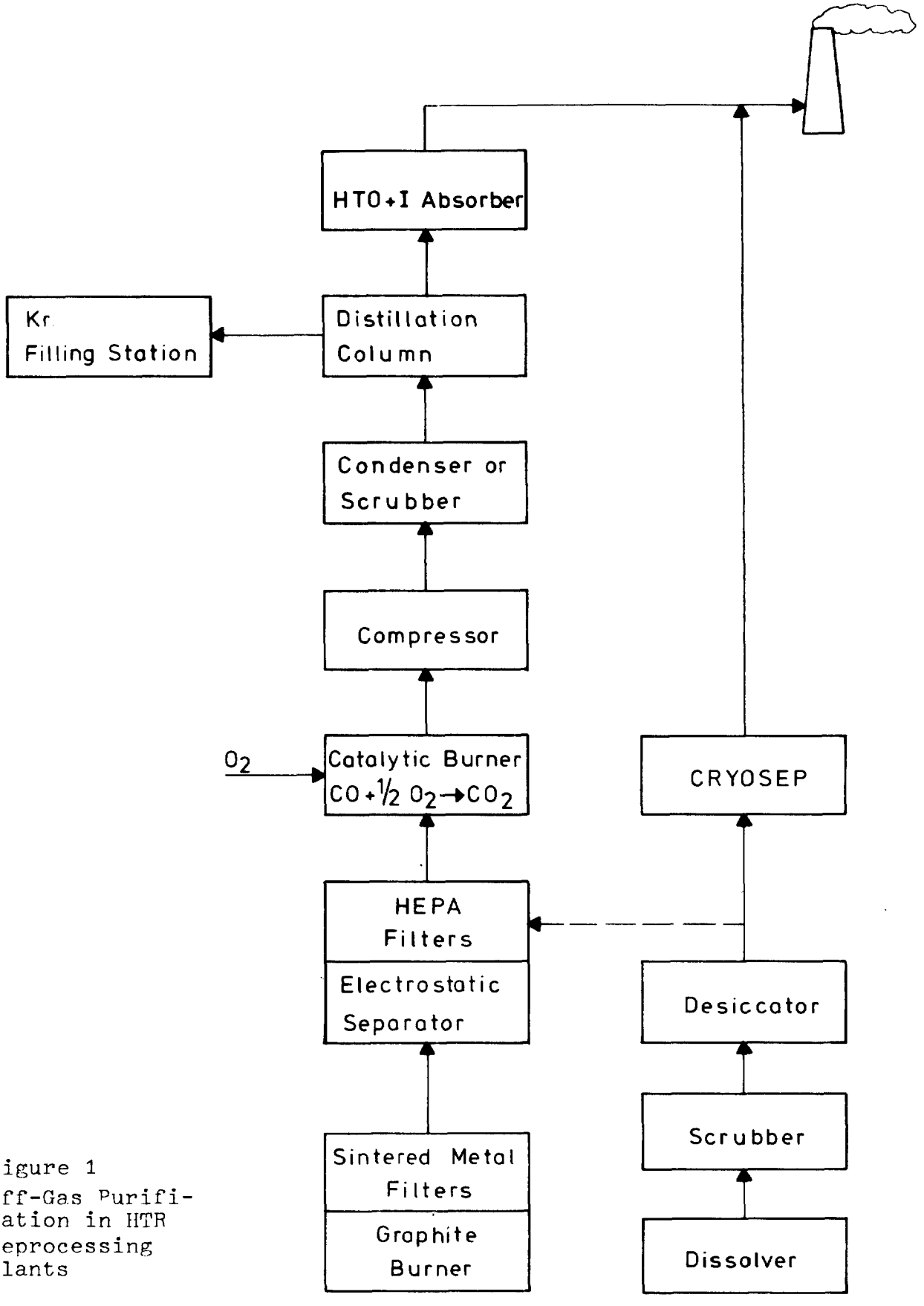

Figure 1
Off-Gas Purification in HTR Reprocessing Plants

After expansion, the purified gas will be discharged through the stack.

The special design of the process steps "scrubbing and/or liquefaction" and "separation of krypton by distillation" strongly depends on the permanent gas content.

The fluidized bed burner designed in Jülich will run with pure oxygen (3). The resulting off-gas contains about 20 to 30% carbon monoxide and 80 to 70% carbon dioxide. After oxidation of the CO the permanent gas content, mainly oxygen, is lower than 5%. This off-gas can be liquefied completely at 20°C and about 80 atm. The distillation of the liquid may occur above 0°C (Figure 2).

The combination of the carbon dioxide rich burner off-gas and the air containing dissolver off-gas results in an unsignificant increase in the permanent off-gas content, because the dissolver off-gas volume from a closed continuously running dissolver is lower by about three orders of magnitude than the burner off-gas volume (4). Therefore the combination of these two off-gas streams before or after the catalytic burner should not cause additional problems.

A higher permanent gas content results from using oxygen enriched air for burning the graphite. At $\leq$20% permanent gas the off-gas can be completely liquefied too, however lower temperatures and higher pressures must be applied (Figure 3).

Between 20 and about 70% permanent gas the gas mixture must be compressed and cooled to about -40°C. Under these conditions the gas is partially liquefied. The remaining gas phase must be scrubbed with the bottom product from the distillation. The combined condensate and scrub solution is fed to the distillation column. The complete process must be run at temperatures between -40 and -50°C (Figure 4).

The utilization of oxygen enriched air is mainly dictated by economic considerations. On the other hand, however, the off-gas cleaning system becomes more and more complicated and expensive with increasing permanent gas content. A detailled economic comparison of ambient and low temperature AKUT process has not yet been finished. However it seems to be evident that burning with oxygen and off-gas purification with ambient temperature AKUT process will be preferable from the economic as well as safety point of view.

In the following chapters both variants of the AKUT process are described. However, so far extensive technical experience is available only for the ambient temperature AKUT process.

Deviating from our early concept (5), this flowsheet dispenses with a separation of the permanent off-gas component before distillation, because surprisingly krypton is enriched to a much higher degree than the more volatile oxygen and nitrogen at the top of the distillation column.

Ambient Temperature AKUT Process

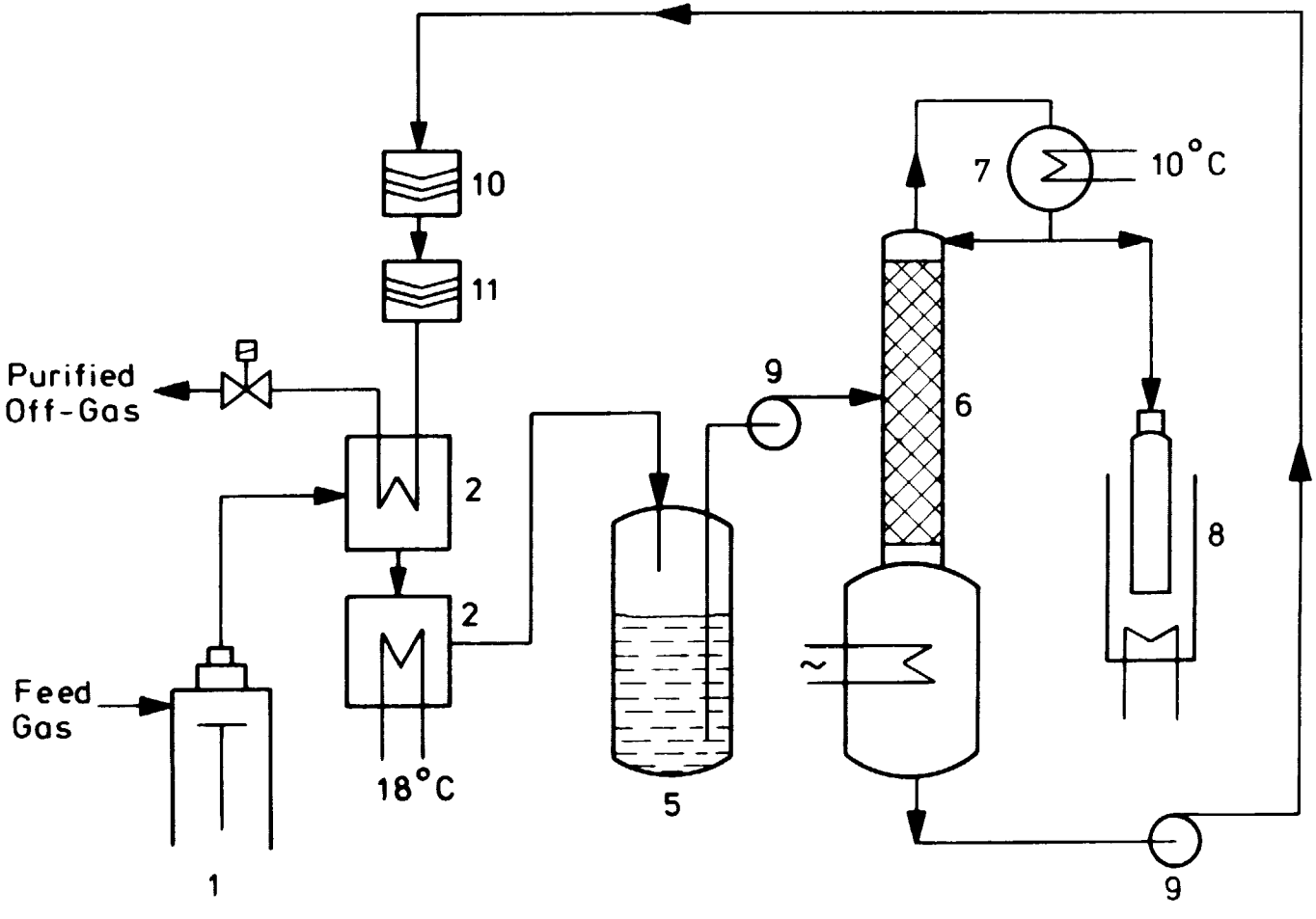

1 Compressor
2 Heat Exchanger
5 Pressure Vessel
6 Distillation Column
7 Condenser
8 Krypton Filling Station
9 Pump
10 Tritium Absorber
11 Iodine Absorber

Figure 2 AKUT Flow Sheet (< 10% permanent gas)

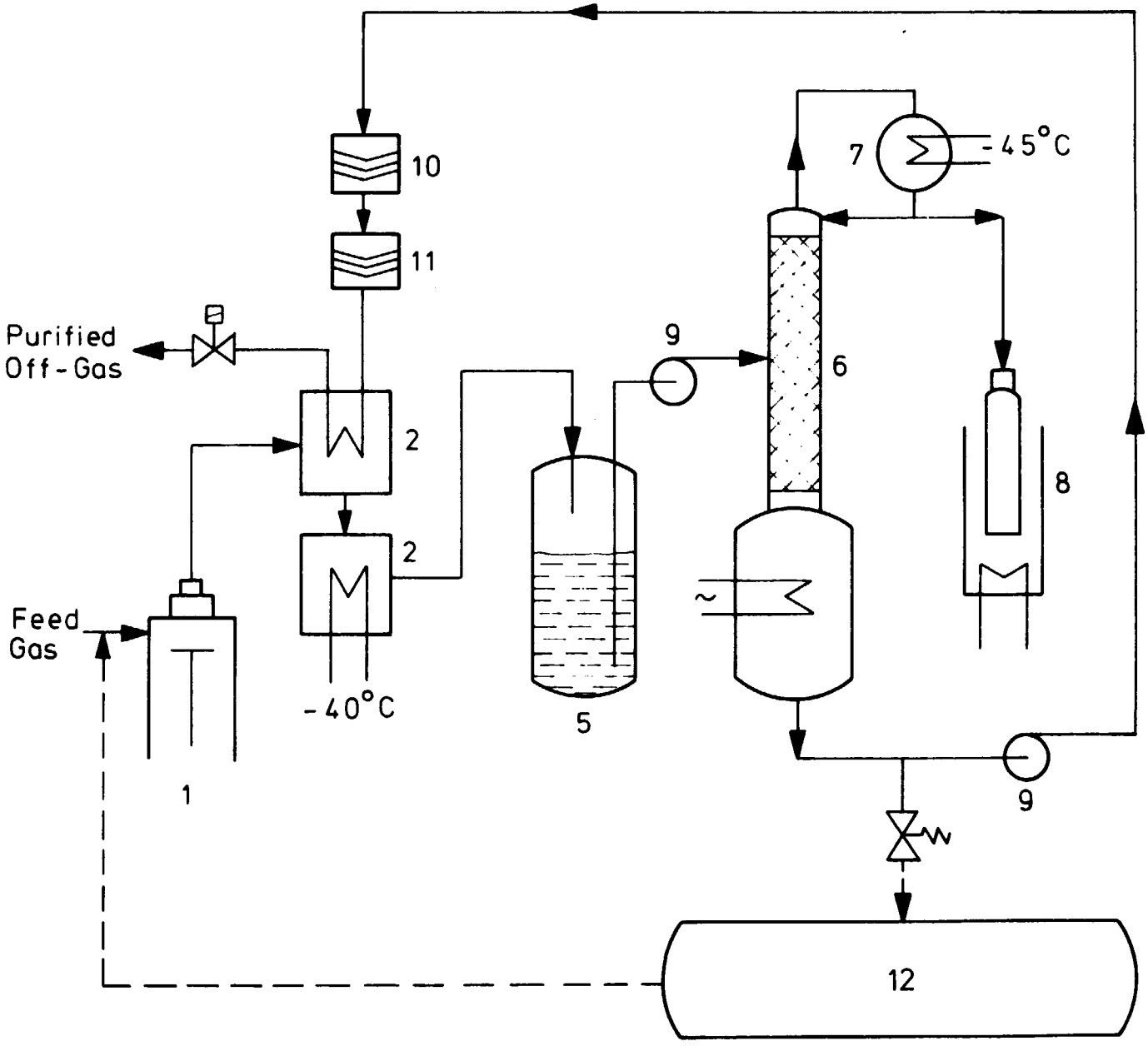

1 Compressor
2 Heat Exchanger
5 Pressure Vessel
6 Distillation Column
7 Condenser
8 Krypton Filling Station
9 Pump
10 Tritium Absorber
11 Iodine Absorber
12 Safety Pressure Vessel

Figure 3
AKUT Flow Sheet
(10-20% permanent gas)

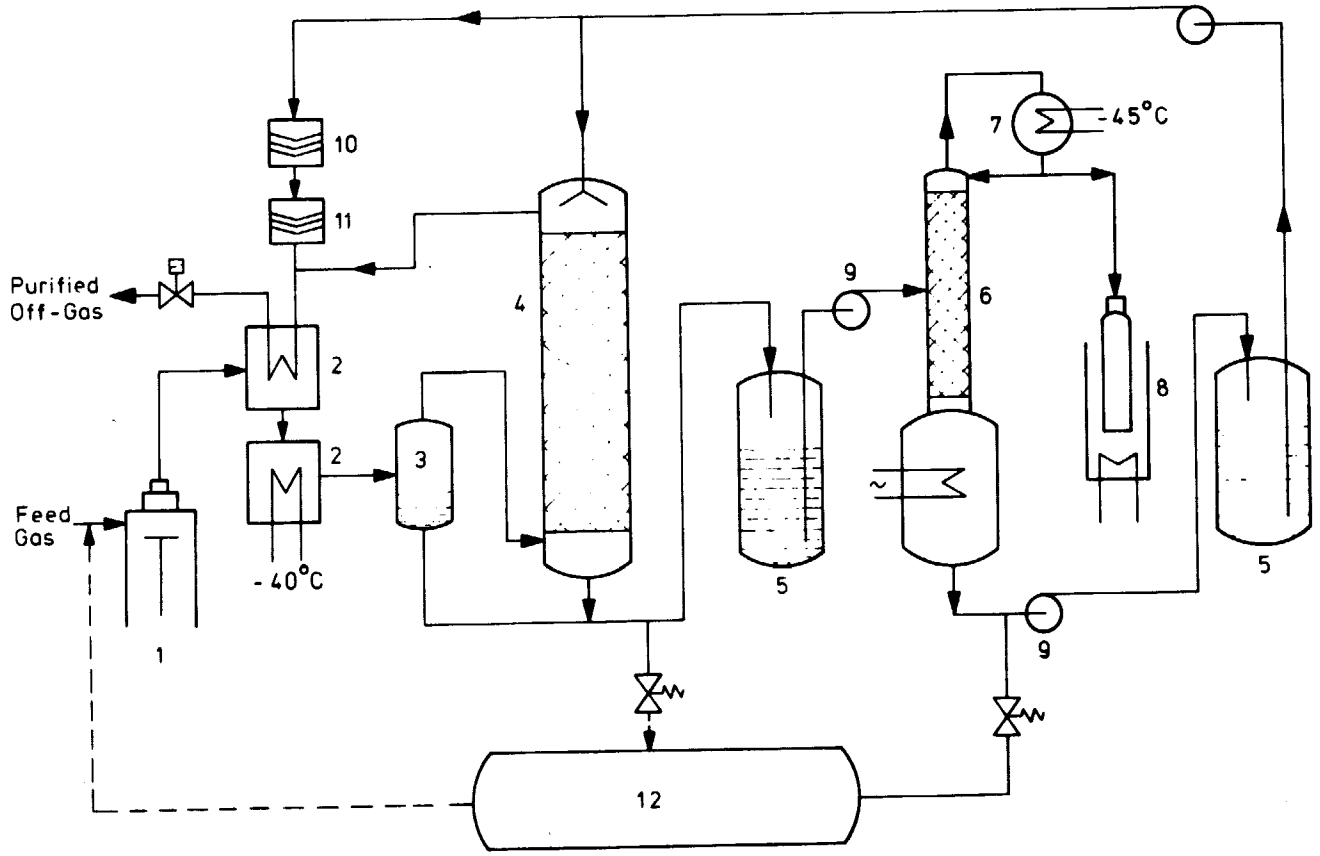

1 Compressor
2 Heat Exchanger
3 Phase Separator
4 Scrubber
5 Pressure Vessel
6 Distillation Column
7 Condenser
8 Krypton Filling Station
9 Pump
10 Tritium Absorber
11 Iodine Absorber
12 Safety Pressure Vessel

Figure 4 AKUT Flow Sheet (> 20% Permanent Gas)

Composition of the Off-gas

Under normal operation conditions the off-gas from burning the graphite matrix of depleted HTR fuel elements consists of about 20 to 30% carbon monoxide and 80 to 70% carbon dioxide. During start-up and shut-down of the burner the CO content may increase up to 80%. Also 10% oxygen were found during these phases.

The radioactivity of the off-gas fluctuated extremely. It depends on the type of the fuel element, its burn-up, the temperature of the furnace and of the sintered metal filters, plate out in the ducts and so on (6). Some typical compositions are given in table II.

Table II Radioactive contamination of burner off-gas

Isotope	Radioactivity Ci/m^3
^{3}H	0.01 - 0.1
^{14}C	$1 - 5 \cdot 10^{-4}$
^{85}Kr	0.1 - 1
^{137}Cs	$10^{-3} - 10^{-1}$

^{134}Cs and ^{137}Cs and eventually ^{131}I are the most important aerosol activities. Other nonvolatile isotopes like ^{106}Ru and ^{144}Ce could be detected only after special analytical separation. Their activities are lower by two orders of magnitude. The favoured cesium release into the off-gas may be caused by passing the hot sintered metal filters as cesium vapour and condensing to aerosols after cooling in the ducts, whereas real aerosols and dust are retained by the sintered metal filters to a high degree.

Aerosol Separation

The aerosol separation is necessary to avoid poisoning of the catalytic burner. The separation process occurs by electrostatic separators followed by HEPA filters.

The electrostatic separator used in our hot cell experiments has been designed by the German company JUCHO - Dortmund. It is equipped with a 4-stage anode and is running with 15 kV and about 50 uA (Figure 5).

In the electrostatic separator mainly cesium and iodine are deposited. The ^{137}Cs activity could be reduced to about $4 \cdot 10^{-6}$ Ci/m^3 independently of the radioactivity before the electrostatic separator. The resulting decontamination factor was in the order of 100 to 10,000 for cesium. For iodine the decontamination factor fluctuated very strongly between about 2 and more than 100. This scattering may result from changing distribution of iodine between the aerosol and

gaseous form.

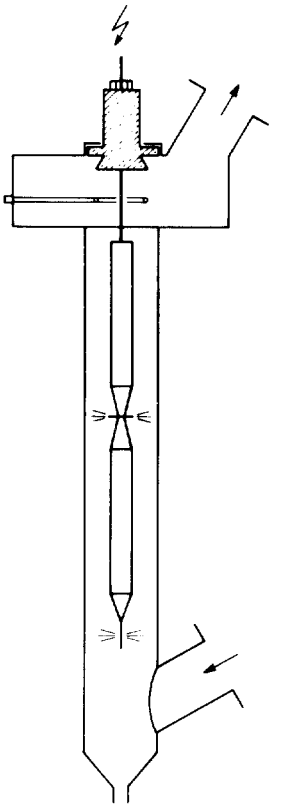

Figure 5 Electrostatic separator

The main advantage of the electrostatic separator is a lower radioactive deposition on the HEPA filters. In a 50,000 MWe reprocessing plant with about 30,000 m^3 burner off-gas per day containing 0.1 Ci $^{137}Cs/m^3$ one must collect about 3000 Ci ^{137}Cs per day. To manipulate HEPA filters with such high contamination would be extremely, difficult and very expensive.

Since the cesium activity can be reduced by electrostatic separators from 0.1 Ci/m^3 to 4.10^{-6} Ci/m^3, the bulk of the radioactivity is removed before the HEPA filters, which then are used for the final purification step. We have found that with HEPA filters the aerosol radioactivity of the electrostatic separator effluent could be further reduced below our detection limit (10^{-10} Ci $^{137}Cs/m^3$).

Oxidation of Carbon Monoxide

The aerosol free off-gas now enters the catalytic burner to oxidize carbon monoxide by addition of oxygen or to reduce an excess of oxygen by addition of carbon monoxide. To be sure that no explosive reaction between carbon monoxide and oxygen may take place in the following high pressure part of the equipment the resulting gas must be free of CO. The permanent gas content however should be lower than 5% for complete liquefaction at room temperature.

The catalytic burner equipment designed by DECATOX Frankfurt/M. is schematically shown in figure 6. The off-gas as well as oxygen or carbon monoxide, respectively, are fed into a circulating off-gas stream and heated to about 350°C. The reaction between carbon monoxide and oxygen is catalyzed by a palladium catalyst. The heat of reaction is discharged in the following heat exchanger. A part of the circulating gas is withdrawn for further processing. The process is controlled by continuous measuring of the carbon monoxide content before the catalytic burner and the oxygen content after the burner.

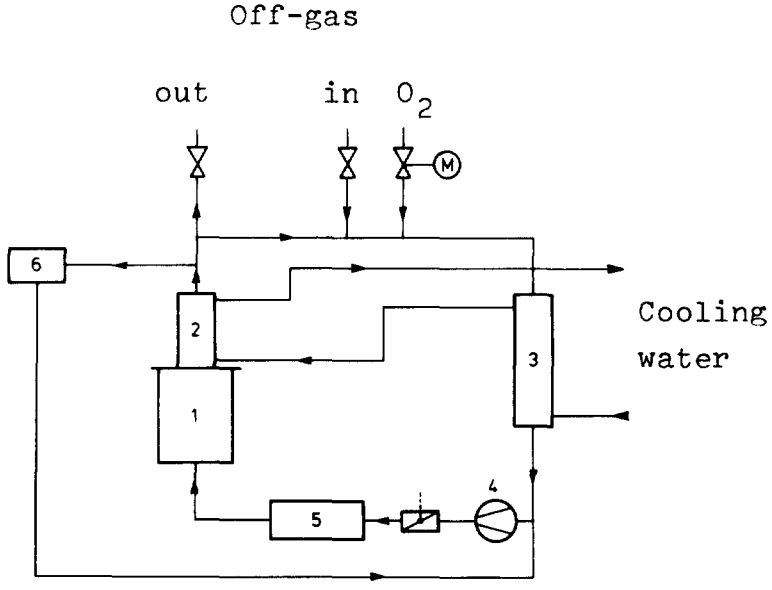

1 Catalyst
2 Heat exchanger
3 Heat exchanger
4 Fan
5 Gas heater
6 O_2 analysator

Figure 6 Catalytic burner

The ratio of the volume of circulating gas to the volume of feed gas is mainly given by the maximum permitted temperature of the catalyst (about 600°). This ratio is about 10 or 20:1. Under these conditions no explosive mixture can be formed.

Special emphasis must be paid to the gas tightness of the equipment, especially of the fan, because inleaking air will produce a relatively high permanent gas content in the resulting gas.

The catalytic burner used in our hot cell experiments has been designed for the oxidation of about 25% CO with oxygen. The resulting oxygen excess should be smaller than 0.5%. During normal operation of the graphite burner these conditions could be met easily. Fast changes in the gas composition during start-up and shut-down periods however result in a higher oxygen excess up to about 8%.

Compression and Liquefaction

The off-gas withdrawn from the catalytic burner is compressed with a 3-stage piston compressor with extremely low leak rate, a so-called helium compressor, to about 70 to 80 atm. Under these conditions the dew point is reached and tritium containing water is partially condensed. After condensation the gas contains about 100 to 200 ppm water.

After passing a heat exchanger, the liquefied gas is stored in a pressure vessel.

Distillation

The liquefied gas is pumped into a distillation column. At the top a krypton rich $Kr/O_2/CO_2$-mixture is withdrawn whereas at the bottom nearly krypton free liquid CO_2-O_2-mixture containing tritiated water is discharged.

It is a surprising effect, that at the top of the distillation column the lower volatile krypton is more enriched than the higher volatile oxygen. This effect is clearly seen from figure 7, which displays a batch distillation of a 0.1% $Kr/0.3\%$ O_2/CO_2 mixture. According to this effect it is possible to separate the krypton without foregoing stripping of the oxygen. This results in a important simplification of the process.

The experiments with a 2 m long, 4 cm diameter distillation column gave enrichment factors for krypton at the top of about 100. Starting from a 1000 ppm Kr containing simulated gas the maximum krypton concentration at the top was about 25 weight-%. With real burner off-gas which contains no more than about 20 ppm krypton also enrichment factors of about 100 could be reached. For final disposal however a further enrichment is necessary. At the bottom the depletion factor was about 100.

These experimental results will be taken into account for the design of the second generation distillation column.

Absorption of Tritium

For the sorption of tritiated water from the liquid off-gas discharged from the bottom of the distillation equipment, molecular sieves, magnesium perchlorate, and phosphorus pentoxide were used. The best results were obtained with phosphorus pentoxide and magnesium perchlorate which reduce the humidity in the effluent to 8

and 12 ppm H_2O, respectively. With molecular sieves a constant humidity could not be reached, presumably because carbon dioxide is strongly adsorbed too.

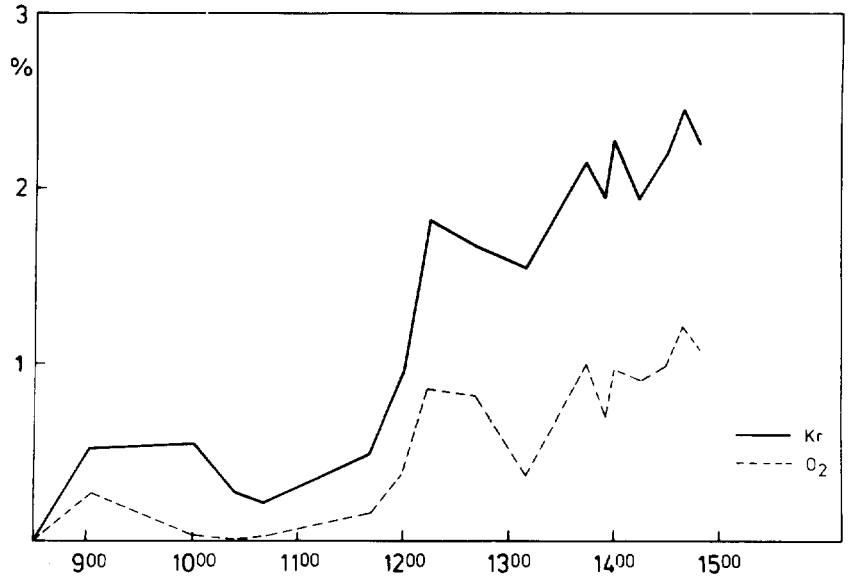

Figure 7 Krypton and oxygen enrichment of a 0.1 % Kr/0.3 % O_2/CO_2 mixture

Considering a water content of the burner off-gas in the order of 1000 ppm, corresponding to about 0.3% water adsorbed by the crushed fuel elements, the overall decontamination factor for tritium is in the order of 100, which is satisfactory.

In the same way an adsorption of iodine from the liquid off-gas should be possible. However the efficiency of the iodine filters could not be tested during the last hot cell runs because of the long decay time of the fuel elements

Low Temperature AKUT Process

The burning of the graphite matrix of the depleted HTR fuel elements with oxygen enriched air results in an appreciable amount of nitrogen in the off-gas. From the technical point of view a feed gas with about 50% oxygen is recommendable. The resulting off-gas composition will be about 50% CO + CO_2, 50% N_2 and 1 to 10 ppm Kr.

From known as well as estimated data the following process may be developed.

The off-gas filtering equipment and the catalytic burner will not deviate in an appreciable manner from the ambient temperature flowsheet.

The oxidized off-gas containing 50% permanent gas cannot be liquefied completely (7). Therefore the gas will be condensed partially at -40°C and the remaining gas phase will be scrubbed with the liquid discharged from the bottom of the distillation column.

First the gas is compressed to 120 atm and cooled to -40°C. Under these conditions 46% of the gas will be condensed. The molar fraction of nitrogen in the gas and in the liquid phase will be 0.22 and 0.74, respectively.

The liquid phase will be fed into the distillation column. The column will operate at -40°C at the bottom and at -45°C at the top. It must have 25 theoretical plates at a reflux ratio of 17,000. From the top of the column a krypton rich fraction with 10% Kr, 76% N_2+O_2 and 14% CO_2 may be withdrawn. A part of the krypton free product from the bottom containing 20% N_2+O_2 and 80% CO_2 is used to scrub the gas phase remaining after partial liquefaction. A smaller fraction of the bottom product corresponding to the amount of feed gas is discharged through the stack after expansion. The most important design data are given in table III.

Comparison of Ambient and Low Temperature AKUT Process

A comparison of the ambient temperature flowsheet for carbon dioxide rich off-gas and the low temperature flowsheet for permanent gas rich off-gas shows that the latter must be much more expensive, because

- a further process step, the scrubbing of the off-gas including recirculation of the liquid gas from the bottom of the distillation column to the scrubber must be applied,
- the throughput of the distillation column must be higher by a factor of about 3 because of the higher off-gas volume and the additionally recirculated liquid gas, and
- a cryogenic unit as well as good insulation are necessary.

Furthermore safety aspects must be considered. Power break down would result in an appreciable increase of the pressure in the case of the low temperature flowsheet. To prevent the blow-off of radioactive gas additional pressure vessels must be provided.

The higher capital costs of the low temperature lowsheet as well as its higher operating costs must be compared with the oxygen enrichment costs. A gross calculation seems to make evident, that the burning of the graphite with oxygen and the following ambient temperature AKUT process are preferable. Detailled cost calculations are under way.

Evaluation

The AKUT process for the separation of aerosols, krypton and

Table III Design data for the low temperature AKUT process

		Molar Fraction of Kr	Molar Fraction of N_2
Burner Off-gas		$2.2 \cdot 10^{-6}$	0.50
Compression and Cooling			
Temperature	$-40^{\circ}C$		
Pressure	120 atm		
Liquified off-gas	46 %		
Gaseous phase		$3.8 \cdot 10^{-6}$	0.74
Liquid phase		$2.0 \cdot 10^{-7}$	0.22
Scrubber			
Theoretical plates	20		
Mole ratio liquid/gas	2		
Liquid before scrubbing		$3.8 \cdot 10^{-9}$	0.22
Liquid after scrubbing		$1.9 \cdot 10^{-6}$	0.22
Gas after scrubbing		$7.7 \cdot 10^{-9}$	0.74
Scrub Solution + Condensate		$1.4 \cdot 10^{-6}$	0.22
Distillation			
Theoretical plates	25		
Reflux ratio	17000		
Temperature Top	$-45^{\circ}C$		
Bottom	$-40^{\circ}C$		
Pressure	120 atm		
Feed (liquid)		$1.4 \cdot 10^{-6}$	0.22
Top (liquid)		0.1	
Bottom (liquid)		$3.8 \cdot 10^{-9}$	0.22

tritium as well as iodine is being developed for the purification of the burner off-gas in HTR fuel element reprocessing. The type of the graphite burner (fluidized bed or block burner) is of minor importance, because a catalytic burner produces an off-gas with constant composition. However, the use of oxygen is recommended because a low permanent gas content is advantageous from the economic and safety point of view. The addition of the relatively small dissolver off-gas volume to the burner off-gas does not change the situation appreciably despite of the higher permanent gas content of the dissolver off-gas.

If the amount of krypton liberated during the burning step is low and its emission may be tolerable, one should dispense with the krypton separation from the burner off-gas because a cryogenic process for the purification of the much smaller dissolver off-gas volume may be more advisable.

References

(1) M. Laser, H. Beaujean, P. Filß, E. Merz, H. Vygen, "Emission of radioactive aerosols from reprocessing plants", Physical Behaviour of Radioactive Contamination in the Atmosphere, IAEA Proceeding Series, in press.

(2) H. Beaujean, J. Bohnenstingl, M. Laser, H. Schnez, "Gaseous radioactive emissions from reprocessing plants and their possible reduction", Environmental Behaviour of Radionuclides Released in the Nuclear Industry, IAEA Proceeding Series STI/PUB/345, p. 63-78

(3) R. Böhnert, "Entwicklung eines Verfahrens zur Verbrennung des Graphits bestrahlter Brennelemente von Hochtemperaturreaktoren in einer inertstofffreien Wirbelschicht", German Report Jül-1041-CT (1974)

(4) F.G. Bodewig, W. Johannisbauer, G. Kaiser, P. Sckuhr, "Komponentenentwicklung für die Auflösung, Speiselösungseinstellung und Extraktion in JUPITER", Reaktortagung des DAtF 1973, ZAED-Karlsruhe, p. 421 (1973)

(5) M. Laser, H. Beaujean, Verfahren zur Abtrennung von Edelgasen aus Kohlendioxid enthaltenden Gasgemischen", Deutsches Patentamt, Offenlegungsschrift 2 131 507, Anmeldetag 25.6.1971

(6) H. Beaujean, P. Filß, U. Grahmann, M. Laser, E. Merz, U. Tillessen, "Reinigung der Verbrennungsabgase bei der Wiederaufarbeitung von HTR-Brennelementen", German Report Jül-925-CT (1973)

(7) G. Kaminishi, T. Toriumi, "Dampf-Flüssigkeit-Phasengleichgewicht in den Systemen CO_2-H_2, CO_2-N_2 und CO_2-O_2, Kogyo-Kagaku-zasshi 69, 175-178 (1966)

DISCUSSION

GLASS: I find the oxygen-krypton behavior, as you say, very surprising. And, I was wondering if you have any reason why the oxygen-krypton behavior is almost 180 degrees from what one would expect, and also, could there be an artifact of batch processing which might not be present in steady state operation?

LASER: The last question first. I don't think it is an effect of batch distillation. We have found this effect in our experiments and we also have an idea why this enrichment occurs but I'm sorry I cannot give details about this in public because our patent office has not authorized me to publish details.

K-L-6338

ABSORPTION PROCESS FOR REMOVING KRYPTON FROM THE OFF-GAS OF AN LMFBR FUEL REPROCESSING PLANT*

M. J. Stephenson, D. I. Dunthorn,
W. D. Reed, and J. H. Pashley
Materials and Systems Development Department
Gaseous Diffusion Development Division
UNION CARBIDE CORPORATION
NUCLEAR DIVISION
Oak Ridge Gaseous Diffusion Plant
Oak Ridge, Tennessee

Abstract

The Oak Ridge Gaseous Diffusion Plant selective absorption process for the collection and recovery of krypton and xenon is being further developed to demonstrate, on a pilot scale, a fluorocarbon-based process for removing krypton from the off-gas of an LMFBR fuel reprocessing plant. The new ORGDP selective absorption pilot plant consists of a primary absorption-stripping operation and all peripheral equipment required for feed gas preparation, process solvent recovery, process solvent purification, and krypton product purification. The new plant is designed to achieve krypton decontamination factors in excess of 10^3 with product concentration factors greater than 10^4 while processing a feed gas containing typical quantities of common reprocessing plant off-gas impurities, including oxygen, carbon dioxide, nitrogen oxides, water, xenon, iodine, and methyl iodide. Installation and shakedown of the facility were completed and some short term tests were conducted early this year. The first operating campaign using a simulated reprocessing plant off-gas feed is now underway. The current program objective is to demonstrate continuous process operability and performance for extended periods of time while processing the simulated "dirty" feed. This year's activity will be devoted to routine off-gas processing with little or no deliberate system perturbations. Future work will involve the study of the system behavior under feed perturbations and various plant disturbances.

I. Introduction

Since 1967, the Oak Ridge Gaseous Diffusion Plant has been engaged in a program to develop and demonstrate a fluorocarbon-based selective absorption process for removing radioactive krypton and xenon from various contaminated off-gases. A pilot plant was built and put into operation to establish general process feasibility and to collect basic engineering mass transfer and performance data. This phase of the ORGDP program proved to be very successful insofar as demonstrating the potential and flexibility of the basic process and ultimately resulted in the generation of absorber column design correlations and process operating procedures[1,2]. Tests designed to demonstrate the specific application of the process

* This document is based on work performed at the Oak Ridge Gaseous Diffusion Plant operated by Union Carbide Corporation, Contract W-7405-eng-26 with the United States Atomic Energy Commission.

to the cleanup of various nuclear reactor off-gases were initiated in 1971. In these tests, radioactive krypton and xenon isotopes were used to prepare simulated reactor vent gases having krypton concentrations ranging from 10 ppb to 4 ppm, and xenon concentrations between about 3 ppb and 15 ppb. In addition to air, nitrogen, argon, helium, and hydrogen were utilized as process gases. Overall process krypton and xenon removals as high as 99.9 and 99.99 percent, respectively, were commonly achieved [3,4]. Krypton concentration factors as high as 1500 were measured in the course of this work. The reactor related tests were concluded in 1972, and it was judged that application of the process to reactor systems was feasible without any further extensive testing.

Development activities prior to 1972 involved work with only the primary or basic absorption system and so called "clean" feed gases. Fuels reprocessing applications had not been actively studied and important questions remained as to how certain impurities common to fuel reprocessing plant off-gas would effect the process operability and performance when introduced into the krypton absorption system and what special modifications or additions might be necessary to the primary process to establish or guarantee process integrity. Since impurities generally compromise the reliability and safety of the other krypton recovery processes, it was decided to undertake scoping tests to provide an initial feel for the tolerance the fluorocarbon process has for fuel reprocessing plant impurities and confirm predicted impurity disposition in the absorption system. In these tests, carbon dioxide, nitric oxide, nitrogen dioxide, and nitrous oxide were fed to the process at impurity concentrations ranging from 500 ppm to over 1 percent. Other tests were performed with iodine and methyl iodide. The scoping studies indicated that the feed gas impurity behavior is predictable and process operability and krypton removal capability appears to be unaffected by the presence of typical feed gas impurities, at least, for short term operation[5].

Based on the operability, performance, and tolerance the fluorocarbon process has for typical fuel reprocessing plant off-gas impurities and the operating experience and flexibility of the Oak Ridge program, development work was proposed in a joint program with the Oak Ridge National Laboratory and subsequently supported by the AEC to adapt the ORGDP-developed process to krypton decontamination of LMFBR fuel reprocessing plant off-gas. This program involved redesign of the absorption pilot plant and development of several auxiliary subsystems to be added to the primary absorption-stripping process to deal with the particular needs of the LMFBR application. The new absorption pilot plant was built at Oak Ridge during 1973 and the first half of 1974 and is now in operation. This facility is described below. Experimental plans scheduled for the next five years to demonstrate the overall proposed process are also discussed.

II. Pilot Plant Description

The Oak Ridge Gaseous Diffusion Plant selective absorption pilot plant, as it exists for the LMFBR fuel reprocessing plant application, consists of a primary absorption-stripping operation and all peripheral equipment required for feed gas preparation, process solvent recovery, process solvent purifications, and krypton product purification. A schematic of the pilot plant is shown in figure I. The new plant is designed to handle a nominal 7 liters/sec (STP) of "dirty" reprocessing plant off-gas and achieve krypton decontamination factors in excess of 10^3 with product concentration factors greater than 10^4. The absorption-stripping section of the plant is the same primary process developed and demonstrated earlier. A photograph of the primary plant, showing the absorber, fractionator, and

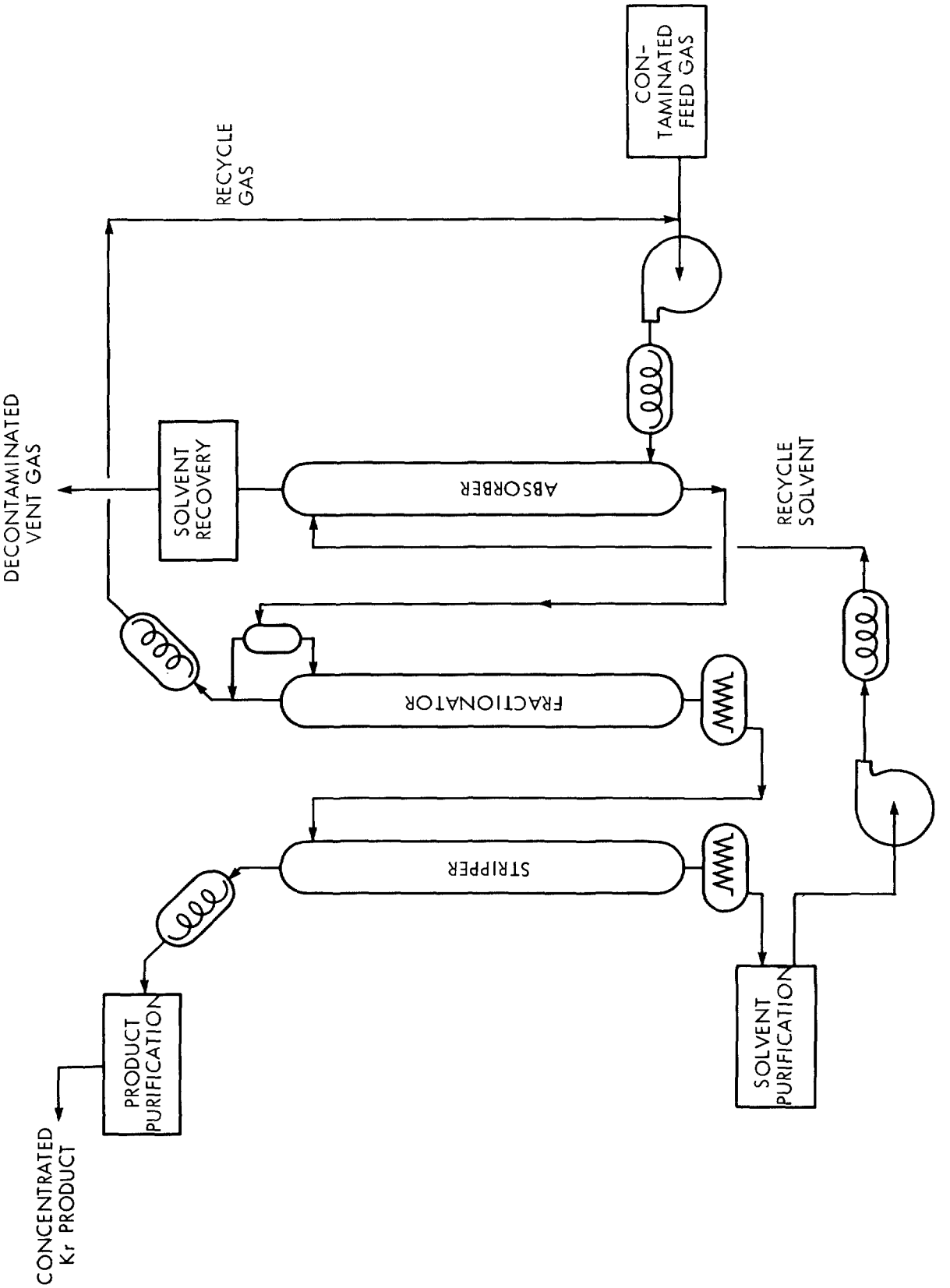

Figure 1 Schematic of the ORGDP selective absorption pilot plant.

stripper before being insulated is shown in figure 2. The absorber column is 3 inches in diameter and contains 9 feet of wire mesh packing, while the fractionator column is 3 inches in diameter with 7.5 feet of packing, and the stripper column is 6 inches in diameter with 12 feet of packing. Figure 3 gives an overall view of the completed pilot plant. The process utilizes conventional equipment designs which have been employed for many years in non-nuclear applications in the chemical industry. The general operating theory and procedures are likewise well known. Pilot plant control and monitoring instrumentation is typical of industrial gas absorption processes. The pilot plant control panel is shown in figure 4.

Three packed columns comprise the main working sections of the process. Each column is designed to exploit certain gas-solvent solubility difference that exist between the solvent and the various feed gas constituents. The main separation of noble gas is accomplished in the first column or absorber. The other two columns, each fitted with a reboiler and an overhead condenser, make-up the fractionator and stripper sections of the plant. The purpose of the fractionator is to remove the bulk of the coabsorbed carrier gas from the loaded solvent, while the stripper produces a highly concentrated krypton-xenon gas product by recovering the remaining dissolved gas from the solvent. The rest of the primary process equipment includes a process gas compressor, solvent pump, gas and solvent heat exchangers, and several refrigeration compressors. The related support equipment items for the LMFBR application include regenerable adsorption and chemical traps for solvent recovery and product purification and a solvent still for solvent purification.

The feed gas, contaminated with krypton, is first compressed to the absorber column operating pressure, typically between 14 and 28 atm, and then cooled to the desired absorption temperature, around minus 30°C. Two single stage diaphragm compressors are used in series to compress the process gas. A photograph of the compressor package is shown in figure 5. The gas is then passed into the bottom of the absorber column and is contacted countercurrently with downflowing solvent. Under favorable operating conditions essentially all of the krypton plus a quantity of the bulk feed gas is dissolved. Other gases, such as xenon, nitrous oxide (N_2O), carbon dioxide, and oxygen, if present, will also dissolve according to their respective solubilities. Soluble solids such as iodine and nitrogen dioxide (NO_2) and miscible liquids such as methyl iodide will also be retained by the solvent. The decontaminated gas leaving the top of the absorber is vented, while the loaded solvent leaving the bottom of the absorber is passed on to the fractionator.

The fractionator is operated at a lower pressure and correspondingly higher temperature than the absorber, for example at 3 atm and 0°C. Upon entering the fractionator flash drum, a large portion of the less soluble gases such as nitrogen and oxygen desorb and pass into the fractionator overhead condenser. The remaining liquid is fed into the top of the fractionator column where it is contacted with upflowing solvent vapor from the reboiler to facilitate further desorption of the less soluble gases. During fractionation, the remaining dissolved gas becomes further enriched in krypton and the other more soluble feed gas constituents such as xenon, nitrous oxide, and carbon dioxide. Since a perfect cut cannot be achieved, however, a measurable amount of krypton is also evolved and, therefore, the fractionator off-gas is recycled back to the absorber. The solvent is next routed from the fractionator reboiler to the stripper for noble gas recovery and solvent purification. The stripper section of the process is similar to the fractionator and the action described for the fractionator is repeated. By operating the stripper column with a higher solvent boilup and under a lower pressure, generally around 2 atm, than that used in the fractionator, the remainder of

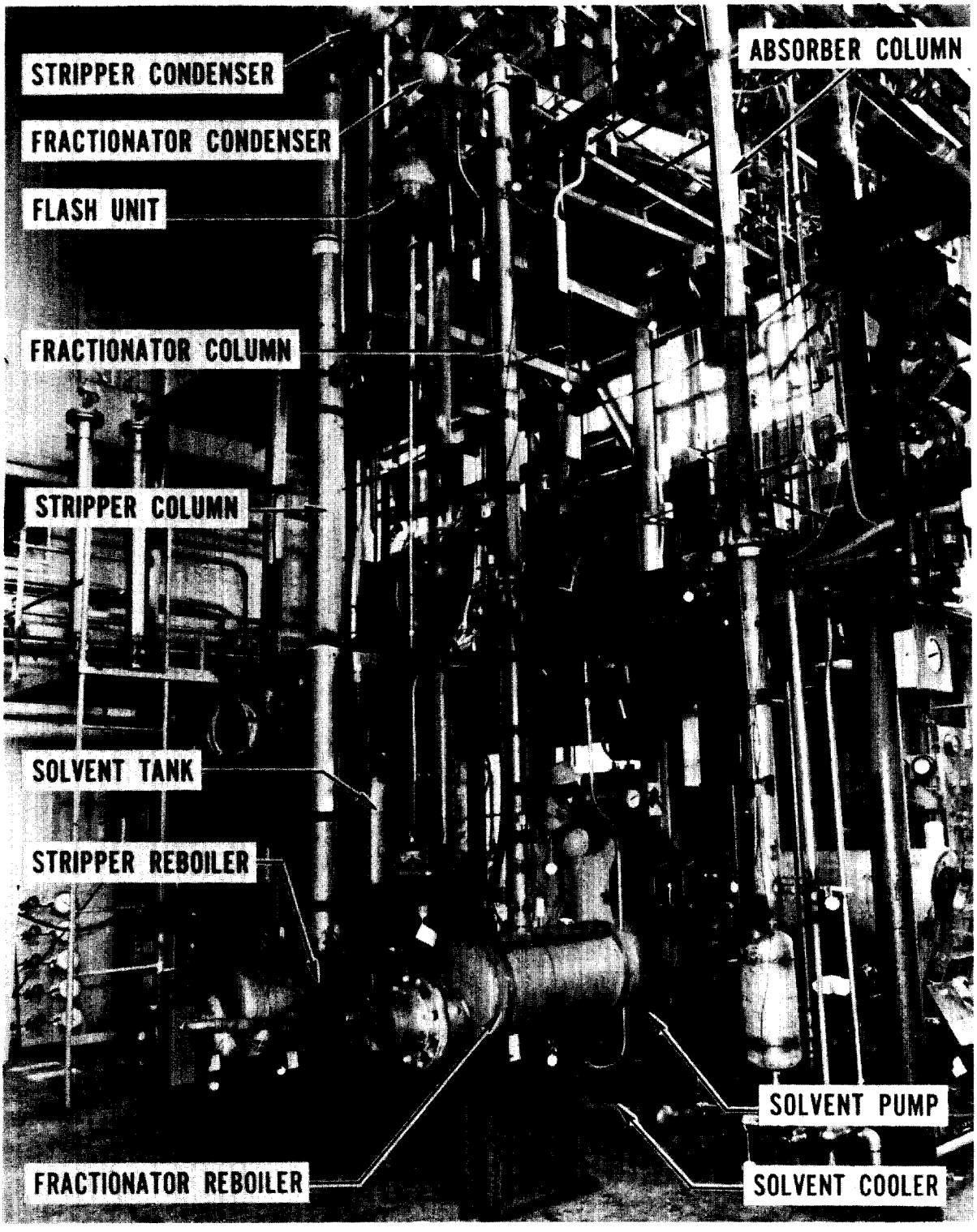

Figure 2 Primary pilot plant without insulation.

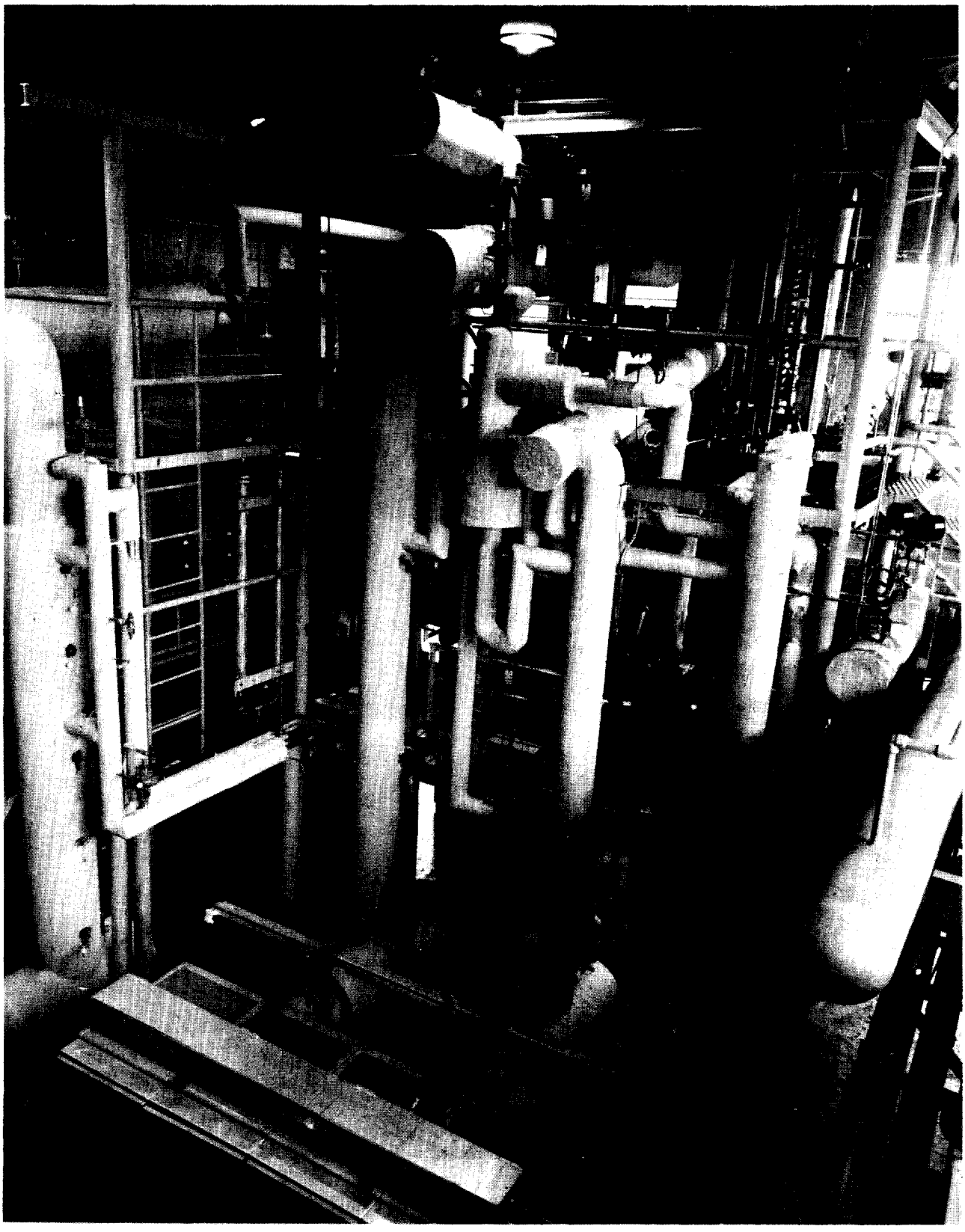

Figure 3 Overall view of the ORGDP facility.

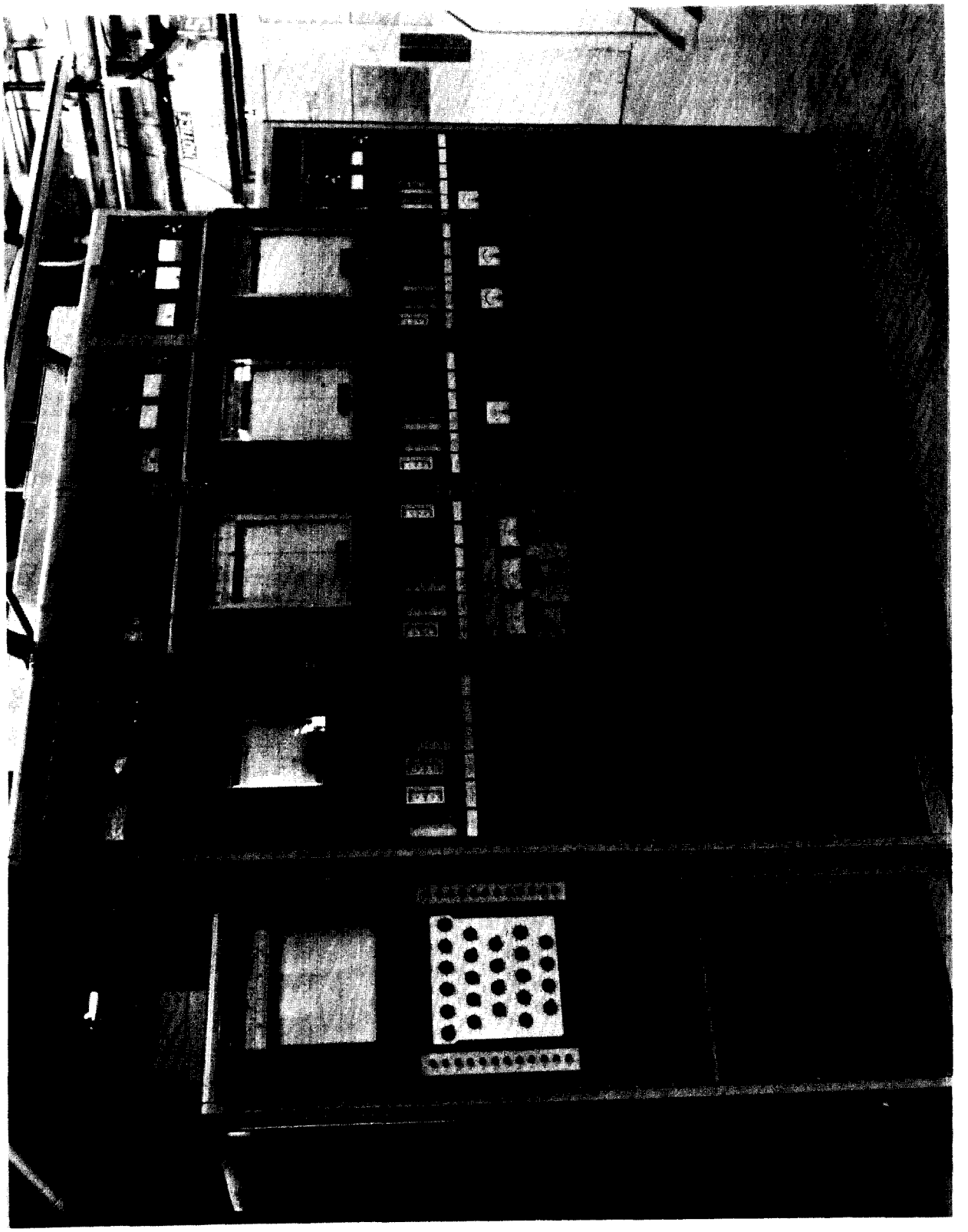

Figure 4 Pilot plant control panel.

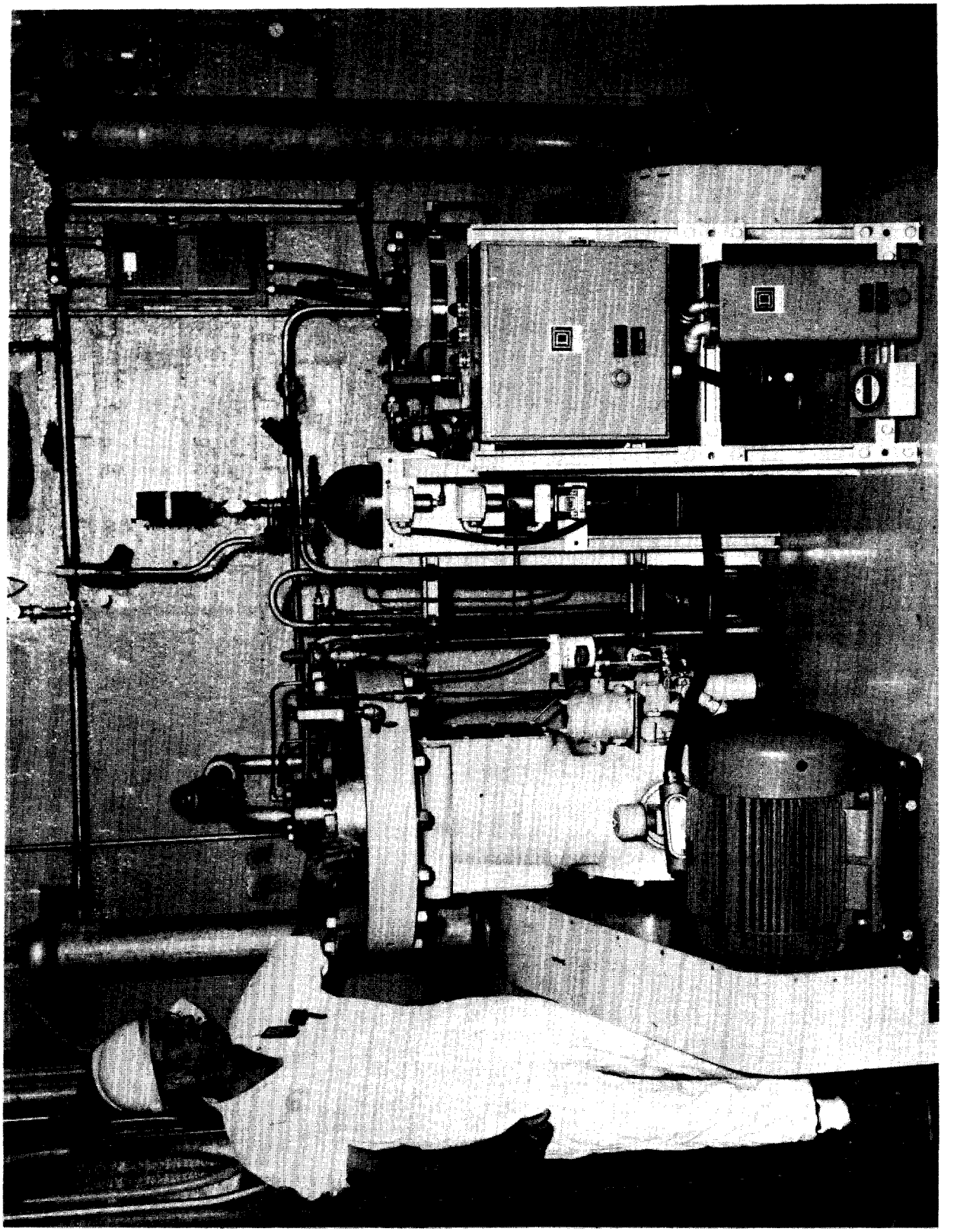

Figure 5 Process feed gas compressor.

the absorbed gas is driven from the solvent and collected as a product. Less volatile feed gas constituents, such as nitrogen dioxide (NO_2), iodine, and methyl iodide if present, remain in the solvent during the fractionation and stripping operation. These reprocessing plant impurities will tend to accumulate in the solvent circuit unless removed via a solvent purification subsystem before recycling the solvent back to the absorber for reuse.

The feed gas preparation station consists of a precision gas metering and mixing manifold capable of providing a pilot plant feed gas containing typical quantities of common or expected reprocessing plant off-gas impurities, including oxygen, carbon dioxide, nitrogen oxides (NO, NO_2, N_2O, N_2O_3), water, xenon, iodine, and methyl iodide.

The process solvent recovery subsystem includes the necessary equipment to evaluate solid adsorbents for removing solvent vapor from the process vent gas. ORGDP laboratory tests indicate that several materials, including 13X molecular sieves, alumina, silica gel, and activated charcoal, can be used to effectively remove refrigerant-12 from air. Charcoal will not be used, however, because of the potential hazards associated with contacting the adsorbent with nitrogen oxides. Operating parameters and regeneration schemes will be defined in the course of the work. Our goal is to reduce the refrigerant content in the process vent gas from its equilibrium value leaving the absorber, typically 3 to 5 mole percent, to less than 1 ppm. Later, we will investigate the use of alternate solvent removal schemes including the use of a turboexpander to cool the vent gas by isentropic expansion and thereby condense the accompanying vapor. Contacts with industrial suppliers of turboexpanders indicate that the solvent content in the process vent gas could be reduced to less than 1 ppm using a commercial expander.

The process solvent purification subsystem plays a critical role in ensuring plant operation when processing waste gas containing high boiling components that dissolve or mix with the solvent in the absorber and tend to otherwise accumulate in the solvent circuit. Based on the obvious needs of the purification equipment and the physical and chemical properties of the system impurities and process solvent, a solvent still was selected to perform the purification task[6]. The still is primarily designed to remove nitrogen dioxide, iodine, and methyl iodide from the solvent but will also remove refrigerants-113 and 114, the radiolytic decomposition products of refrigerant-12. Figure 6 is a photograph of the solvent still.

The purpose of the product purification subsystem is to further reduce the krypton storage volume by removing the accompanying solvent vapor and all miscellaneous feed gas constituents that, according to component solubilities, totally or partially collect with the krypton product. Essentially all xenon, carbon dioxide, and nitrous oxide (N_2O) fed to the absorption process will utimately end up with the krypton product because the solubilities of these feed gas constituents approximate that of krypton in refrigerant-12. Smaller quantities of oxygen and nitrogen will be present because these components are not very soluble. Diluent components will be removed from the krypton product by passing the mixture through a series of one or more physical and chemical sorbent traps as required. These traps are relatively small since the flow rate of gas at this point is very low, normally being two to three orders of magnitude less than the process feed gas flow. First, a 5A molecular sieve trap will be used to catch the carbon dioxide and most of the nitrous oxide. Next, a 13X molecular sieve trap will be used to remove the refrigerant-12 vapor. Then, oxygen and nitrogen plus the remaining nitrous oxide will be chemically reacted in heated chemical traps. Manganese oxide will be the primary getter to remove the oxygen while titanium sponge or

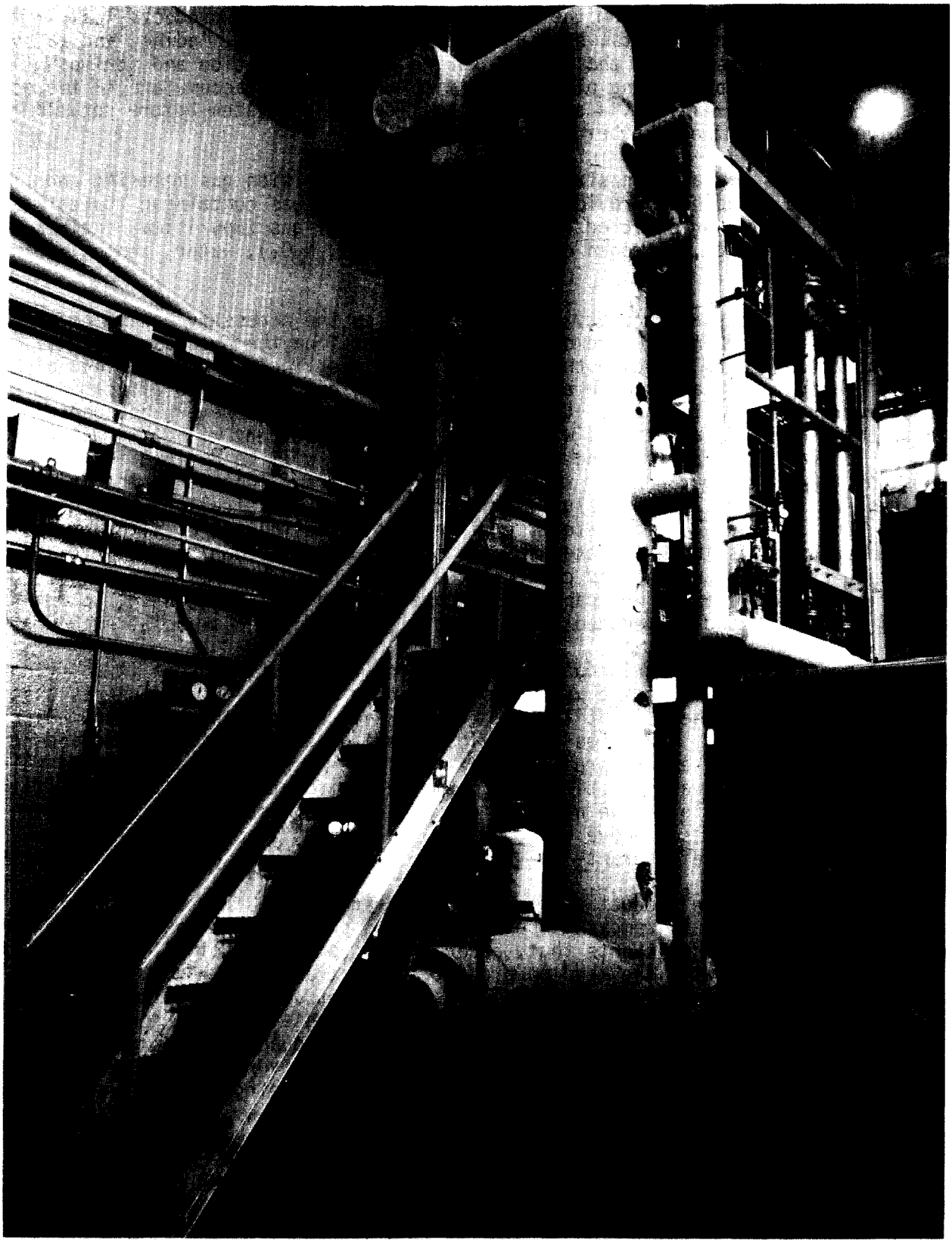

Figure 6 Solvent purification still.

calcium turnings will be used to remove the nitrogen. The resulting product will be essentially pure krypton and xenon with only minute traces of the other process feed gas components. Later in the program methods separating the krypton-xenon product will be evaluated to recover the valuable xenon and thereby further reduce the krypton storage requirement.

It should be emphasized at this point that an alternative philosophy for application of the selective absorption process at reprocessing plants is possible. If stringent feed pretreatment requirements were imposed, like those necessary for cryogenic processing, product and solvent purification subsystems would not need to be as inclusive as planned. The current feeling is that from both an economic and reliability standpoint, the tolerance of the absorption system for impurities should be exploited, and this is the basis for the direction of our current work.

III. Experimental Program Plan

The Oak Ridge Gaseous Diffusion Plant selective absorption process development program is currently scheduled to be completed by 1979. The overall effort appears to be broad enough in scope to effectively evaluate the proposed process and provide data necessary to the design of larger systems and yet remain flexible enough to respond to the needs of the overall LMFBR fuel recycle program. Pilot plant shakedown operations were completed during the first half of this year and a detailed operating procedure was prepared. The first pilot plant campaign simulating the LMFBR fuel reprocessing plant application is now underway. The major objective of the work is to demonstrate overall process operability and performance for extended periods of time while processing simulated reprocessing plant off-gas. In addition to providing subsystem performance data, this program will also provide more fundamental data from the primary process, primarily related to the stripping operation. Next, realizing that system perturbations will occur in actual application, tests will be conducted in which deliberate attempts will be made to disrupt plant operation. The objectives of this program are to define process limitations and to develop preventative or corrective operational procedures as necessary to counteract system disturbances and re-establish normal operations. Work will involve the study of the system behavior under feed perturbations and various plant disturbances such as the failure of an upstream air cleaning or control device and the introduction of much larger quantities of iodine, methyl iodide, nitrogen dioxide, or particulates in the process, the failure of various components such as a refrigeration compressor, or the failure of one of the process subsystems such as the solvent purification still. Completing the formal program, pilot plant tests will be conducted as necessary to satisfy or explore application questions posed by industry. Peripheral matters will also be considered along with the main development effort, such as evaluation of methods to separate the cold fission product xenon from the krypton product, and process flowsheet alterations reflecting energy conservation measures.

IV. Conclusions

We have constructed a pilot plant at Oak Ridge to evaluate and demonstrate a fluorocarbon-based absorption process exclusively tailored to remove krypton from the off-gas of an LMFBR fuel reprocessing plant. The process utilizes conventional heat and mass transfer equipment commonly employed by the chemical industry and requires only moderate process pressures and temperatures. An extensive evaluation program is scheduled over the next five years to provide design and operational

data for process scaleup. Acceptance of the proposed process for use at a reprocessing plant will undoubtedly be enhanced if the ongoing development work continues to show that the system tolerance for impurities is good. Previous laboratory tests with iodine and methyl iodide suggest that the krypton absorption process could serve as a secondary or backup system for fission product iodine removal. Certainly, this possibility will be explored. Likewise, the process might also be used to remove nitrogen oxides from the reprocessing plant off-gas.

V. References

(1) Merriman, J. R., et al., *Removal of Radioactive Kr and Xe from Contaminated Off-Gas Streams*, USAEC Rep. CONF-700816-4 (1970).

(2) Stephenson, M. J., et al., *Experimental Investigation of the Removal of Kr and Xe from Contaminated Gas Streams by Selective Absorption in Fluorocarbon Solvents: Phase I Completion Report*, USAEC Rep. K-1780 (1970).

(3) Stephenson, M. J., et al., *Application of the Selective Absorption Process to the Removal of Kr and Xe from Reactor Off-Gas*, USAEC Rep. K-L-6288 (1972).

(4) Stephenson, M. J., et al., *Experimental Demonstration of the Selective Absorption Process for Kr-Xe Removal*, USAEC Rep. CONF-720823 (1972).

(5) Merriman, J. R., et al., *Removal of ^{85}Kr from Reprocessing Plant Off-Gas be Selective Absorption*, USAEC Rep. K-L-6201 (1972).

(6) Dunthorn, D. I., and Stephenson, M. J., *Solvent Purification System for the Fluorocarbon Absorption System*, USAEC Rep. K-L-6325 (1973).

DISCUSSION

KABELE: Two questions: would you comment on problems of radiolysis of the fluorocarbon and what, if anything, would that mean in terms of putting a halogen in your principal product if you want to store in a steel vessel?

STEPHENSON: We have looked into the decomposition of refrigerant-12, which is our primary solvent, and the radiolysis of the material does not pose a significant problem. If you want to talk about the exposure that the solvent might receive, we're talking about one mega-rad for a 5 ton/day FRP. The noble gas inventory is small. The primary products of decomposition are refrigerants -114, -113, and -13. Refrigerants-114 and -113 will come out of the system via the solvent distillation column. Refrigerant-13 is volatile and will vent from the process at any off-gas point. Some chlorine will also be evolved, but in the absence of water, is not corrosive. Free chlorine will be removed from the krypton product via the product purification traps. If water is present, we would consider putting a sacrificialmetal in the system.

T.E. WILLIAMS: I was wondering if the solvent recovered from the absorber vent gas is re-cycled back to the process?

STEPHENSON: All solvent will be re-cycled from the solvent recovery subsystem. Later in the program we will consider using a commercial turboexpander to recover the process solvent from the process vent.